USING GEOPHYSICAL METHODS TO LOCATE ARCHAEOLOGICAL FEATURES AND ARTIFACTS FROM LA PLACITA DE LOS TRUJILLOS, BURIED BY THE SANTA ANA RIVER DURING THE GREAT FLOOD OF 1862

A Thesis

Presented to the

Faculty of

California State Polytechnic University, Pomona

In Partial Fulfillment

Of the Requirements for the Degree

Master of Science

In

Geology

By

Chloe Sutkowski

2020

SIGNATURE PAGE

THESIS: USING GEOPHYSICAL METHODS TO LOCATE ARCHAEOLOGICAL FEATURES AND ARTIFACTS FROM LA PLACITA DE LOS TRUJILLOS, BURIED BY THE SANTA ANA RIVER DURING THE GREAT FLOOD OF 1862

AUTHOR: Chloe Sutkowski

DATE SUBMITTED: Spring 2020

Department of Geological Sciences

Dr. Jascha Polet
Thesis Committee Chair
Geological Sciences

Dr. Stephen Osborn
Geological Sciences

Dr. Jonathan Nourse
Department Chair
Geological Sciences

ABSTRACT

In the mid-1800s, La Placita de Los Trujillos (La Placita) was situated alongside the Santa Ana River (SAR) in what is now Colton, CA. The settlement had grown to be the largest non-native community between New Mexico and Los Angeles, until the river washed away or buried all adobe structures and settlers' belongings during the Great Flood of 1862. Historical archives reveal that a significant portion of San Salvador is buried approximately 3 meters beneath sandy flood deposits of the vacant, 200-acre lot of Pellissier Ranch. The motivation for this study was to provide the Spanish Town Heritage Foundation with data they could use to advocate the cultural importance of Pellissier Ranch in their attempt to stop the city from developing the site for warehouses. From April 2018 to January 2020, we conducted eleven days of geophysical field surveys in search of buried adobe structural remains, household items composed of wood and iron, and large farming equipment that would have existed in La Placita. Over 7,000 meters of ground-penetrating radar (GPR) profiles were acquired with both a GSSI-SIR 3000 and 4000, using the 400 MHz and 350 MHz HyperStacking antennas respectively, and 25 km of magnetic gradiometry data was acquired using a GEM GSM-19T Proton Precession Magnetic Gradiometer.

GPR profiles imaged several 'adobe melt' signatures at a depth range of 1.4 - 3.8 meters, and two buried canals with surfaces reaching 1.3 meters below the surface, and bottom depths of 2.5 meters. Additional structural GPR anomalies vary in size from 9 - 70 meters at a depths of 1 - 3.8 meters. We hypothesize that some of the shallower buried (sub-2-meters) anomalies exist for a few reasons: the portion of the anomalous feature closer to the river absorbed the majority of the river's force, which shielded the more intact part, or the location did not experience the full strength of the river's force, causing less destruction and burial beneath the sandy flood deposits.

Contemporary debris from trespassers resulted in many false-positives in gradiometer results that needed to be excluded from mapped vertical gradients. We therefore focused more heavily on GPR results, using the gradiometer as a complementary technique to at-

tempt to verify anomalies we imaged with GPR. In two locations, we observed a positive correlation between the two data-sets, attributed to a sub-2-meter burial of anomalies. This confirms claims made by other researchers that features / artifacts with low magnetic content cannot be seen if buried deeper than 2 meters.

From our results, we conclude with confidence that several anomalies we imaged in GPR profiles can be related to structures / features of La Placita, and the depth range of the settlement at Pellissier Ranch is primarily 2 - 3.8 meters.

Based on our surveys, we suggest to focus any future investigation in the middle of Pellissier Ranch. There is one east-west dirt road that cuts through the middle of the 200-acre site. At about the halfway point of that east-west road, we found a collection of promising anomalies.

Table of Contents

List of Figures

1 Introduction

In the mid-1800s, La Placita de Los Trujillos (La Placita) was situated alongside the Santa Ana River (SAR) in what is now Colton, CA. The settlement had grown to become the largest non-native settlement between New Mexico and Los Angeles, until the river washed away or buried all adobe structures and settlers' belongings in a single night during the Great Flood of 1862. Historical archives reveal that a significant portion of La Placita is buried 3-5 meters beneath sandy flood deposits of the vacant, 200-acre lot of Pellissier Ranch (Figure 1).

(a) Pellissier Ranch location in southern California, denoted by red dot (Google Maps, 2018).

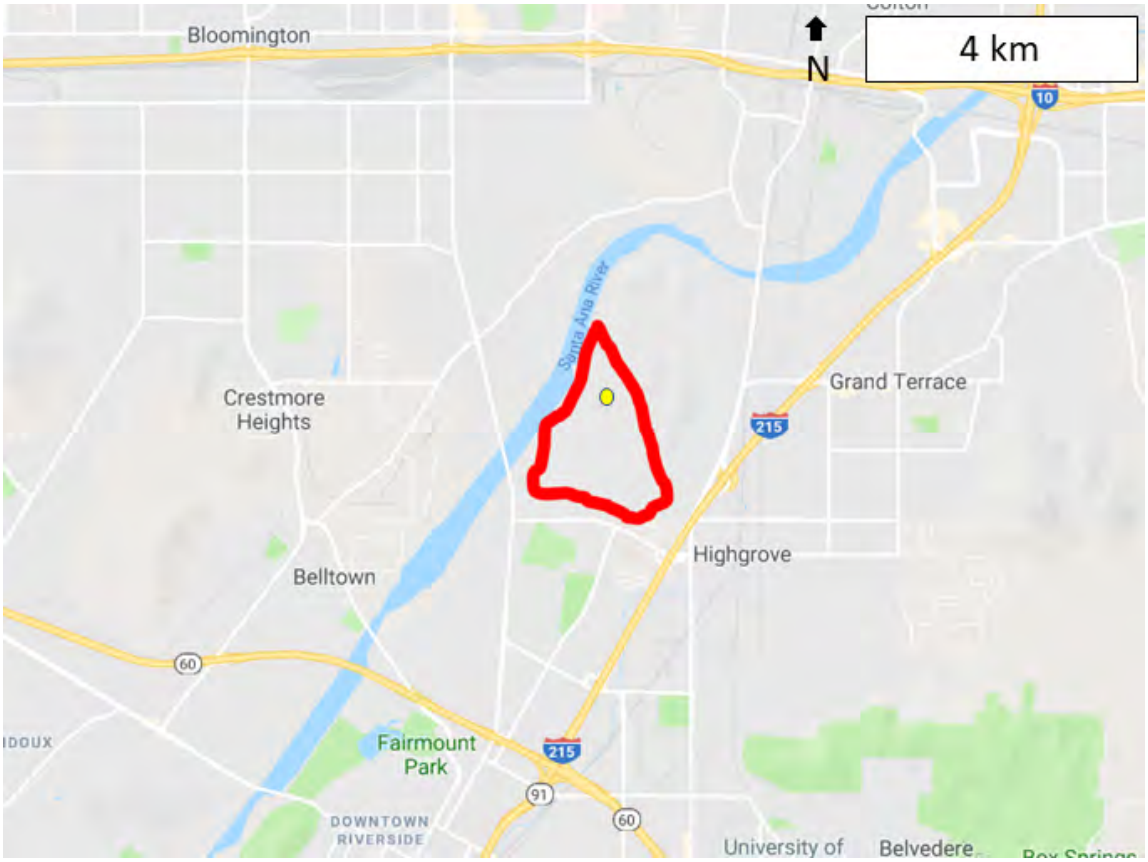

(b) Survey area of Pellissier Ranch in Colton, CA, denoted with a red outline. Yellow dot within Pellissier Ranch marks approximate location of test dig (Figure 6) (Google Maps, 2018).

Figure 1: Study location

Some artifacts may have been carried far from the settlement. We hope to locate larger artifacts, and artifacts that were inside homes that likely collapsed and trapped everything inside of them. Accounts claim that a layer of sandy flood deposits approximately 3-5 meters thick was left atop the settlement after the flood waters retracted (personal communication Nancy Melendez, 2018). This relatively shallow depth range makes a geophysical survey feasible.

Before this study, no surveys had been conducted at Pellissier Ranch. How we became involved in this project, was the Spanish Town Heritage Foundation. Officers of the foundation were seeking help in proving the historical importance of the site after learning of the city's plans to develop Pellissier Ranch as industrial complexes.

1.1 Brief Overview of La Placita de Los Trujillos

In the mid-1800s, San Salvador (the name of the entire settlement spanning both sides of the SAR: La Placita and Agua Mansa) was the largest settlement between New Mexico and Los Angeles and was comprised of settlers from Abiquiu, New Mexico (Vickery, 1984). The land had been given to them for free under one condition: to protect the nearby rancher's property from Native American raids.

While the able bodied defended the area from Native American raids per their contract, other settlers took to farming crops and livestock. The land by the SAR was fertile and the settlers made their living trading produce in downtown Los Angeles and livestock as far as New Mexico (Vickery, 1984). For decades, San Salvador prospered and expanded. Then, an epic rain season began at the end of December 1861 and led to the greatest flood on record in the Upper SAR basin (Sidler, 1968). This Great Flood of 1862 destroyed San Salvador in a single night. Calculations done in 1937 using Manning's Formula estimated that the peak flow of the SAR during this flooding event was 9,000 m^3/s (Sidler, 1968).

Luckily, the pastor had been able to alert the settlers to evacuate in time by ringing the church bell in the middle of the night and no fatalities occurred (Vickery, 1984). Witnesses watching on high ground claimed that billows as high as 50 feet raged out of the confined channel (Mount Slover to the north and La Loma Hills to the south) that the SAR's overflow was funneled through (Beattie et al., 1939). An overview of the river's flow from the northeast, where it originates in the San Bernardino Mountains, to the southwest is shown in Figure 2.

Figure 2: The SAR flows (path and direction indicated with blue arrows) from the San Bernardino Mountains to the Pacific Ocean. Pellissier Ranch is highlighted in aqua (circled). The river takes a sharp turn (red arrow) before it arrives at Pellissier Ranch, as its flow is confined through two topographic highs: Mount Slover and La Loma Hills (Google Earth Pro, 2018).

When morning light broke, the settlers looked upon a wasteland of muddy flood-water where just hours before, their homes had been. The overwhelmed SAR had created a 4-feet-deep, 4-mile-wide, inland sea that remained for approximately one month (Jones, 2018). Peter C. Peters, from Colton was a witness the morning after the Great Flood of 1862 and claimed he watched from the bluff near the cemetery as the adobe homes melted down in the flood-waters and disappeared (Beattie et al., 1939).

Efforts to farm the area post-flood were thwarted by the harsh, sandy deposits that the river had blanketed over the once fertile land (Vickery, 1984). Eventually, the settlers surrendered and moved to nearby communities, but the question remains: what became of the remains of San Salvador, the largest settlement between Los Angeles and New Mexico in the mid-1800s? Despite a brief period during which the area was used as a dairy farm, the land of Pellissier Ranch has remained vacant. The city of Colton is looking to change that, with plans of developing the land into warehouse space. The STHF seeks to prevent this development by proving the cultural importance of this land and appropriating Pellissier Ranch as a historic park instead. A subsurface geophysical investigation could help their

cause by locating anomalies in the subsurface that are buried in the estimated depth range.

The application of geophysical techniques to archaeology is a rapidly growing field. Surveys conducted in 2019, for example, found a buried, 12-meter-long Viking ship (Paasche, 2019) and mass graves from the Tulsa Race Riots of 1921 (Witten et al., 2019). The advancement of technology and computer processing has made various non-invasive techniques highly desired for their efficiency in determining the archaeological importance of sites (Conyers, 2013). Another option for identifying artifacts in the subsurface would be to perform invasive surveys (i.e. excavating). However, invasive techniques become extremely costly when the location is large and it is unknown where buried artifacts may be located. This study aims to identify subsurface anomalies that could be associated with buried La Placita artifacts through the application of several geophysical techniques at Pellissier Ranch.

1.2 Archaeological Geophysics

The first successful application of geophysics to archaeology was an electrical resistance survey conducted in 1946 (Atkinson, 1958). Through this method, Richard Atkinson was able to detect ditches from a previous settlement in the United Kingdom (UK). The next major survey was also conducted in the UK with a proton magnetometer in 1958 (Aitken, 1958). Buried kilns and earth-filled pits were detected in Aitken's survey, the latter having major implications for United States applications as they are the most common feature of prehistoric, Native American settlements. John Weymouth and Bruce Bevan conducted the first major surveys in the United States in the 1970s (Bevan, 1977), (Weymouth, 1976). An early Ground-Penetrating Radar (GPR) survey in the United States took place in 1975, and located buried walls in New Mexico (Clark, 1986). As computer processing power has improved, GPR has become an increasingly popular method for its ability to map a variety of different objects and features in three dimensions.

Across all studies, the most critical element of conducting a successful survey is know-

ing which methods to employ. This depends heavily on the subsurface properties, as some methods will work better than others in imaging artifacts. For example, GPR works best at sites that have a low clay content, as clay will negatively impact the depth of penetration of the electromagnetic waves, while magnetic gradiometry will not be susceptible to this limitation. It is therefore advantageous to use at least a few different methods in a study to enhance the probability of detecting artifacts and/or structural features. Additionally, confidence in results gathered is improved if interpretations can be made with datasets from multiple geophysical methods, with different strengths and weaknesses.

For example, in this study, if an anomaly appears to image a subsurface canal in GPR profiles, the magnetic gradiometer could confirm this by recording a drop in the gradient of magnetic intensity at the canal's location. The low would occur due to the fact that the sand (predominately quartz monzonite) that buried the canal would have a lower magnetic susceptibility than the soil the canal was buried in (predominately quartz diorite; average rock type values from Klein et al. (1983). Another example would be a large scale metallic artifact imaged by the magnetic gradiometer as a significant contrast in the total magnetic field intensity at that location, also appearing as a hyperbolic reflection (discussed in Section 2.1.1) in a GPR profile over the same location.

A proper analysis of the targets and surrounding environment materials is a well-established requirement for a successful geophysical investigation (Sambuelli et al., 2002). For the purposes of this study, this includes knowing if there are any modern surface or subsurface structures/utilities that could create false positives in results, and research on the approximate depth to the water table and local soil type. This information helps determine what method/methods will be successful at the site. An overview of this research is provided in the next sections.

After archival research, we chose and imaged areas within Pellissier Ranch in search of remains from the settlement using various geophysical methods that have been successful in previous archaeological geophysics surveys (Conyers, 2013; Bevan, 1998; Bigman, 2011;

Leckebusch et al., 2001; David et al., 2008; Clark, 1996; Bristow, 2009) including success in locating buried structures specifically (Bevan, 2006; Conyers, 2012).

1.3 Location and Geology

Pellissier Ranch (Figure 3) is located on the border of Colton and Riverside in southern California between interstate 215 and the Santa Ana River.

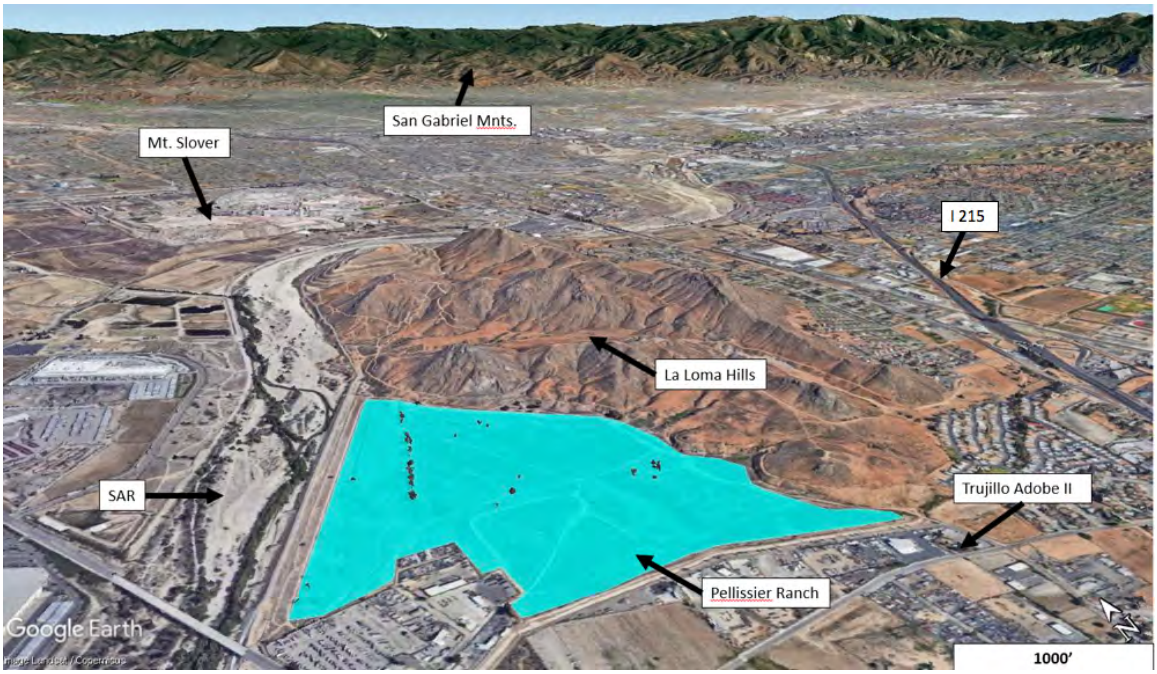

Figure 3: Pellissier Ranch highlighted in aqua, as viewed from an angle to emphasize its absence of topography. La Loma Hills borders the northeast side of the site, and the SAR borders the northwest side of Pellissier Ranch after a distinct curve it takes just north of La Loma Hills. The San Bernardino Mountains are visible in the distance (Google Earth Pro, 2018).

The site is relatively flat, at an elevation of around 257 meters with a 1.5 meter variation. Bordering the north side of the ranch are La Loma Hills, composed of Cretaceous quartz diorite (Figure 4).

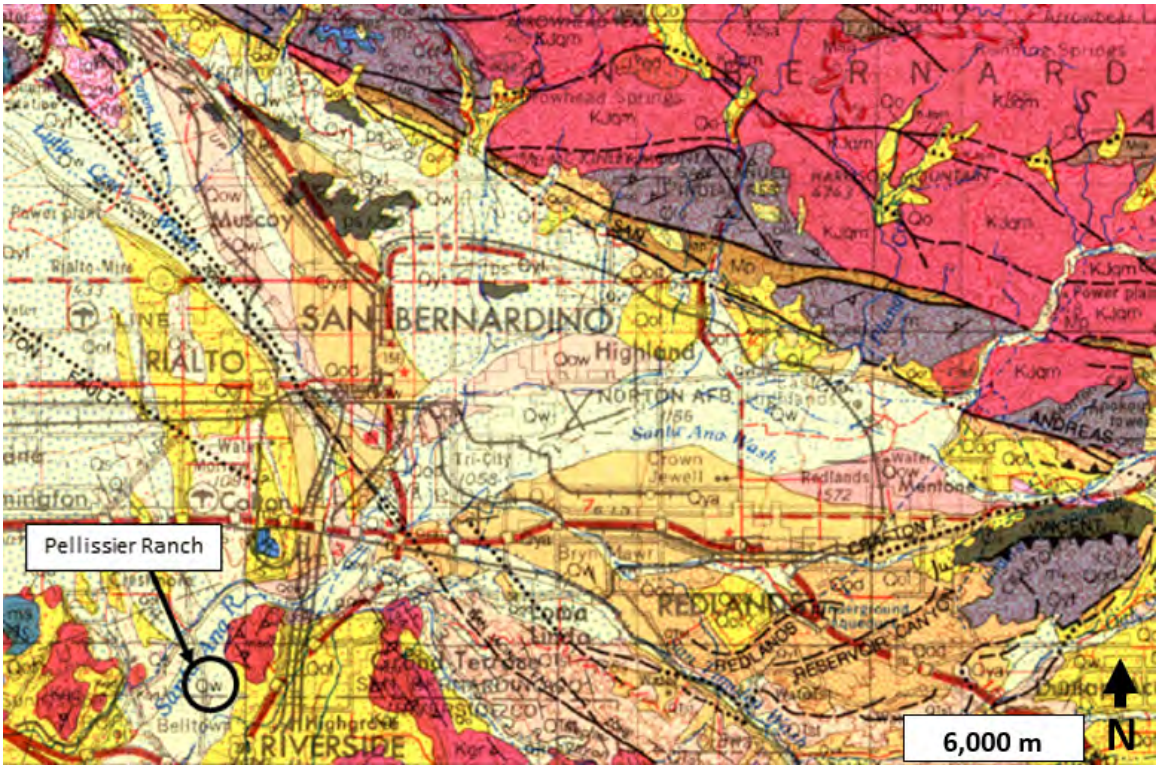

Figure 4: Geologic map of Colton, CA, with Pellissier Ranch circled and labeled. Quaternary wash deposits (Qw) dominate the entire site. La Loma Hills to the northeast of the site are composed of Cretaceous quartz diorite (Kqd) with beds dipping to the east. The Santa Ana River originates in the San Bernardino Mountains on the northeast corner of the map, which are composed primarily of Cretaceous or Jurassic quartz monzonite (KJqm). Map from Bortugno (1986).

Industry surrounds the ranch on its south and west side, while residential homes surround the eastern side. Powerlines border the northwest side along the Santa Ana River, a radio tower for KDIF AM Riverside sits in the southwest corner, concrete towers and observation wells are scattered across the site, and a petroleum pipeline runs along the base of La Loma Hills at the northern border (see Figure 5 for marked locations). Observation wells are read biweekly by Riverside Public Works; the depth of the groundwater from the surface varies between 4.5 and 7.5 meters throughout the year.

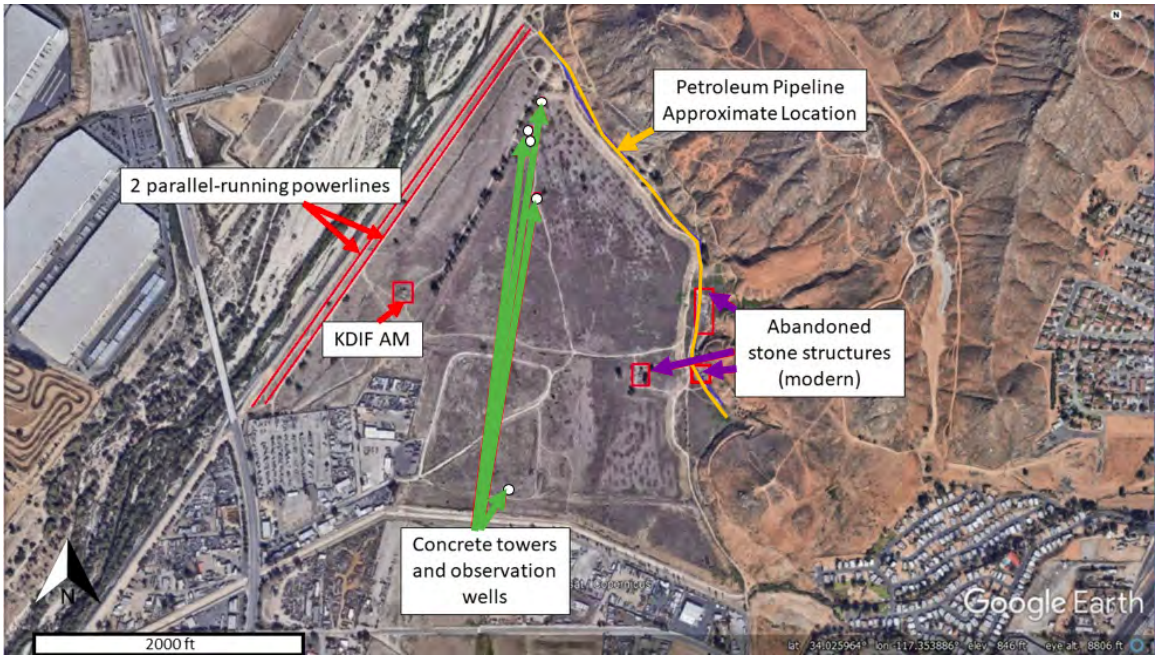

Figure 5: Pellissier Ranch map indicating all large scale features that could affect a geophysical survey (Google Earth Pro, 2018).

Quaternary wash deposits make up the shallow subsurface of Pellissier Ranch. These wash deposits originate from the San Bernardino mountains, where the SAR originates. The San Bernardino Mountains are mostly composed of Cretaceous or Jurassic quartz monzonite. Eroded quartz monzonite is carried downstream and deposited along the the river until it meets the Pacific Ocean. Quartz monzonite is composed of potassium, sodium, calcium, silicon, and aluminum, along with trace amounts of iron and magnesium.

The modern surface soil of Pellissier Ranch has been classified by soil scientists from the United States Department of Agriculture as sandy loam (Rolfes, 2017). It has been 156 years since the Great Flood of 1862, which has allowed for the deposition of this loamy sand atop the flood deposits. A test dig at a location in the center of the site found that the sandy loam extends approximately 0.5 meters deep. At this depth, light-colored sands, most probably deposited during the Great Flood of 1862, are reached (Figure 6).

The wash deposits are medium-sized, light-colored sand. Sand has the largest pores of the three different grain types (sand, silt, and clay) and therefore, a low surface area to

volume ratio. This results in water infiltrating quicker through sandy soil, preventing the soil from holding onto nutrients necessary for crops to thrive.

Historical archives indicate the settlers were forced to abandon the land post-flood due to the flood deposits being inhospitable for farming (Vickery, 1984). La Placita pre-flood was a fertile land, rich with agriculture that led to the settlement's prosperity, so we can assume that there must have been a more loamy soil at the surface pre-flood. Loamy soil is ideal for farming as it is a mixture of all three soil types: clay, silt, and sand. The loamy soil's advantage is that it can hold water long enough for crops to acquire necessary nutrients before the water drains downward. We therefore infer there will be a measurable difference in material properties such as dielectric constant and magnetic susceptibility between the two soil types.

Figure 6: Photo of 2-meter-deep hole, dug 10/27/2019 within the GPR profile shown in Figure 37 (see Results section). Noticeable contrast between the tan, loamy sand (marked by black, double-ended arrow) and the sandy flood deposits, most probably deposited during the Great Flood of 1862.

Given this knowledge of the local geology, water table, and soil conditions, magnetic gradiometry and GPR should both be effective techniques in this study. The next step was to determine where to concentrate our field surveys within the 200-acre lot of Pellissier Ranch. This would require some archival research: speaking with STHF officers, who are descendants of La Placita settlers, and utilizing library archives and Google Scholar.

1.4 Archival Research

On February 19, 2018, officers of the STHF, Nancy Melendez and Darlene Elliot, met with Dr. Jascha Polet and me at Pellissier Ranch. They walked with us along the eastern-

most dirt road on the site. They did not have any information regarding locations of structures or features that comprised the settlement. Information they shared with us pertained to the types of structures that once resided on this land, such as the remains of a footbridge that had been stumbled upon years ago and since lost, and the remains of Trujillo Adobe. The Trujillo Adobe was erected as part of La Placita II (the replacement settlement that La Placita settlers built post-flood), and remains in a fragile state up against the southern edge of Pellissier Ranch. They shared images of it with us to give us a better idea of the size and material we could expect of the structures (Figure 7).

(a) All that remains of Trujillo Adobe. Walls are about 1-meter thick, composed of adobe bricks. Square shaped home, with approximately 10-meter long walls on each side.

(b) Close-up of adobe bricks that make up the Trujillo Adobe.

Figure 7: Images taken by STHF officers of the Trujillo Adobe, the last remaining structure of La Placita II (personal communication STHF, 2018).

An inhabitant of La Placita II had previously hand drawn a map documenting the layout of La Placita II and a simplified illustration of a La Placita II home, which was shared with us in August 2018 (Figure 8; personal communication Darlene Elliot, 2018).

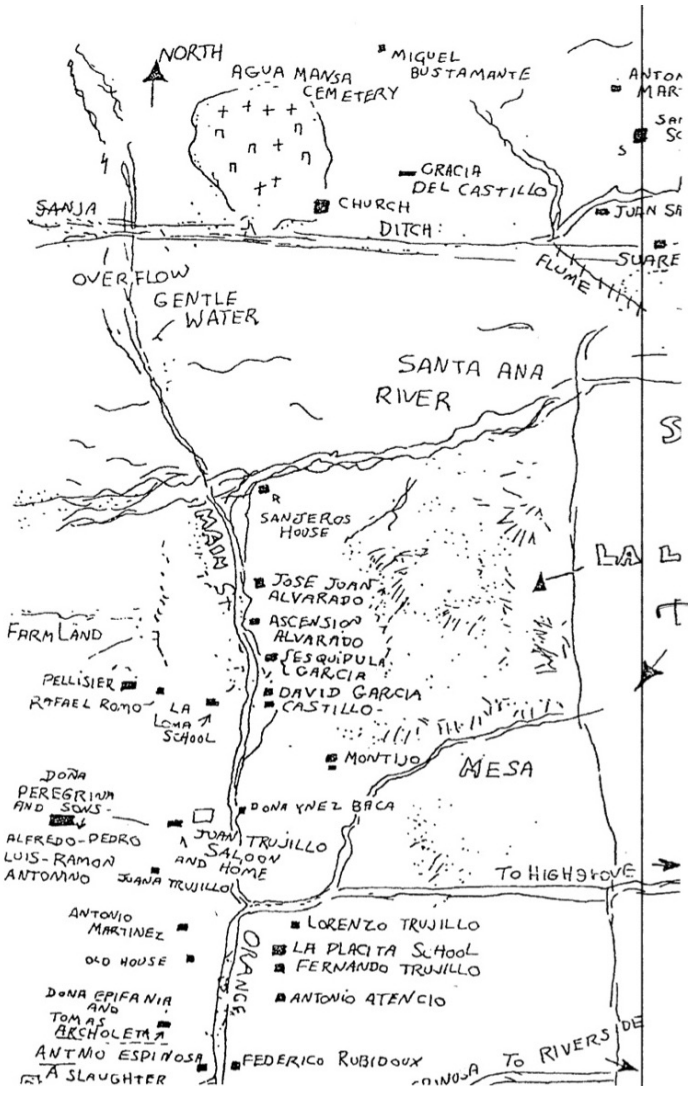

(a) Approximate layout of the La Placita II adobe settlement. Provided by STHF, 2018.

(b) Illustration of a typical La Placita II adobe home. Provided by STHF, 2018.

Figure 8: Historic map and illustration of La Placita II.

Upon review of this map from Alex King, the Director-at-large of the Old Spanish Trail Association, it was determined that it was an unsuitable document to use directly as the basis of our experiment design as the original La Placita settlement is documented as being located much closer to the river than the second settlement. The only clue we had to work with was that the original Trujillo Adobe existed somewhere directly between the path of its post-flood replacement, and the Agua Mansa Cemetery (personal communication Darlene Elliot, 2018) (Figure 9).

Figure 9: The original Trujillo Adobe is said to have resided within Pellissier Ranch (outlined in red), somewhere along the NW trending line, which starts at the Trujillo Adobe and ends at Agua Mansa Cemetery (personal communication STHF, 2018).

La Placita was established as a New Mexico style town similar to Abiquiu, from where

the original group of about 50 emigrated (Harley, 2003). Figure 10 is an image taken in 1920 of the Abiquiu, New Mexico, plaza. Adobe homes are close together and a church lies at the heart of the plaza.

Figure 10: The Abiquiu, New Mexico, adobe settlement photographed in the early 1900s. The original settlers set out to model La Placita after the Abiquiu plaza from which they emigrated (Harley, 2003). Image from (Parkhurst, 1920).

We analyzed photographs of Martinez Hacienda (an early 1800s adobe structure in Taos, New Mexico) to better anticipate artifacts, and the likely look and materials of the 1800s adobe structures of La Placita (Figure 11). This was a suitable comparison as the structure sits within 50 miles of Abiquiu, and was completed at approximately the same time that the La Placita settlers would have lived in Abiquiu. Many wooden and clay household items can be expected, with metallic cookware, blankets, hides, tables, benches, and kilns also present (Figure 10).

(a) Interior of Martinez Hacienda.

(b) Exterior of Martinez Hacienda.

Figure 11: This adobe structure was from the early 1800s in Taos, New Mexico (approximately 50 miles from Abiquiu, from where La Placita settlers emigrated, erected about a decade before they left New Mexico). Images showing Martinez Hacienda from (Aragon, 2012).

Also documented was a church, built in 1852, that ”collapsed in quicksand” on the morning the very first mass was to be held (Harley, 2003). Archives claim this church was in La Placita and very close to the river (Vickery, 1984).

From the time of the original La Placita settlement to now, much has changed in the surrounding area as industrial complexes and residential homes were built. With the exception of Pellissier Ranch, the area has been heavily urbanized in the last half-century. In order to better imagine the SAR's flow in a major flooding event, a birds eye view, with all the buildings stripped away, was needed.

1.5 Elevation Analysis

Digital elevation model (DEM) data from the United States Geological Survey (USGS) was collected for Pellissier Ranch and used in ArcMap 10.5 to perform an elevation analysis. A more comprehensive analysis of available DEM data is included in Appendix A of this thesis. Two important observations may be made based on this analysis. The contour dataset we derived from digital elevation rasters (Figure 12) allows us to imagine the flood plain. It is clear from the datasets that without the levies erected on the SAR's border, Pellissier Ranch is highly vulnerable to spillover. In the center of the map, the river's flow is confined by topographic highs (Mount Slover, which reached a much higher elevation before cement mining began in the mid-1900s, to the north and La Loma Hills to the south), where maximum width is limited to 550 meters. A river that was flowing at 9,000 m^3/s could easily have exceeded the confines of this 550-meter passage and witness accounts do confirm this, claiming that billows 50 feet high came raging out of the narrow corridor (Sidler, 1968).

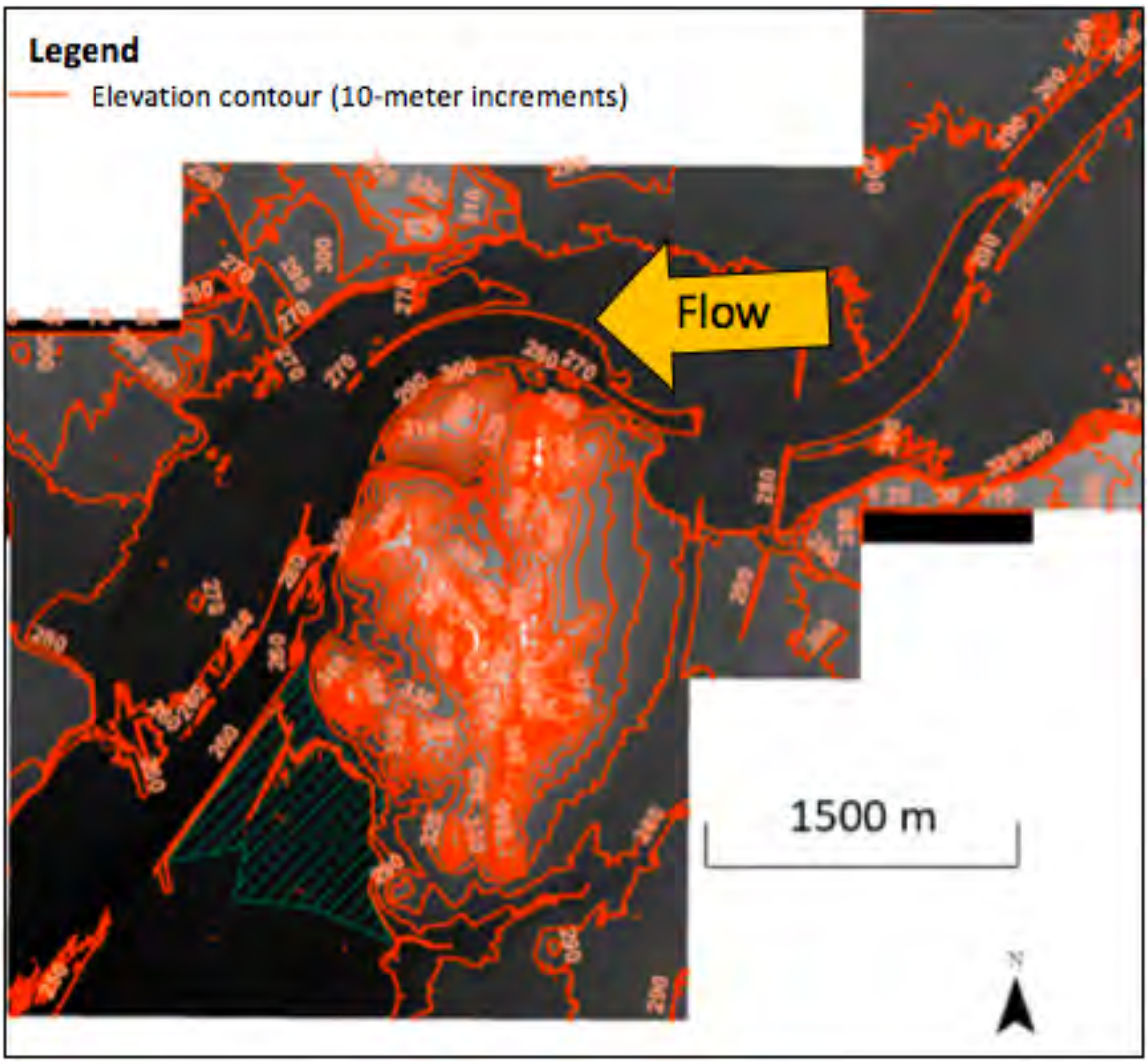

Figure 12: Contour raster derived from elevation raster with an interval of 10 meters. Vast spillover area is observed in the northeast portion of the map, leading the river into a narrow channel confined by two topographic highs, before it reaches Agua Mansa and La Placita. Hashed, aqua colored area denotes Pellissier Ranch (ArcMap, 2018).

The second observation from derived DEM datasets was that Pellissier Ranch is flat, with the average slope across the site less than 1° with the exception of a few very small, isolated areas where there is a slope of up to 5° (Figure 13). This gives confidence that topography corrections for GPR profiles will not be necessary.

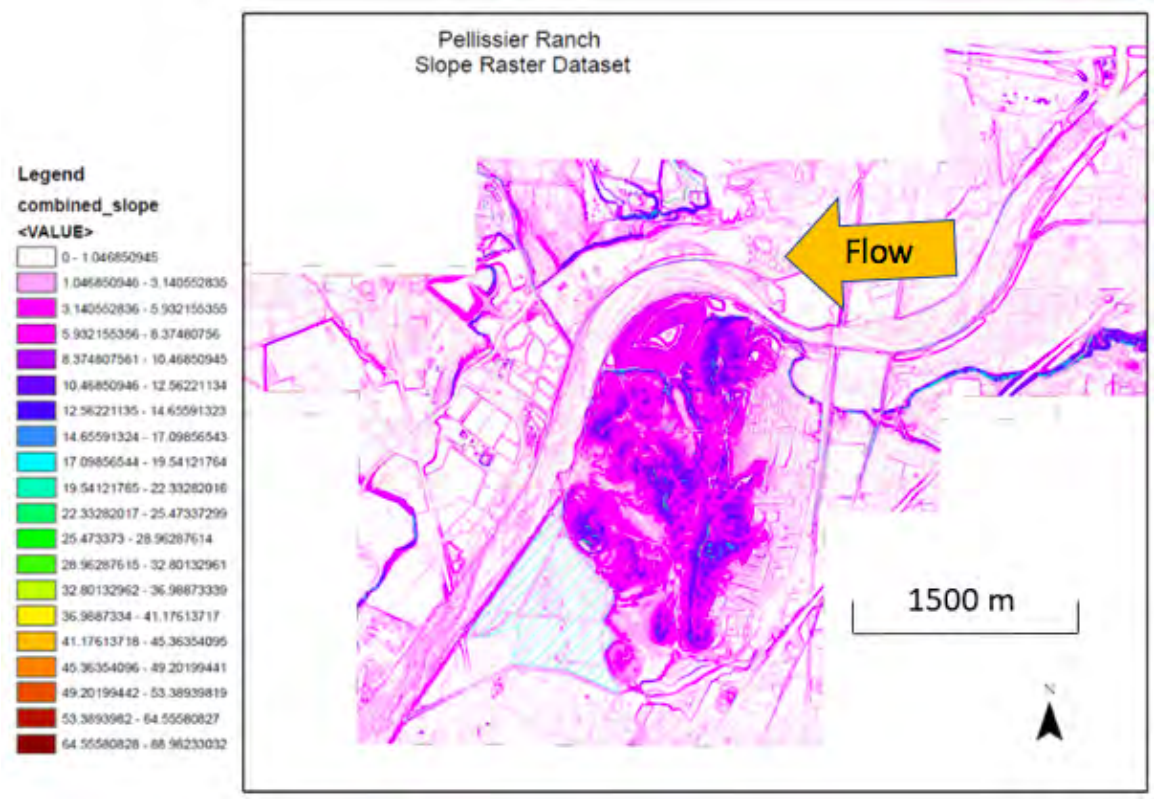

Figure 13: Slope raster derived from elevation raster showing 20 different classes of slope values. Pellissier Ranch slopes are mostly in the 0-1° range. Hashed, aqua colored area denotes Pellissier Ranch (ArcMap, 2018).

With a better understanding of how the SAR would have inundated the original La Placita settlement, we began to investigate what other purposes this land might have served. Best case scenario for our study, would be if the land was untouched. That would indicate that every major anomaly found in the subsurface within the depth range of La Placita (3 - 5 meters), would have a high probability of being related to the settlement.

1.6 Land Use

Most of the land usage from the time of the flood to present is unclear. Immediately afterwards, the settlers had tried to revive the once fertile farmland that had made La Placita prosperous (Vickery, 1984). However, the layer of sandy deposits that covered the original land made it too difficult to farm and they abandoned it. For decades, this portion of the

Bandini claim remained untouched until a Frenchman, Antoine Pellissier, purchased it. From 1903 to 1917 he operated the land as a vineyard and dairy farm, eventually ceasing operation due to low profits (Peninou, 2004). The land was then abandoned and from that time until recently, it is not well documented what use the land served. A few compost piles (that we avoided in our surveys) occupy the site, but currently, the land remains abandoned.

There are three observation wells for groundwater monitoring on Pellissier Ranch, several tall concrete structures, and a few mostly non-intact stone structures constructed about 100 years ago during the land's brief dairy farm days. The groundwater wells reveal the water table to be at about 6 meters depth. Dirt bike and dune-buggy riders frequent the dirt roads of the ranch and account for much of the modern debris that litters the site. This could make interpretation of results more complicated, and it will be necessary to weigh results from some methods heavier than those that rely solely on magnetic properties (ex. magnetic gradiometer). Future plans for this land are to develop it for warehouses, which leads to our motivation for this study.

1.7 Motivation

A major motivation for this study is to aid the Spanish Town Heritage Foundation in assessing whether remains from La Placita exist in the subsurface of Pellissier Ranch. Any artifacts and structural remains that lie in the subsurface could be a source of inspiration for the community. Given the current plans to develop the site for warehouses, a geophysical investigation is timely as a historical imperative.

Studies have been conducted by Dr. Michael J. Eula from the University of California, Irvine to determine the importance of a community knowing its history. Through years of research, he found that the past offers significant comfort to people as "when one is faced with challenges in one's own time, there is a measure of solace in realizing that people who came before us faced equally daunting problems in a myriad of ways" (Eula, 1993). The benefits seen are most noticeable in young people. Through his observation of teaching

young people history, many are disengaged when discussing global or national history. However, the same disengaged students become excited when learning about their own neighborhoods (Eula, 1993).

An in-depth demographic analysis was completed for Colton, CA in 2016 (DataUSA, 2017). It determined that Colton has a young, primarily Hispanic or Latino population, with a higher percentage of non-citizens than the national average. Their economic status overall is lower than the national average. Preserving Pellissier Ranch and the history that lies beneath its surface would have many benefits to this community. La Placita was made up of immigrants who came from nothing in Abiquiu, New Mexico. The group was comprised of Mexicans and former genizaros (term for Native Americans who had been made slaves, most notably their leader, Lorenzo Trujillo). Many current residents have past ties to settlers from La Placita, such as Nancy Melendez and Darlene Elliot who run the Spanish Town Heritage Foundation and are descendants of Trujillo.

Evidence of geophysical anomalies that can be determined to be probable La Placita artifacts / features may influence the city's decision on what to develop at Pellissier Ranch. Instead of warehouses being erected, a historic park could be established. The community retaining a connection with its roots would be invaluable for Colton's self-image, and a vital source of inspiration for young people to turn to in difficult times. Knowing that those who first inhabited this land were hardy settlers who prospered because they worked together, even in the most difficult times of losing their homes, food, and belongings in the winter season, would be instrumental. The STHF has noted that during their annual tamale festival, most attendees tell them they had no idea of the rich history associated with the city. It would be unfortunate to permanently lose the potential to preserve land that could offer inspiration to the community.

2 Methods

To investigate the potential presence of artifacts in the subsurface, GPR and a magnetic gradiometer were employed. Of the two techniques, we expect GPR to be the most successful for several reasons. First, modern metal left by site visitors at and near the surface could cause many false positives in our data. Second, previous research has found that buried, non-metallic archaeological remains is optimally imaged by the gradiometer if buried at depths less than 2 meters, with a maximum depth of 3 meters (Clark, 1996). The STHF estimates the depth of burial to be 3 - 5 meters. Therefore, we focus more heavily on using the GPR, with the gradiometer as a complementary technique to attempt confirmation of GPR results. A major advantage of GPR in archaeological surveys is that it is one of the few methods that provides depth information. Electromagnetic induction was considered for this study, but was ruled out as a suitable method as artifacts are deeper than the current Cal Poly Pomona Geological Sciences Department-owned EM-Profiler can image, and the results would be greatly affected by surface metal.

Buried artifacts, features, and structures that potentially remain from San Salvador include metallic and wooden artifacts, compacted flooring, 'adobe melt', and buried canals. The structures themselves were composed of adobe, which is primarily a sun-dried mixture of mud, straw, a little sand, and water. Towards the later years of the settlement, the people of La Placita had begun melting down the limestone mined at nearby Mount Slover using simple kilns to create a whitewash that protected local homes from the elements (Landis, 2017). This white, outer layer is seen clearly in Figure 7. As the primarily mud homes, coated in limestone, were buried under a greater than 2-meter layer of sand, we expect the GPR to image this contrast in material properties. Household and farming items that San Salvador settlers owned were wooden and metallic, with physical properties that will contrast with the local earth material. However, the general rule of thumb for identifying artifacts with geophysical methods is that they can only be imaged if they are buried no

deeper than they are large (Ernenwein et al., 2007). Many artifacts were small household items such as food containers, cookware, and farming equipment, which would have been less than a meter in size. However, larger scale objects such as plows and benches would represent suitable targets.

2.1 Ground Penetrating Radar

In this study, a GSSI Utility Scan Pro GPR was used with two different antennas that operated with two different control units. An SIR 4000 control unit with a 350 MHz Hyper-Stacking antenna, and an SIR 3000 control unit with a 400 MHz antenna were employed. Our GPR set up in the field is shown in Figure 14.

(a) Chloe Sutkowski with GPR.

(b) Example of real-time data as seen by operator during this study.

Figure 14: Both images feature the SIR-4000 and 350 MHz HyperStacking antenna at Pellissier Ranch on 11/10/19.

2.1.1 Key Concepts of GPR

GPR data is acquired through the use of electromagnetic (EM) radar waves. Pulses of the waves at a pre-set frequency are emitted into the ground via a transmitter coil. As they travel downwards, they may encounter buried objects, features, or geological bedding contacts. When a contrast in conductivity, permittivity, or dielectric properties (due to e.g. compaction, water content, soil type, metallic artifact) is encountered, a portion of the wave's energy is reflected back to the surface, where the receiver coil records the amplitude of the return (in millivolts), along with the time it took to receive the return. If the contrast is large, the wave's reflection will be strong. When analyzing GPR profiles, a strong reflection appears as either a bright white or dark black signal. If the materials do not differ greatly, the reflection will be less noticeable. The equation that represents the reflection strength is:

$$R = \frac{\sqrt{\epsilon_1} - \sqrt{\epsilon_2}}{\sqrt{\epsilon_1} + \sqrt{\epsilon_2}}$$

with "epsilon" representing the dielectric permittivity of the original ("1") and encountered ("2") material. If "1" and "2" differ greatly, the resulting reflection is stronger.

A hyperbolic reflection occurs when a wave hits a point-source reflector (i.e. chair), instead of a planar reflector (i.e. 'adobe melt'). This difference is shown in Figure 15. As waves are transmitted from the GPR antenna, they can hit artifacts obliquely. This allows the GPR to image an object even when it is not directly below the antenna. However, the time it will take for a wave to travel the oblique path to reach the reflector and return is longer. The return time of the point-source reflection will then vary as the GPR approaches the artifact, with the shortest return time (the apex of the hyperbola) marking its true location along the surface (Leckebusch, 2003).

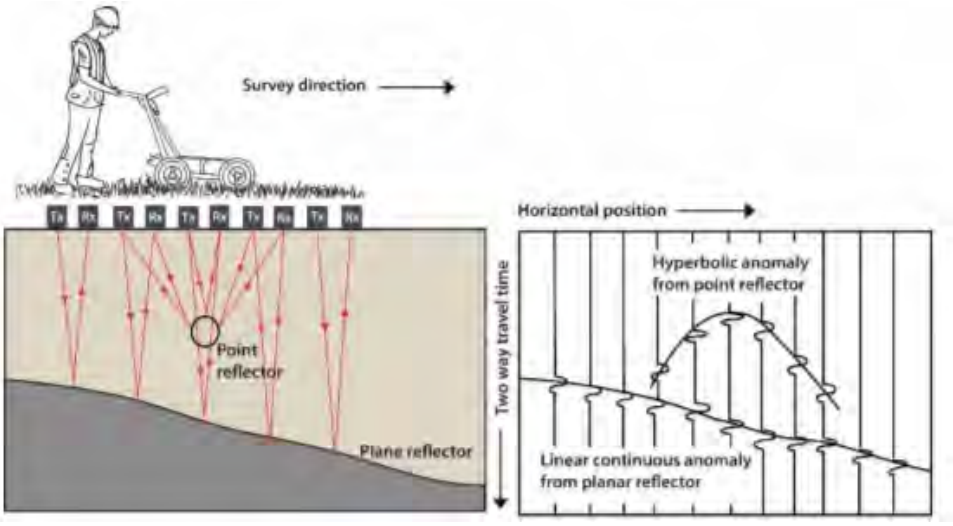

Figure 15: GPR data collection method. Figure from (Conyers, 2013).

A 2-dimensional profile of the subsurface is compiled from GPR traces, and most commonly shown in greyscale. A trace is the single waveform representation of all waves that were reflected back up to the receiver coil, at a surface location (Conyers, 2013). In a 40 meter transect, 1,500+ traces may be collected. Using computer software like Reflex2DQuick (Sandmeier, 2018), profiles can be created from the traces and analyzed for archaeological artifacts and features. The process of how a GPR profile is created from traces is shown in Figure 16.

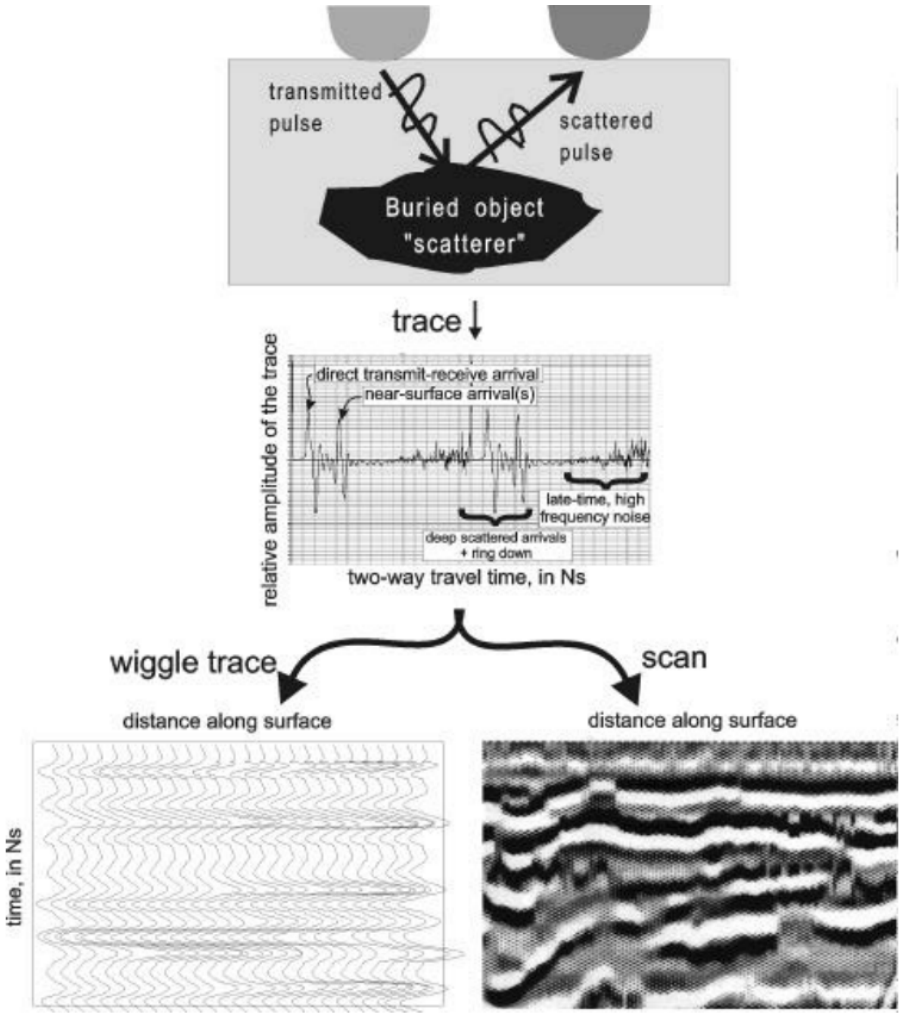

Figure 16: The process of creating a GPR profile of the subsurface. GPR emits an EM pulse into the subsurface. This pulse has a portion of its energy reflected up to the receiver each time it encounters a change in material properties, which is recorded as amplitude in the wave's "trace." All traces recorded along a GPR survey line are stacked alongside each other in space to construct a 2-dimensional (usually greyscale) profile of the subsurface. Image from (Daniels, 2000).

Snell's Law can predict the resulting angle of the wave's path through objects / materials / layers via the equation:

$$\frac{sin\theta_1}{sin\theta_2} = \frac{v_1}{v_2}$$

with "theta" representing the angle of the wave from vertical, "v" representing the velocity, "1" representing the original material, and "2" representing the encountered material. As the wave travels through the subsurface, it continues to lose energy until eventually,

full wave attenuation occurs. This is a limiting factor in GPR imaging depth, along with conductivity.

Electrical conductivity is present to at least a minimal degree in all media in the subsurface. This causes EM waves to become more dissipated as they travel downward until full attenuation of the wave occurs. Attenuation affects waves not only as they propagate down, but also when they are reflected back up. In highly conductive material like clay, EM waves will struggle to penetrate the subsurface and reach deeper layers or artifacts due to the wave's energy experiencing high attenuation. Another factor affecting EM wave propagation is the frequency of the emitted wave. Higher frequencies will be better equipped to image small and shallow objects at higher resolutions, while lower frequencies will be preferred for imaging deeper into the subsurface. This is due to the high frequency wave's shorter wavelength pulse when compared to a low frequency wave's longer wavelength pulse (Figure 17). Archaeological artifacts from San Salvador are not expected to be located at greater depth than 5 meters, making a higher frequency antenna desired in this study.

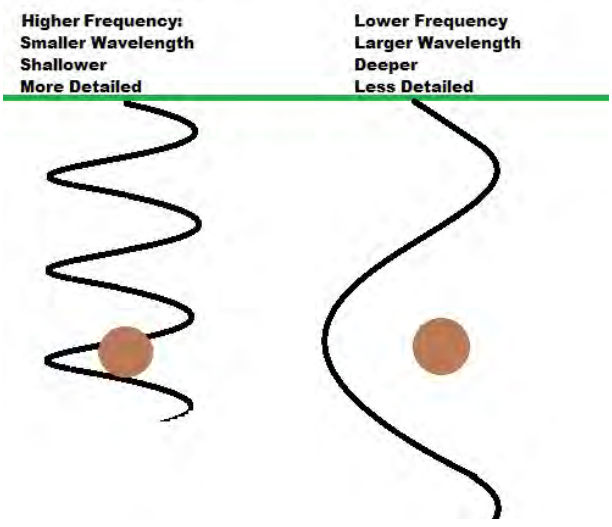

Figure 17: Comparison of the difference between a higher frequency antenna vs. lower frequency antenna, and why a higher frequency is better suited for archaeological surveys (Bevan, 2006).

The Cal Poly Pomona Geological Sciences Department owns two GPR antennas (400

MHz and 350 MHz). In the dry, sandy soil of Pelissier Ranch, GSSI rates their 400 MHz antenna successful at imaging down to a depth of 4.5 meters, and their 350 MHz Hyper-Stacking antenna to a depth of 6 meters. Both depths are sufficient for the purposes of this study, as our research determined that artifacts are likely to be buried at depths shallower than 5 meters.

To best model our study for success, we review in the section below previous research in the American Southwest that successfully located adobe remains.

2.1.2 Previous Site Successes

From historical archives of San Salvador, materials and artifacts expected in the subsurface of Pellissier Ranch include: iron cookware, metallic utensils, wooden ladders / chairs / tables / fences, kilns, farming equipment, and remains of adobe structures. Past research has proven that the size, shape, and location of buried artifacts can be approximated by use of GPR (Cezar et al., 2001), along with 'adobe melt' off adobe structures buried at southwestern sites (Conyers, 2012).

Cultural features from Marana Mound (A.D. 1150-1300) had been buried by 50-100 centimeters of fluvial and alluvial silts and sands from the Santa Cruz River that flowed alongside it. Floor features, walls, and irrigation canals were imaged with a GSSI SIR-3000 system using a 400 MHz antenna (Conyers, 2012). Figure 18 shows (a) a floor from this ancient settlement as a strong amplitude, horizontal reflector about 7 meters long in profile view and (b) the outline and bottom of a 2-meter-wide irrigation canal when crossed perpendicularly. Both showed as strong amplitude reflections due to the measurable difference in dielectric properties between the sandy flood deposits that buried the compacted, plastered floor and the material into which the irrigation canal had been dug (Conyers, 2012).

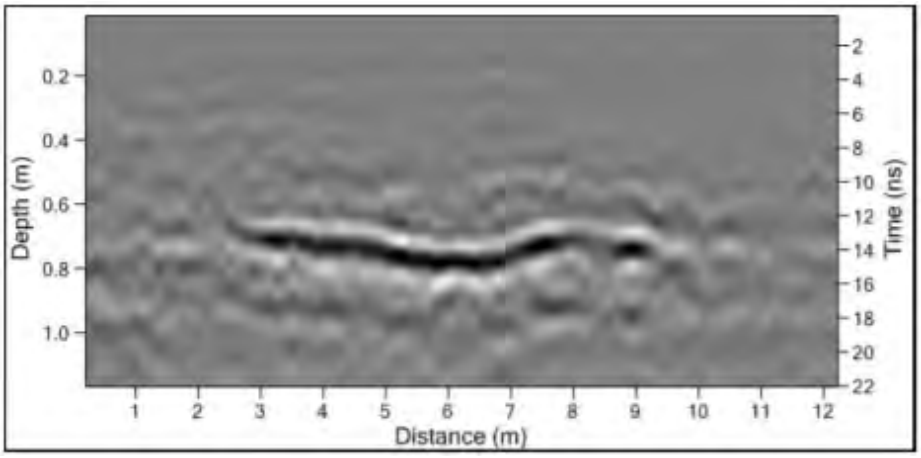

(a) A compacted, plastered floor buried beneath sandy flood deposits.

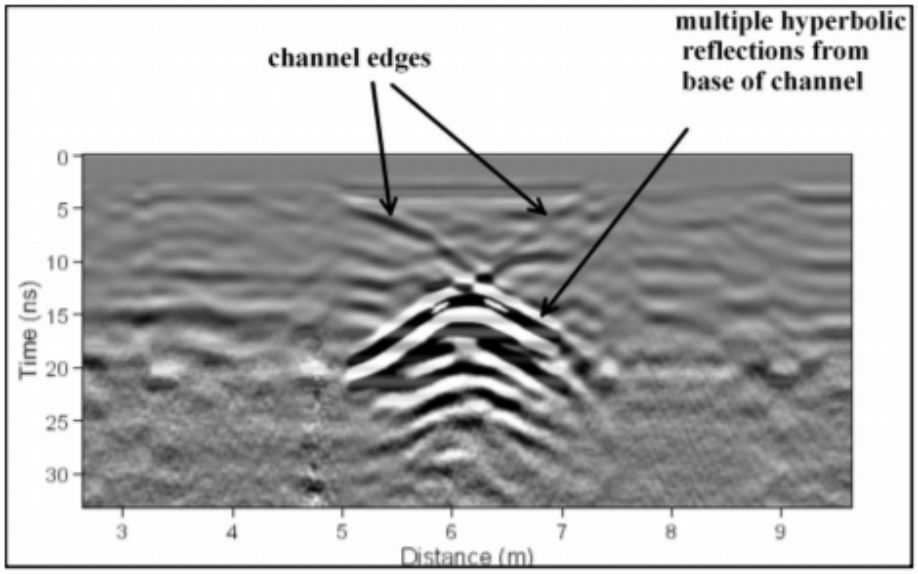

(b) An irrigation canal buried beneath sandy river deposits.

Figure 18: GPR profiles collected with a 400 MHz antenna of cultural features buried by about a meter of fluvial deposits at Marana Mound (Conyers, 2012).

Another example from the same site is shown in Figure 19. In this case, an abandoned adobe structure had been disintegrated over time by rainfall. The material of which the adobe walls were composed were redeposited on the ground surface adjacent to the walls and appear as high-amplitude, horizontal reflections on what had been the living surface (Conyers, 2014).

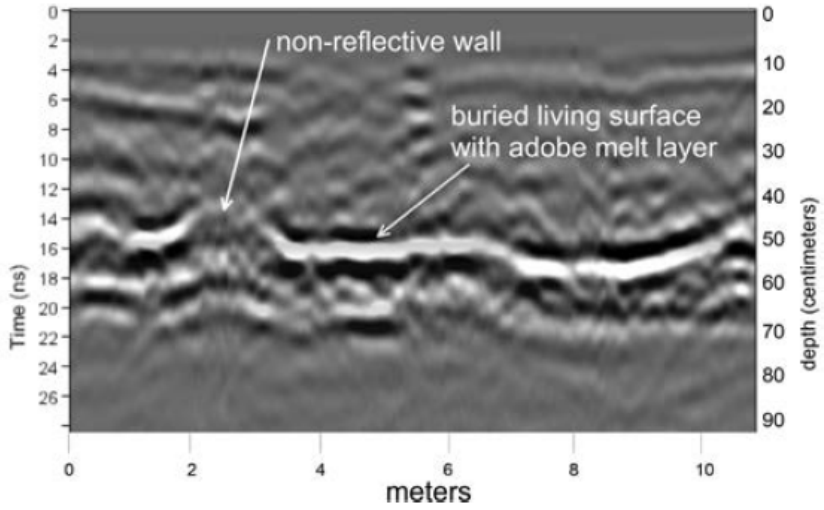

Figure 19: A GPR profile collected with a 400 MHz antenna at Marana Mound of 'adobe melt' buried beneath sandy deposits. The structure had been abandoned and the adobe wall disintegrated by rainfall. The material redeposited adjacent to the wall as a distinct, horizontal layer atop the previous living surface (Conyers, 2012).

At University Indian Ruin to the east of Tuscon, another survey had been completed to attempt mapping adobe structures buried by aeolian deposits, differing from the fluvial deposits that buried Marana Mound. In this circumstance, it is observed that the adobe wall remains non-reflective as with the buried Marana Mound adobe walls, but instead of a long, single layer deposit of 'adobe melt', there are several layers of short 'adobe melt' segments adjacent to the wall's location (Figure 20). This likely due to the fact that the fluvial or rainfall process would redeposit the adobe quicker and closer to the wall. In an aeolian environment, it would take a longer amount of time to disintegrate the wall and may carry the material further from the wall and not have as strong a reflection as seen in the fluvial environment.

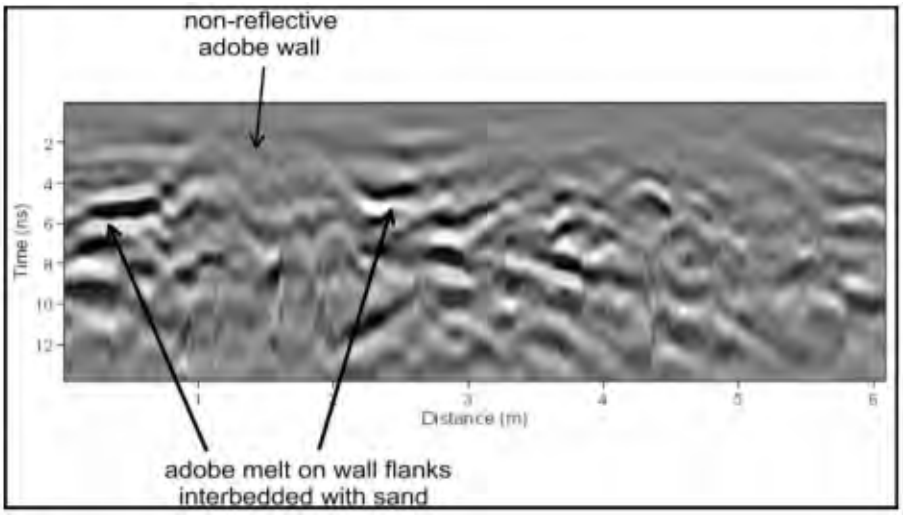

Figure 20: A GPR profile collected with a 400 MHz antenna at University Indian Ruin of 'adobe melt' buried in an aeolian environment by sand. The structure had been abandoned. the adobe wall disintegrated by wind and the material redeposited adjacent to the wall as short, high amplitude layers (Conyers, 2012).

GPR has seen success in both fluvial and aeolian burials. The adobe structures of San Salvador are anticipated to have been melted down during the Great Flood of 1862 (Beattie, 1939) and redeposited as a layer separate from the flood deposits. Historical documents have described that several irrigation canals, homes, farms, a school, and a church made up the original La Placita settlement pre-flood. We anticipate imaging the 'adobe melt' remains of these structures, similar to those imaged in Figures 18 and 19, and potentially some household and/or farming objects, with responses similar to those produced by 0.5-meter urns imaged in Brazil (Cezar et al., 2001) (Figure 21).

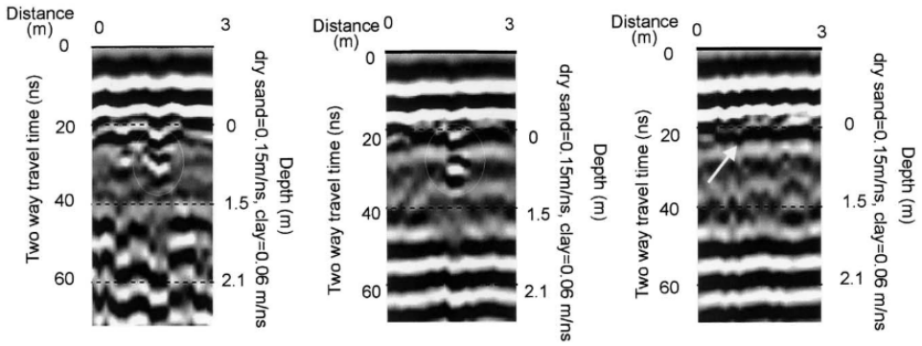

(a) GPR profile showing anomaly buried in the top meter.

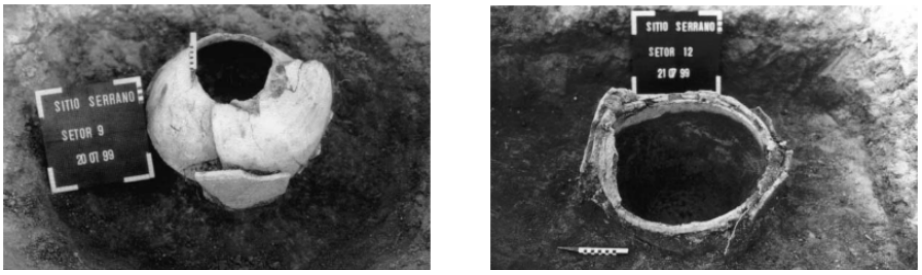

(b) Urns located after excavating at anomalies seen in GPR profiles.

Figure 21: GPR profiles over anomalies in Brazil that were found to be buried urns through excavation. Profiles and figures from Cezar et al. (2001).

To improve confidence in data we collected at Pellissier Ranch, it was advantageous to anticipate potential problems. This aids in survey design and processing collected data. In the below section we briefly review any potential issues or anticipate any data corrections that must be applied.

2.1.3 Anticipating Pellissier Ranch GPR Data

During the Great Flood of 1862, adobe homes were melted away and their contents chaotically buried. Because of this, artifacts are likely to be piled on top of each other in many locations. In trying to locate artifacts buried beneath others, the interpreter of results should account for ”ring-down”. ”Ring-down” occurs when the EM wave encounters an impermeable object in the subsurface (e.g. metallic artifact). This causes issues when trying to image artifacts buried beneath others. A controlled GPR experiment in a sandbox consisted of one concrete (fairly impermeable) block buried beneath another. When tra-

versed with GPR, the ”ring-down” from the first block made the lower buried block invisible to the survey (Leckebusch et al., 2001) (Figure 22). This makes the vertical resolution of the GPR important for data anticipation. In common practice, vertical resolution is about 1/4 of the radar signal wavelength in the subsurface (Bristow, 2009). To first calculate the wavelength of the signal, we use the equation:

$$\lambda = \frac{V}{f}$$

with ”lambda” representing the wavelength, ”V” representing the velocity of the signal, and ”f” representing the frequency of the signal. Since the frequency of our signal is 400 MHz, and the velocity of the signal is anticipated to be approximately 0.14 m/ns (dry sand velocity given in (Leckebusch, 2003), we can determine the wavelength to be 0.35 m. This gives a vertical resolution of 0.09 m (i.e. to be identified, targets must be buried at a vertical separation of 0.09 m from one another).

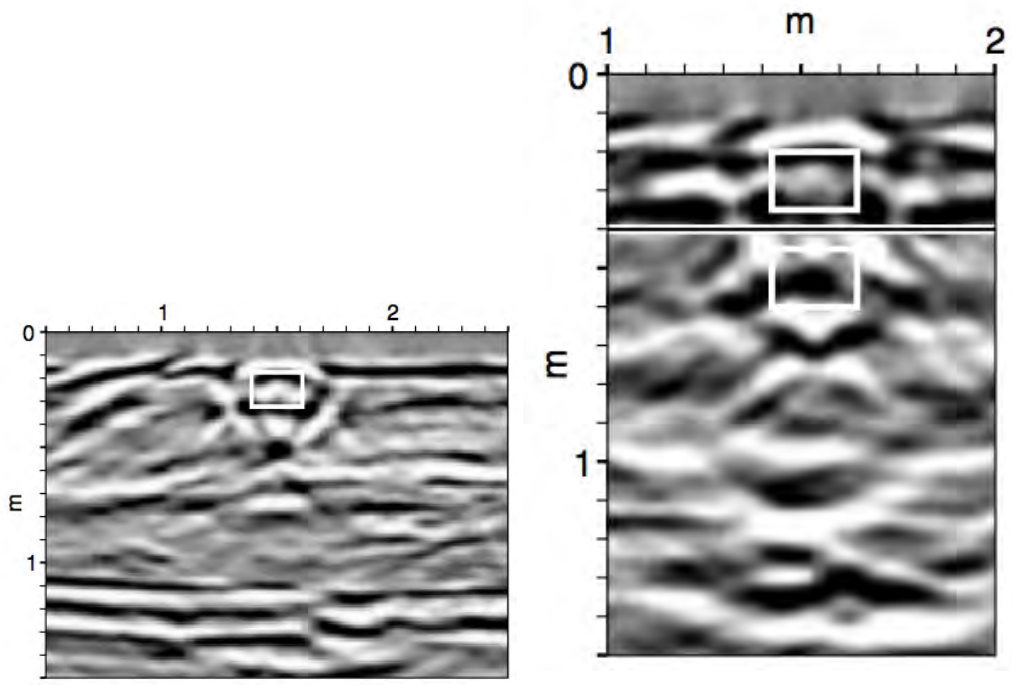

(a) GPR profile over single buried block of dimensions 0.77 m x 0.22 m x 0.15 m.

(b) GPR profile over two buried blocks of dimensions 0.77 m x 0.22 m x 0.15 m, with the second block buried 0.10 m below the first block.

Figure 22: GPR profiles across concrete blocks to show method's ability to image objects buried beneath other objects. The white squares show the actual locations of the buried blocks. Profiles from (Leckebusch, 2001).

Possible noise sources include a radio tower in the western portion of the site, along with power lines that border the northwestern edge of the site (Figure 5), which could cause reflections in GPR profiles that are not related to artifacts in the subsurface (Conyers, 2014). To mitigate their effect, we keep a minimum of 200 meters from these noise sources and use a background removal filter when processing GPR data. The lack of trees, buildings, and other modern development to the site will make additional data processing simpler, as we will not have to account for much other potential noise or false positives in GPR data.

To our good fortune, Pellissier Ranch is on flat land (as evidenced in Section 1.5). This makes it a safe assumption that antenna tilt will not be a factor in our survey and all anomalies can be simply located without any modification of results necessary (Conyers, 2014).

Raw GPR data collected includes the strength of the reflected waves as a function of the waves' two-way travel time. When the velocity of the subsurface material is known, the two-way travel time can be converted to depth. The next section discusses how we determine the material's velocity, so we can calculate depths of reflectors.

2.1.4 Depth Calibrations

In archaeological surveys, depth calibrations are desired as they can tell the artifact's location for excavation purposes. There are a few ways to determine the velocity of the subsurface. The first is traversing the GPR over a known object / interface at a known depth. The depth is then divided by the time it took to travel to the object / interface (the two-way travel time divided by 2). This gives the velocity of the subsurface, which is input into the below equation to determine anomaly depths:

$$d = \frac{vt}{2}$$

with "d" representing depth, "v" representing velocity, and "t" representing time. If burying an object is not feasible, another method is "hyperbola-fitting." This method utilizes GPR data processing software to calculate the velocity based on the dimension of point-source hyperbolas (Cassidy, 2009). It involves applying a variety of different velocities to the data until the shape of the computer-generated hyperbola matches the shape of the hyperbola in the GPR profile. "Hyperbola-fitting" using Reflex2DQuick software will be the method we perform in this study.

2.1.5 Summary of GPR

With knowledge of previous projects that successfully located 'adobe melt' and 0.5-meter urns, and after reviewing aspects of our site that could skew results so we can best avoid false-positives, as well as methods to calibrate depth information from two-way travel time, we were confident GPR would be a valuable method in our study. Dense surveys with

traverses averaging less than 1 meter apart in promising sections will be performed across the site.

2.2 Magnetic Gradiometry

A GEM GSM-19T Proton Precession Magnetic Gradiometer was used in this study with a resolution of 0.01 nT (nanoTeslas) and a sampling frequency of one reading every two seconds. In the case of our set up, two sensors set 0.5 meters apart are carried on a backpack with an attached GPS and computer unit (Figure 23).

Figure 23: Chloe Sutkowski operating a GSM-19T Proton Precession Magnetic Gradiometer at Pellissier Ranch on 7/5/18.

2.2.1 Key Concepts of Magnetic Gradiometry

Magnetic gradiometry is a passive geophysical technique. A magnetometer measures the total intensity of the magnetic field by utilizing the precession of spinning protons of hydrogen atoms in a hydrocarbon fluid (Smekalova, Voss, & Smekalov, 2008). This is done via a coil of wire that generates its own magnetic field to polarize the spinning protons that behave as magnetic dipoles. When the field is removed, it causes the spinning protons that had been polarized to precess around the direction of the Earth's magnetic field (Smekalova et al., 2008). This process generates a small signal in the coil that was used to polarize the

precessing protons at a frequency that is precisely proportional to the total field intensity (Smekalova et al., 2008).

In the case of a gradiometer, there are two fluid-filled sensors at a set distance from each other. The sensor on the bottom will always be closer to the ground, and therefore, more sensitive to archaeological features than the top sensor. Top sensors are further away and suffer a greater drop-off in magnetic field strength, which can be calculated with the equation that defines the proportional relationship between magnetic strength and distance:

$$Strength \propto \frac{1}{d^3}$$

with "Strength" representing the magnetic field strength and "d" representing the total distance from the sensor to the anomaly. This process is illustrated in Figure 24.

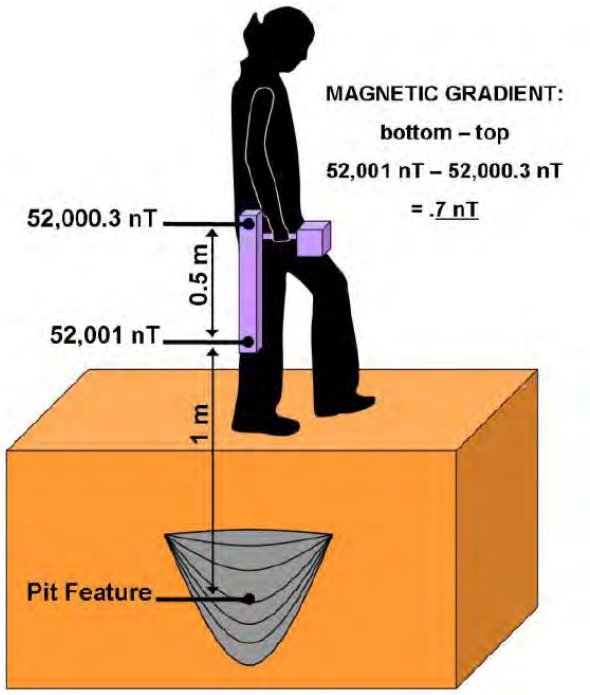

Figure 24: The distance between the two sensors causes the different strengths each sensor measures of the same anomaly. This difference is used to derive the magnetic gradient in nT/m by dividing by the distance between the two sensors. Figure from (Ernewein, 2007).

Our gradiometer also contains a GPS sensor that records the coordinates of each mea-

surement, allowing for easy generation of 2-dimensional maps of magnetic gradient in nanoTeslas per meter (nT/m). In the case of archaeological geophysics, differences between ancient structures / features and the soil surrounding them is usually minor, but detectable if buried within the top 2 meters. Anything deeper than 2 meters is unlikely to be detected due to the weakly magnetic material expected from adobe settlements, paired with the magnetic field strength drop-off with depth (Ernenwein & Hargrave, 2007). Figure 25 illustrates different archaeological objects / features a gradiometer can detect if buried sufficiently shallow.

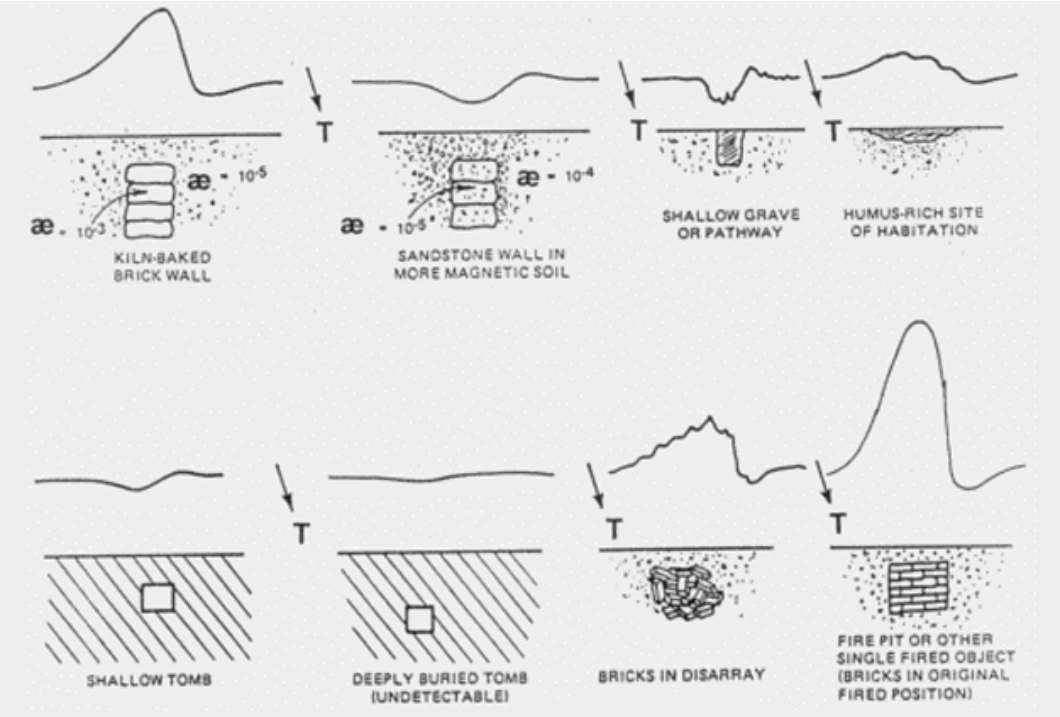

Figure 25: Examples of magnetometer results when traversing over various archaeological artifacts buried in the soil. Figure from (Smekalova, 2008).

The gradiometer was chosen over the magnetometer as it is more adept at locating archaeological artifacts due to its better spatial resolution (Smekalova et al., 2008; Mekkawi et al., 2013; Colombero et al., 2019). Another benefit is that we are able to combine multiple days of gradient data, and do not have to worry about diurnal variation. This is because regardless of how the total magnetic field strength will vary from one day to

another, the difference between magnetic properties of the object / feature and the local soil will not change. It would be imperative to use a base station in archaeological surveys if just measuring the total field intensity as diurnal variation is usually far more substantial than the total field intensity change caused by archaeological features (Clark, 1996).

Magnetic surveys in archaeology are successful even when metal is absent due to iron naturally being present in approximately 6% of the Earth's crust, dispersed through soils, clay and rocks as chemical compounds which are magnetically weak (Smekalova et al., 2008). The intensity of the magnetic field in a weakly magnetic medium that contains iron is enhanced when the medium is burned at high temperatures over an extended period. This process is significant to our survey as we expect buried kilns to be present in the subsurface (as mentioned in Section 1.4). Kilns with strong thermoremanent magnetization can possess a magnetic field up to one-hundredth the strength of the Earth's, making magnetic prospecting effective for detecting buried human occupations (Clark, 1986).

In the next section, we describe previous archaeological surveys that successfully used a gradiometer to locate buried structures / features.

2.2.2 Previous Archaeological Gradiometry Successes

The first magnetic survey for archaeological prospecting was completed in 1958 (Aitken, 1958). Over the years, it has grown to become one of the top methods for detecting and mapping large archaeological sites (Clark, 1996), (David, Linford, & Linford, 2008). A magnetic survey in 1986 over a henge monument found that magnetic highs recorded during traverses matched up with locations of concentrated burnt flint that were later carefully excavated (Clark, 1986). More recent surveys include locating ancient Roman walls buried 0.2 meters below the surface in Italy (Colombero, Elia, Meirano, & Sambuelli, 2019) and ancient Egyptian structures buried at 3 meters (Mekkawi, Arafa-Hamed, & Abdellatif, 2013). In both cases, the structures were only identifiable after filtering of the data to leave only relatively-low values of magnetic gradient in maps of anomalies (Figure 26 and 27).

In the search for buried Roman walls, the wall could not be identified in a map of unfiltered magnetic gradient data. After the range was narrowed to show only lower values (typically from 30 nT/m to -30 nT/m), portions of the wall became visible. Diffuse magnetic noise was present in this smaller value range, likely caused by Fe-rich minerals containing a low-intensity magnetization. Aside from this noise, geometric patterns that match with excavated data can be seen in the maps of magnetic gradient.

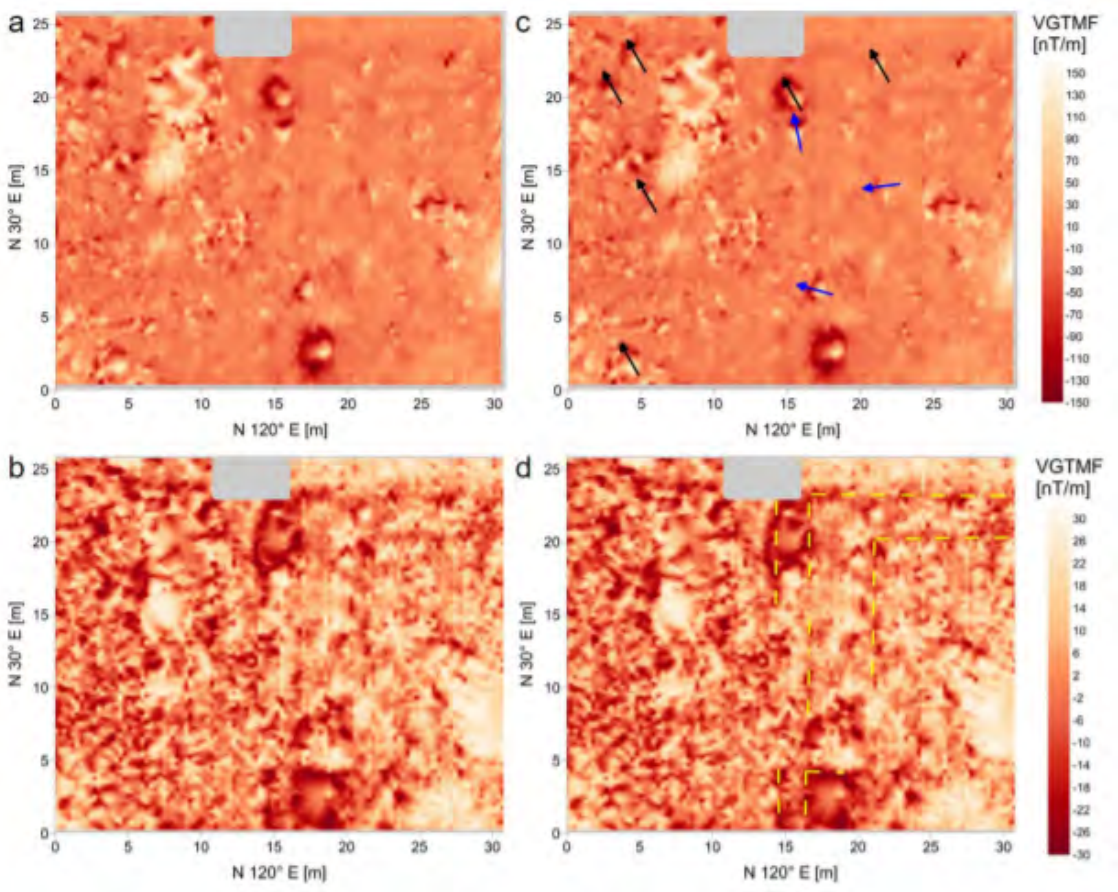

Figure 26: Magnetic gradient data from a Roman site in search of buried structure. All figures show the same location. a) (uninterpreted) and c) (interpreted magnetic field direction with blue arrows) are the unconstrained values from 150 nT/m to -150 nT/m, while b) (uninterpreted) and d) (interpreted buried wall with yellow dashes) were constrained from 30 nT/m to -30 nT/m. Data range of 150 nT/m to -150 nT/m was unsuccessful at delineating buried Roman wall. Data range of 30 nT/m to -30 nT/m was able to identify the remains of the ancient wall. Mapped values from (Colombero et al., 2019).

In the search for buried Egyptian structures composed of mud, even smaller ranges

of magnetic gradient were necessary to successfully identify remains (Figure 27). As the study searched for structures made of mud (as La Placita homes were) and buried in a sandy environment (similar to the environment of Pellissier Ranch), we were most interested in noting how they filtered data to maximize noise elimination and enhance the signature of the structures. Also of interest was that the magnetometer, when measuring only the total field intensity, was not able to locate any structures / features (Mekkawi et al., 2013). It was only when analyzing the magnetic gradient that structures / features became visible (Figure 28).

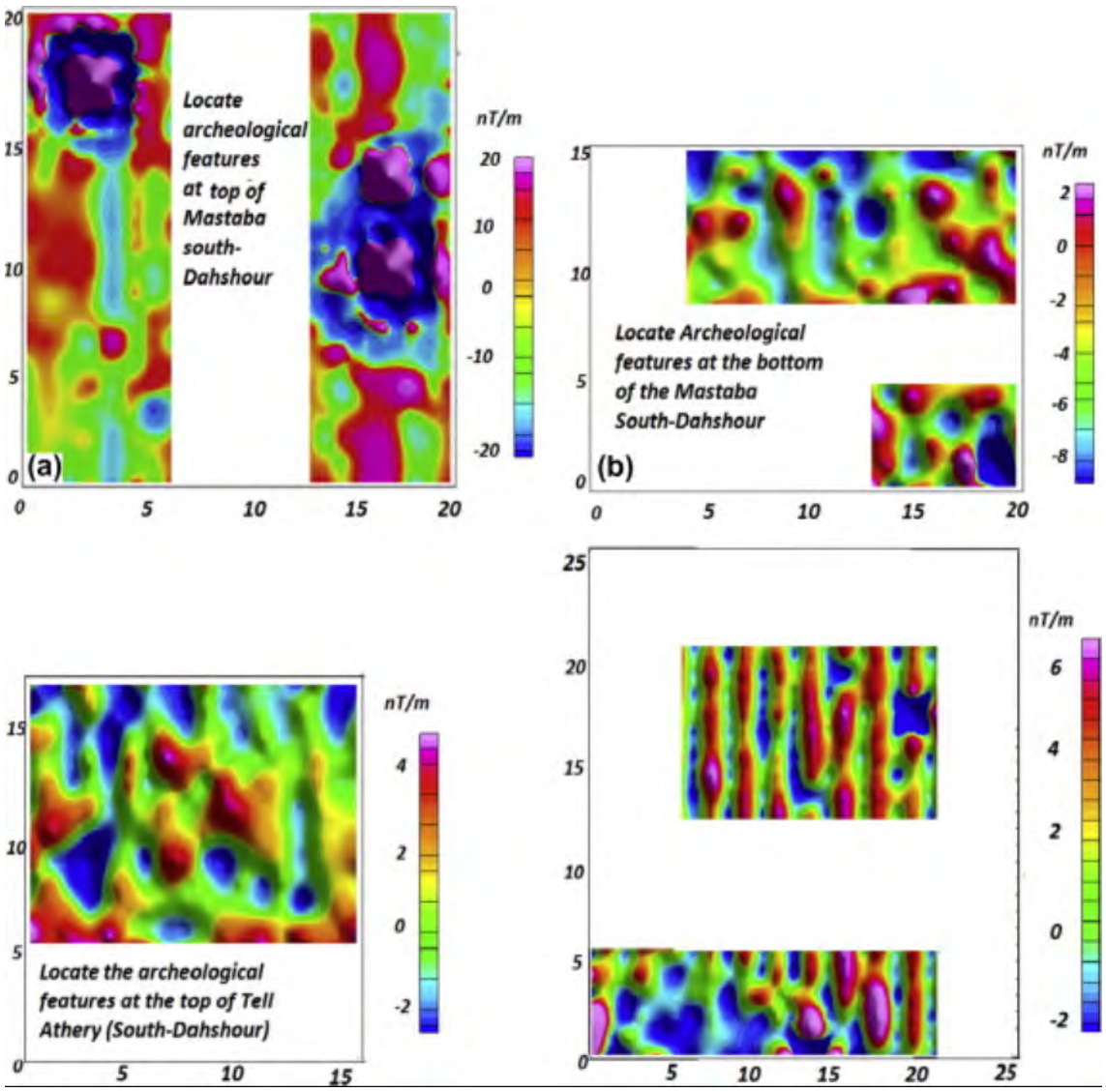

Figure 27: Data filtered to show ranges no larger than from 20 nT/m to -20 nT/m were successful at locating buried, Egyptian archaeological structures composed of mud buried 3 meters below the surface. Figure from Mekkawi et al. (2013).

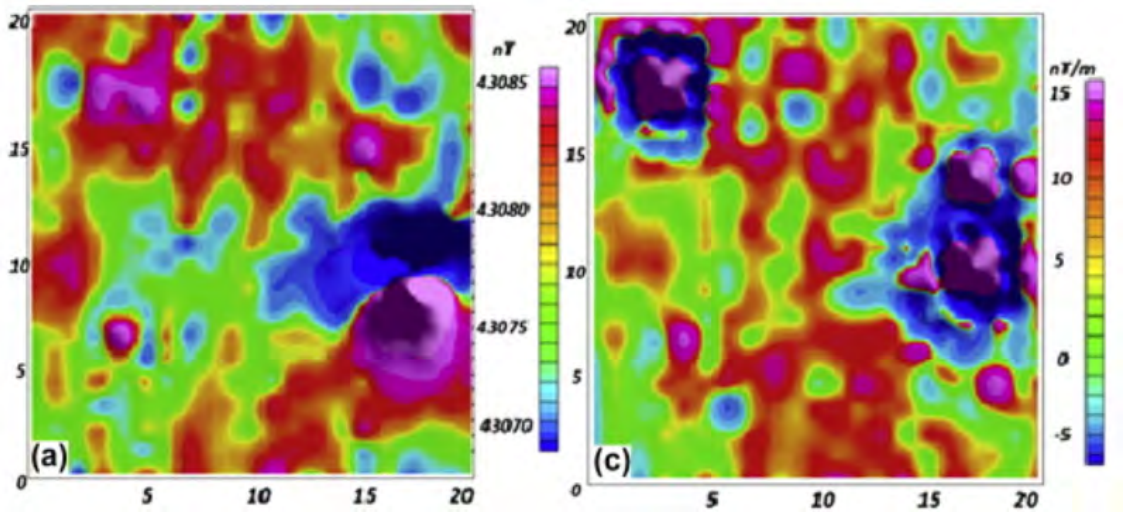

Figure 28: Maps of total field intensity did not indicate location of structures / features. Constraining the gradiometer range of values from 15 nT/m to -5 nT/m successfully detected mud walls within a tomb buried 3 meters beneath the surface in Egypt. Distances marked in increments of 5 on the x- and y-axes are in meters. Figure from Mekkawi et al. (2013).

2.2.3 Summary of Magnetic Gradiometer Technique

(Mekkawi et al., 2013) and (Colombero et al., 2019) proved that when using appropriate processing techniques, magnetic gradiometry is a feasible approach to use in archaeological surveys such as ours. The issue of modern metal at and near the surface would appear in data as spikes in values. Removing spikes will reduce this effect, and since we are interested in smaller value ranges (ex. 20 nT/m to -20 nT/m), does not overall hinder our ability to detect structures. As mentioned at the beginning of this chapter, magnetic gradiometry will serve as a complementary technique to the GPR. We utilize it in this study to test the technique's limits. As it will not be reliable enough to use independently, we will use the gradiometer only at locations we already have GPR data. Matching anomalies seen by the gradiometer with GRP anomalies seen at depth, will give confirmation. Dense traverses of a less than 1-meter spacing will ensure sufficient coverage over any archaeological structures / artifacts.

3 Results and Discussion

In total, we completed 11 field surveys at Pellissier Ranch. The first was completed 4/28/2018 and the last was completed 1/12/2020. Each field experiment took 3 - 5 hours, adding up to an estimated 45 hours in the field. Winter, spring, and fall temperatures were moderate; between 70 and 80 F. Summer temperatures were high, so data was collected only between the hours of 6 am and 11 am for field volunteer safety and to ensure equipment did not overheat.

Exact dates in the field were: 4/28/2020, 6/22/2020, 6/26/2020, 7/18/2020, 8/5/2020, 8/25/2020, 10/27/2019, 11/9/2019, 11/10/2019, 11/26/2019, 1/12/2020.

3.1 Ground-Penetrating Radar

In this study, over 7,000 meters of GPR data was acquired using two different antennas (350 MHz HyperStacking and 400 MHz) and GSSI control units (SIR-4000 and SIR-3000). All profiles collected are shown in Figure 29.

Figure 29: Overview of all GPR lines collected at Pellissier Ranch represented by blue lines (Google Earth Pro, 2018).

3.1.1 GPR Collection Parameters and Data Processing Software

After careful consideration of the parameters used in previous studies that successfully located archaeological features of the same general type, we set up our GPR equipment using similar parameters as in Agrawal et al., 2018; Conyers et al., 1998; Lowe et al., 2014 listed in the below table:

Parameter	Value	Value
Antenna (Hz)	400	350
Samples/Scan	512	512
Scans/Meter	50	50
Bits/Scan	16	16
Range (ns)	130	130
Dielectric Constant	4	4
Low Pass Filter	100	100
High Pass Filter	800	800

All data was processed using Reflex2DQuick. Tall grasses and sandy terrain that contained deep tire marks (from tractors that mowed the site once a year to reduce fire hazard) caused difficulty with coupling to the ground. This made a gain increase of 5 (+/- 2) across all profiles necessary to enhance the visibility of reflections at depth. Other filters applied to all profiles were: static correction to first arrival, background removal to remove any horizontal banding noise (e.g. from the operator of the GPR), and ”dewow” to remove the low frequency ”wow” of data (i.e. drift from the mean). A DC-shift, needed to adjust the signal so that the mean is zero, is applied automatically during data collection by the control units.

Profiles generated by Reflex2DQuick have very small labels that are difficult to read. The x-axis for all GPR profiles is ”distance” (in units of meters), and the y-axis is ”two-way travel time” (in nanoseconds). Both axis increments on profiles are by 10s. Profiles were colored in greyscale, with white and black showing the highest amplitude reflectors in each profile relative to surrounding material (grey).

To better examine the details of anomalies, the two-way travel time of profiles on the y-axis were trimmed (most to 67 ns, with the deepest to 100 ns), eliminating the noise at greater travel times. Figure 30 shows an example of the full, 180 ns, of collected data along a profile that is analyzed again in Figure 41 post-trim. Making out details of the imaged anomalies is easier after the two-way travel time is constrained.

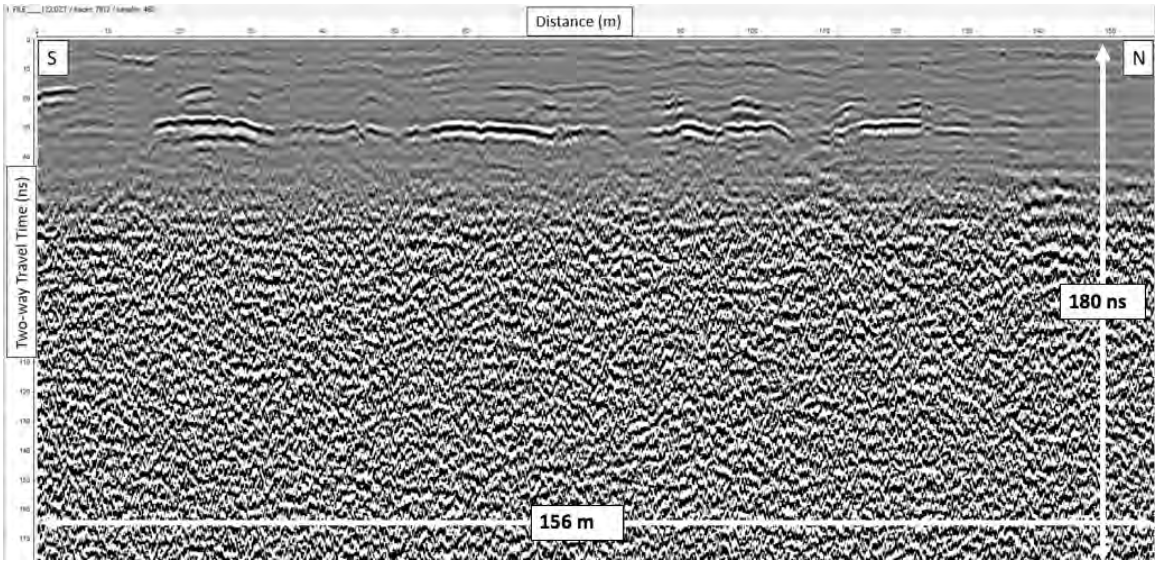

Figure 30: Untrimmed, 180 ns profile containing a large amount of noise at greater depths (due to wave attenuation). Trimming the profile makes details of shallowly buried anomalies clearer. Figure 41 contains this profile (c) after it was trimmed to 67 ns.

As mentioned in Section 2.1.4, we used a hyperbola-fitting technique to determine the average velocity of the EM wave in the subsurface. Reflex2DQuick allowed us to simply input potential velocities until a best fit was found (Figure 31). The best-fitting average wave velocity was 0.14 m/ns for most profiles, with the exception of profiles collected one week after rain (1/12/2020 profiles). Hyperbola-fitting in the 1/12/2020 profiles yielded a lower velocity of 0.11 m/ns, which is explained by the additional water in the subsurface effectively slowing the wave. We use these two values to perform depth calibrations of anomalies in GPR profiles.

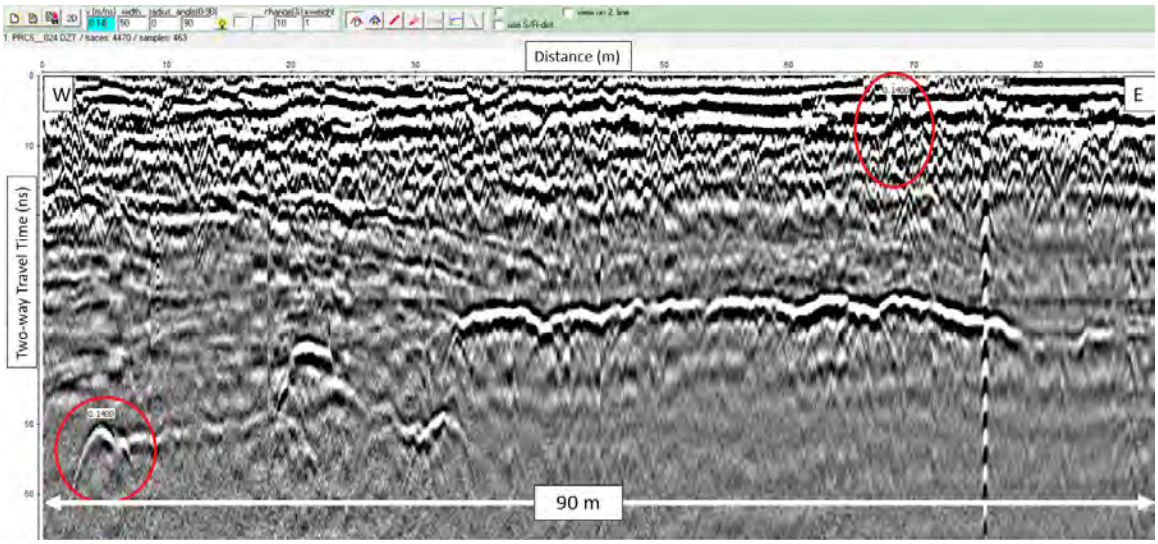

(a) Hyperbolas both shallow and deeper (circled in red to better see) are matched with subsurface velocity of 0.14 m/ns. Additional coverage of this anomaly in Figure 44.

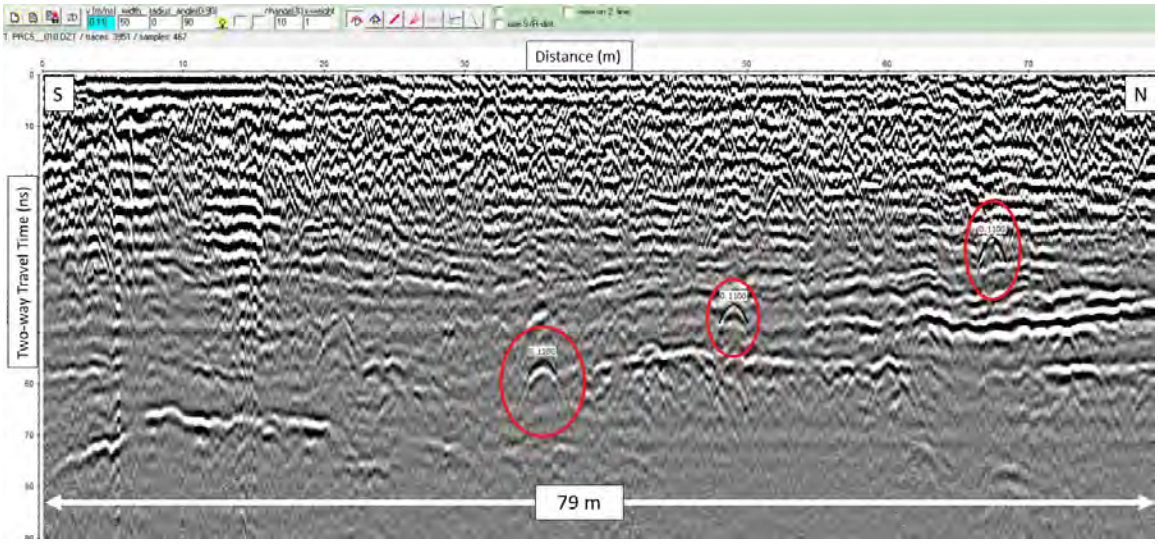

(b) Acquired 1 week after rains. Hyperbolas, both shallow and deeper (circled in red to better see), are matched with a subsurface velocity of 0.11 m/ns. Additional coverage of this anomaly in Figure 43.

Figure 31: Hyperbola-fitting was performed on these profiles using Reflex2DQuick. The program's text containing the velocity value is very small; the value is typed in the caption below each image.

In all profiles, with the exception of 1/12/2020 profiles, two-way travel times of significant reflections did not exceed 60 ns. Rain one week prior to 1/12/2020 profiles accounts for the longer travel times; we undertook the post-rain survey to test how successful the GPR was in wet subsurface conditions (see Figure 32 for an example profile) and to ex-

amine whether the wet conditions would result in larger GPR anomalies due to enhanced contrasts in the subsurface.

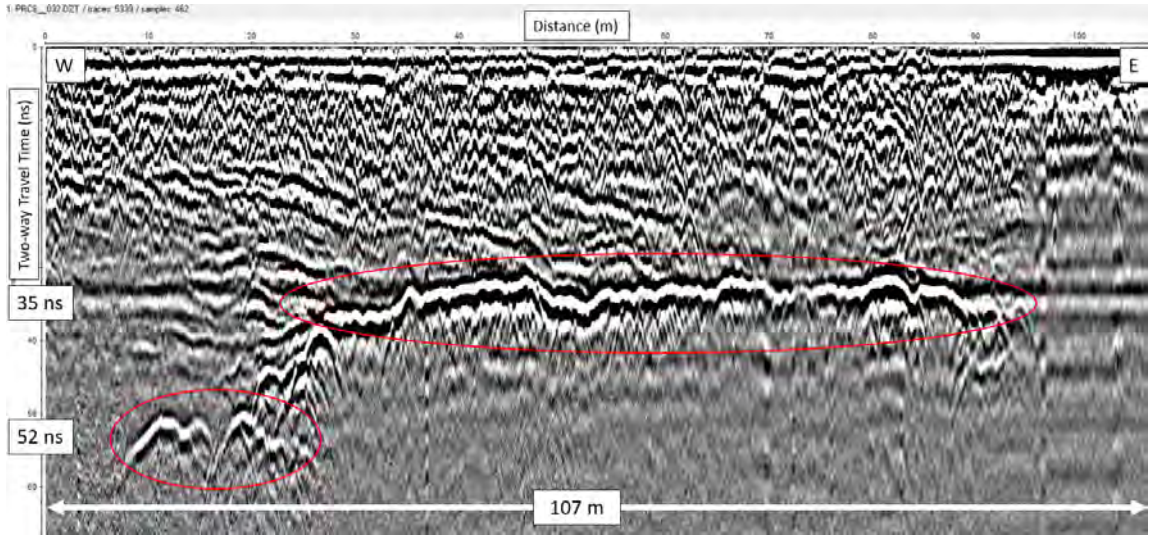

(a) 11/26/2019 profile of anomaly.

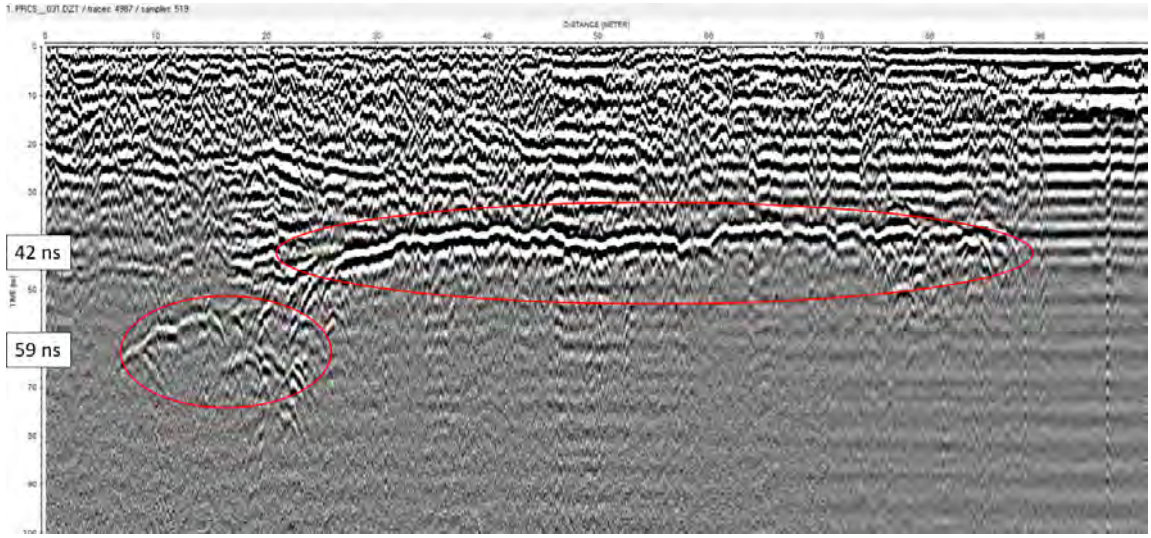

(b) 1/12/2020 profile of anomaly taken 1 week after rain.

Figure 32: GPR data acquired with SIR-4000 and 350 MHz HyperStacking antenna. Profile (b) was taken within 0.5 meters (with the desert grasses and soft sand, it was impossible to traverse over the exact same location) of profile (a) in attempt to confirm that the GPR can successfully locate the anomaly through a wet subsurface. The post-rain travel time (b) is longer than the dry travel time (a) by about 7 ns. Accounting for the difference in subsurface velocity between the two as given by the hyperbola-fitting method (demonstrated in Figure 31 with (a) at velocity of 0.14 m/ns and (b) at 0.11 m/ns), the upper layer of the anomaly is located at a calculated depth of 2.4 meters +/- 0.05 meters in both. A longer time axis (y-axis) was given on (b) to account for the slower subsurface velocity and thus greater two-way travel time due to water saturation. The size and characteristics of the anomaly are defined almost exactly the same in dry and wet conditions. Interestingly, the ”ring-down” effect of a metal pipe at the very eastern edge of the profile is much more pronounced across most of the profile (b).

3.2 GPR Data Analysis

In this analysis section, we first show a representative profile for a GPR section that contains no major anomalies along its entire 172-meter length (Figure 33). All profiles void of any significant anomalies that could potentially be related to La Placita were mapped in Figure 34.

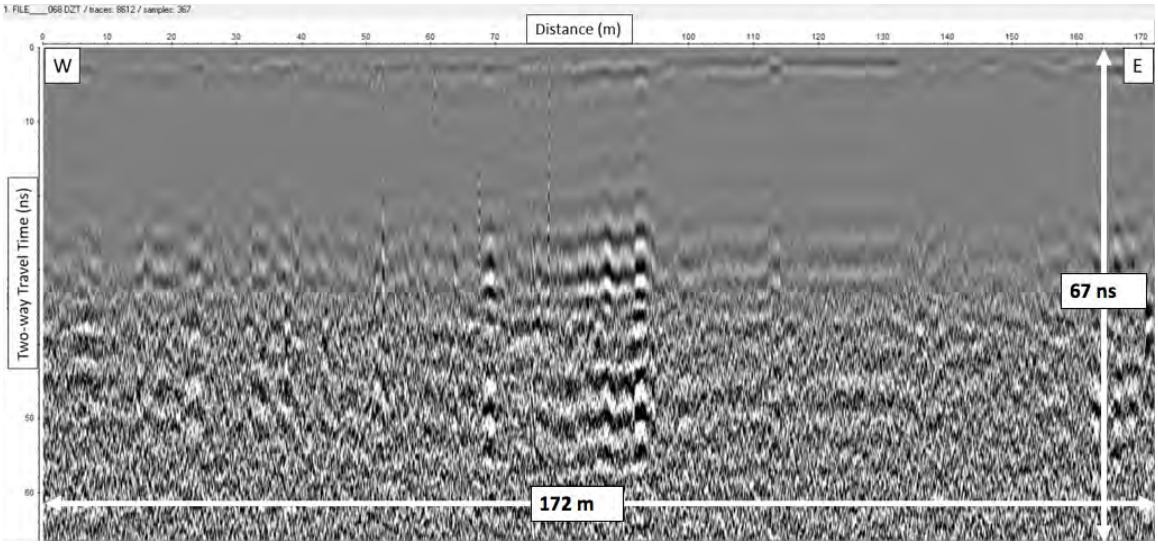

Figure 33: GPR profile taken 4/28/2018. This is a typical example of a profile that we consider to contain no significant anomalies.

Figure 34: Map of all GPR profile locations (circled in red) that we considered void of any significant anomalies potentially related to La Placita.

Our next step was to attempt to image a feature we expected in the subsurface. Being as Pellissier Ranch is adjacent to the SAR, and was historically prone to flooding, floodplain features should be present in the subsurface. In the literature we found profiles from a floodplain in Germany and we will compare them to what we saw in profiles closest to the SAR (Figure 35). Sloping layers of flood deposits in the floodplain indicate washover deposits, with chaotic hyperbolas representing lag deposits (i.e. boulders and cobbles) that a waning river's strength could no longer carry.

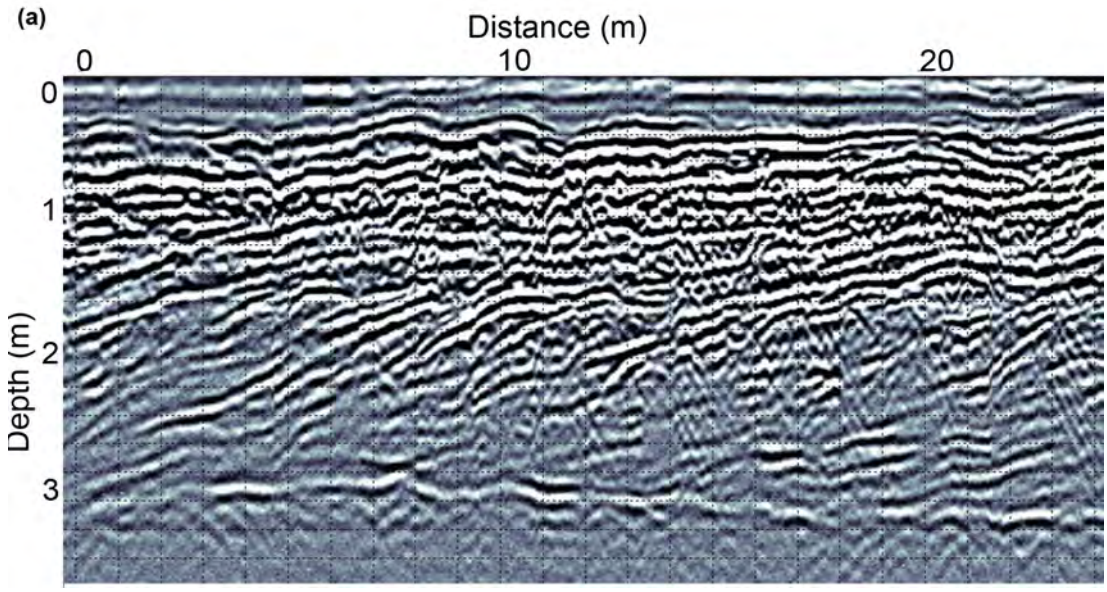

(a) Characteristic profile of washover deposits in a floodplain. Chaotic hyperbolas present are likely lag deposits. Profile from (Jasper et al., 2018).

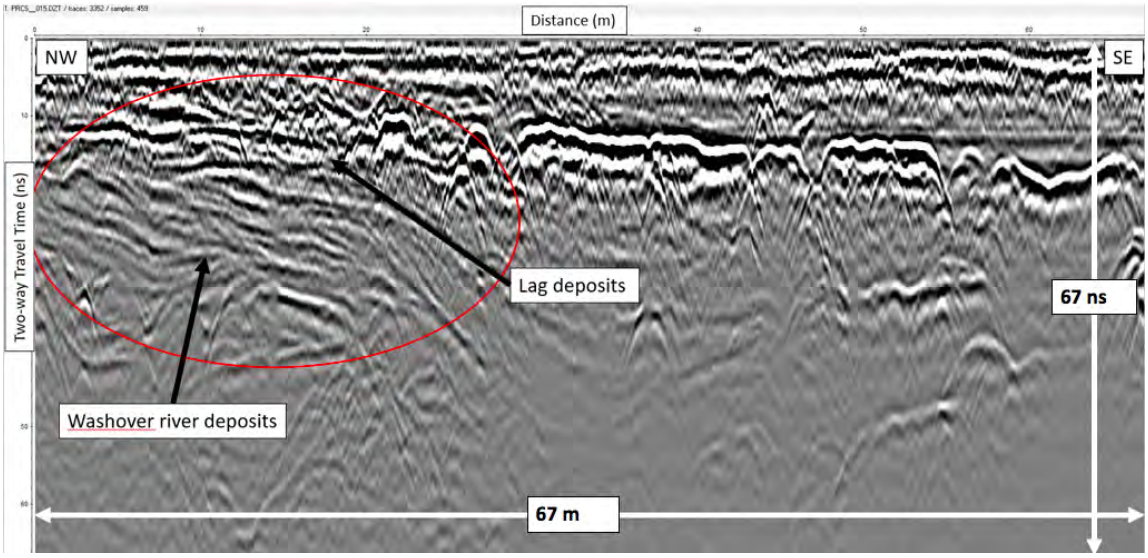

(b) GPR profile acquired on 11/9/2019 with SIR-4000 and 350 MHz antenna. Left-right is Northwest-Southeast. This profile was the closest taken to the SAR. Imaged on the northwestern side of the profile (circled in red) are sloping layers of washover flood deposits in the floodplain, with chaotic hyperbolas representing lag deposits.

Figure 35: Comparison of washover and lag deposits seen in Jasper et al. (2018) with washover and lag deposits seen in our profiles closest to the SAR.

Many profiles collected across the site contained anomalies. Profiles that we show in this section were limited to those that contained anomalies with strong reflections (i.e.

features / artifacts that contrasted greatly with the local soil) and buried within, or close to, the 3 - 5 meter depth range anticipated for La Placita. We located all analyzed anomalies on Google Earth Pro and label them by Figure number (Figure 36). We consider that the canal that we image in both Figure 38 and 39 connects and is one of the major irrigation canals from La Placita, used to bring water from the SAR to the farmland for crops and livestock.

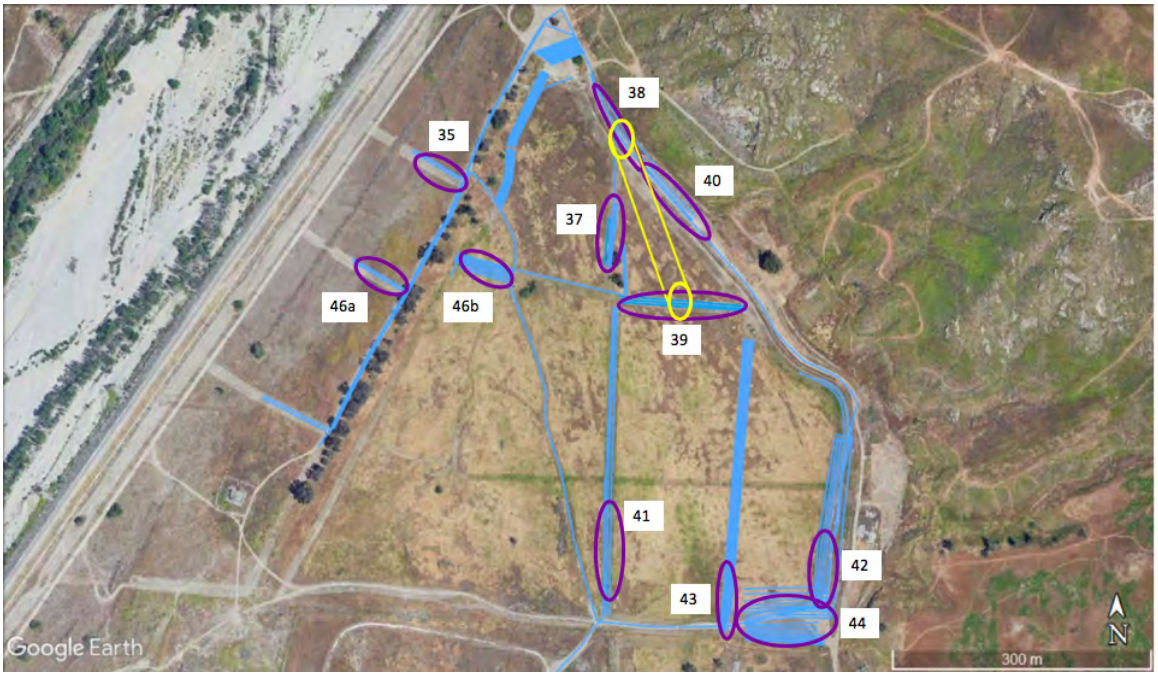

Figure 36: Locations of GPR profiles analyzed in this section are circled in purple and labeled by Figure number (Google Earth Pro, 2020).

The anomalies we deemed significant were based on their strong reflectors, size, burial depths, and characteristics. Several transects were taken adjacent to one another to determine if and how anomalies evolved over space. This practice helped differentiate whether or not an anomaly is a small buried feature / hole as opposed to a structure / irrigation canal or other large-scale subsurface structure. Major anomalies shown in this section we hypothesize to be: a canal, collapsed structure, two-layer structure, low-energy deposition of 'adobe melt', compacted floors and collapsed adobe walls, and a 3-meter, metallic artifact.

We image what we hypothesize to be a canal in two locations. Based on documentation

we had read of the site, we anticipate it to connect and be a major irrigation canal of Pellissier Ranch. In the northernmost location we image the canal, it's width is 13 meters (Figure 38). This is wider than we would expect of a canal, but we theorize that we hit the canal diagonally instead of perpendicular, making it appear wider than it is in profile-view. The 5-meter width we image in a profile further south, we consider to have hit perpendicularly and be of actual width (Figure 39).

Just 50 meters southeast of the 13-meter-wide canal feature, we image a large cluster of high-amplitude anomalous material (Figure 40). We hypothesize this to have been an area of lower-energy deposition of 'adobe melt' and artifacts due to the location of these profiles being at the base of La Loma Hills, which would have made the area less susceptible to the flood's full force. Another area of lower-energy deposition would have been in the eastermost profiles we collected at the site. We image a buried pile of very high contrast with the subsurface material (Figure 42). Many hyperbolas seem to be present as well.

Again in the northern portion of the site, we image what we hypothesize to be a 10-meter-wide, collapsed structure (Figure 37). We make this assertion based on the characteristics of how the anomaly evolves across traverses. In the profiles closest to the river, we see a pile. As profiles move 1-meter further from the river, the pile becomes progressively more intact as planar layers. It would make sense that the portion of the structure closest to the river absorbed the full force of the flood and then collapsed, acting then as a shield for the further away portion of the structure.

In another eastern section of the site, we imaged several compacted floors and most significantly, a very strong hyperbolic reflection at a depth of 3.2 meters (Figure 43). We hypothesize that this is metal due to the prominent hyperbola that the GPR recorded. Earthen-material would be a weaker hyperbola of not as clear and prominent geometry as the one we image.

In the furthest south and east profiles that we collected at Pellissier Ranch, we imaged a two-layer, large anomaly (Figure 44). The top portion is at a depth of 2.4 meters and starts

at 70-meters long in the profile. As profiles move south, the upper layer shrinks as the lower layer (depth of 3.5 meters) grows and then disperses so much that we see a weaker reflection and hyperbolas instead of a strong, continuous layer.

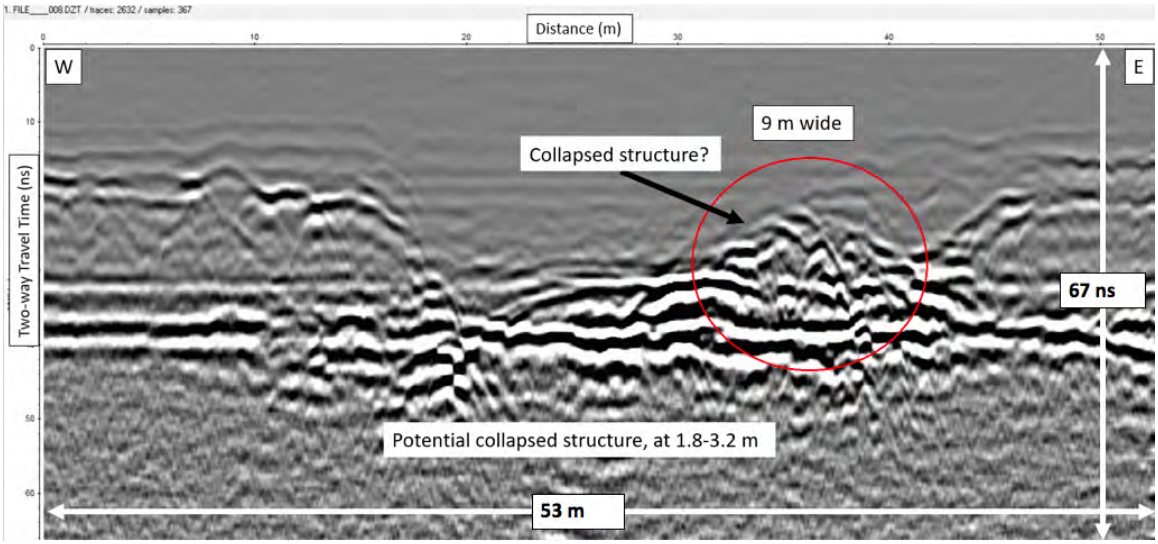

(a) Westmost traverse over anomaly (closest to SAR)

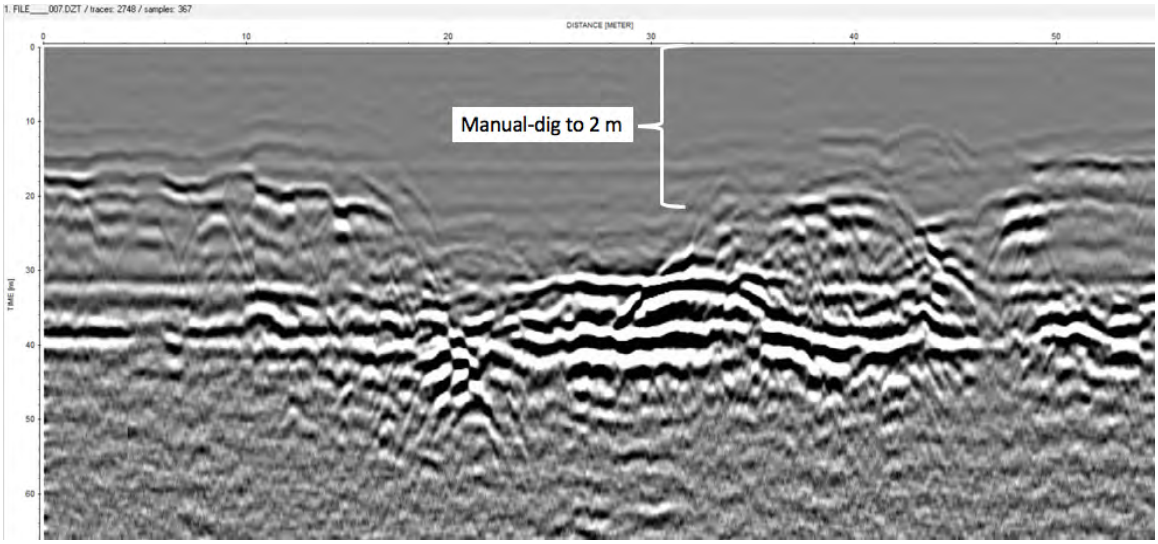

(b) Middle traverse over anomaly. Digging of hole over collapsed ”pile” by three people alternating turns. Depth of 2 meters was stopping point for the dig due to safety concerns and extreme difficulty. Based on depths calibrated using hyperbola-fitting, the anomaly barely escaped us at 2.1 meters.

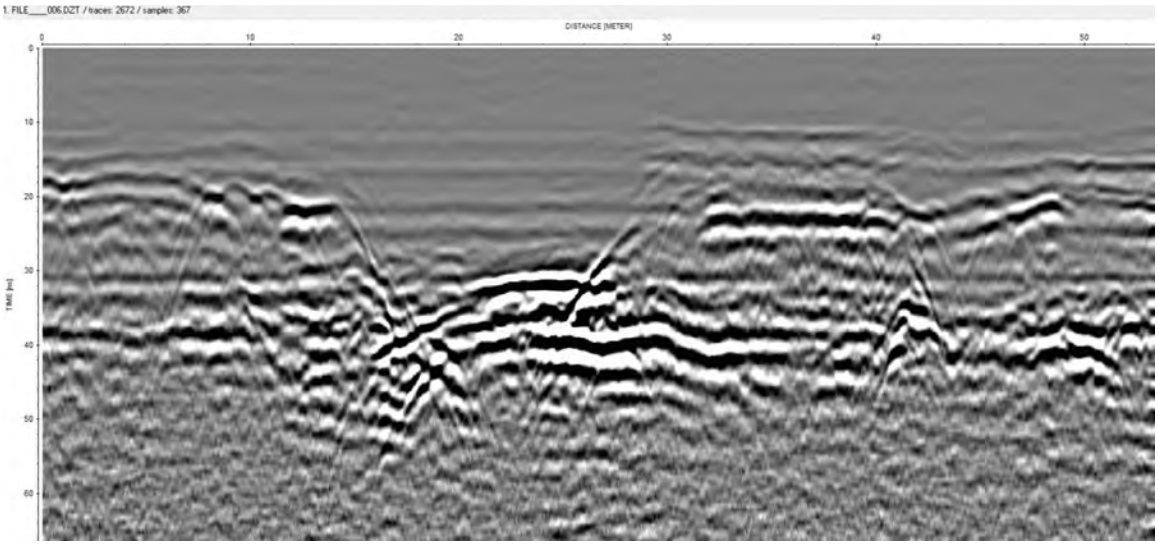

(c) Eastmost traverse over anomaly (furthest from SAR)

Figure 37: GPR data acquired on 8/25/2018 with SIR-3000 and 400 MHz antenna. High-amplitude, 9-m-wide ”pile” (circled in red) at depth of 1.8 - 3.2 m. ”Pile” become progressively more intact as each traverse moves 1 m eastward (further from the SAR).

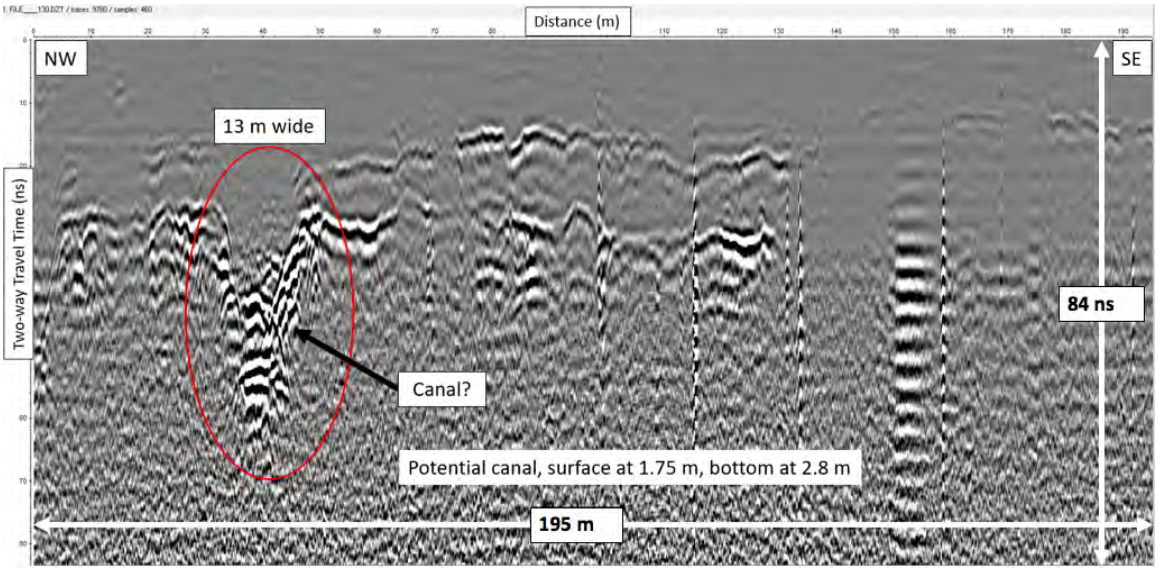

(a) Northmost traverse over anomaly.

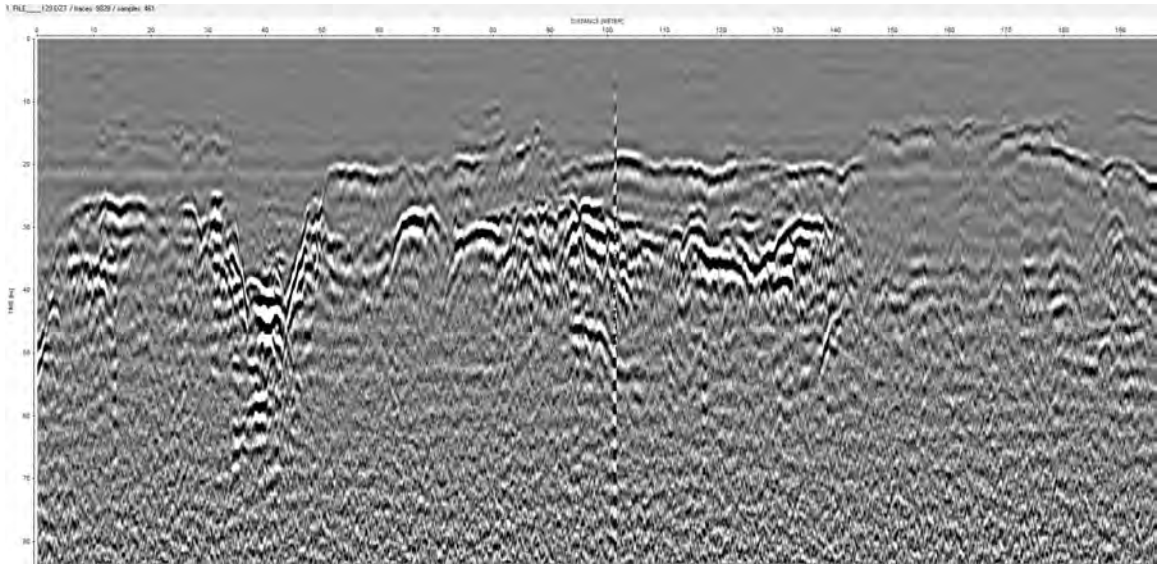

(b) Middle traverse over anomaly.

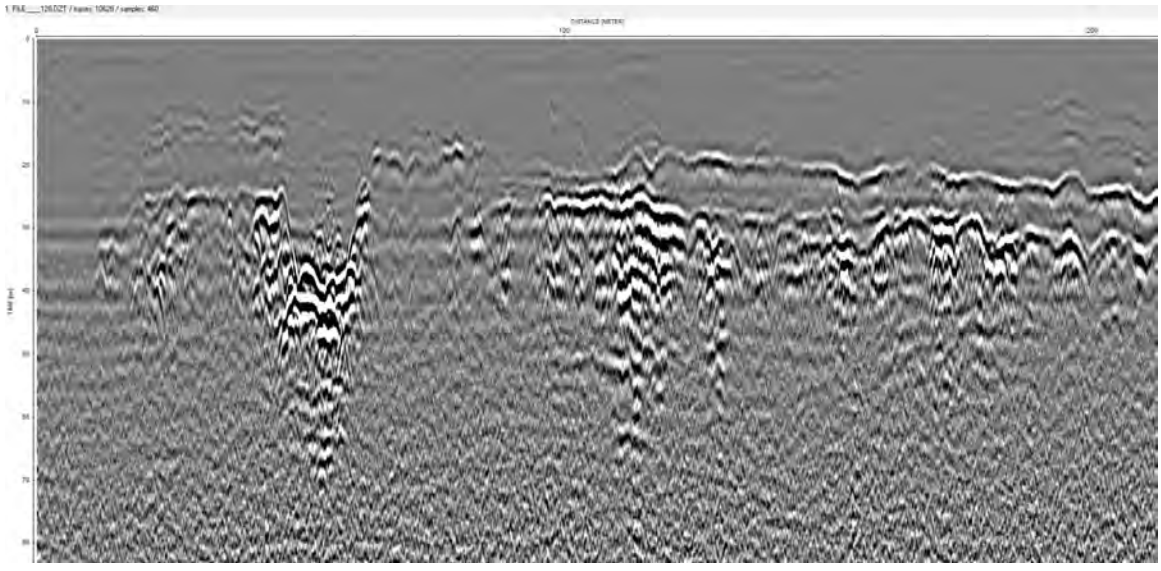

(c) Southmost traverse over anomaly.

Figure 38: GPR data acquired 8/5/2018 with SIR-3000 and 400 MHz antenna. Feature (circled in red) we hypothesize to be a canal of 13-m width that cuts across the site from the SAR for irrigation purposes. Canal surface at 1.75 m; canal bottom at 2.8 m. Distance between each chosen traverse is 1 m.

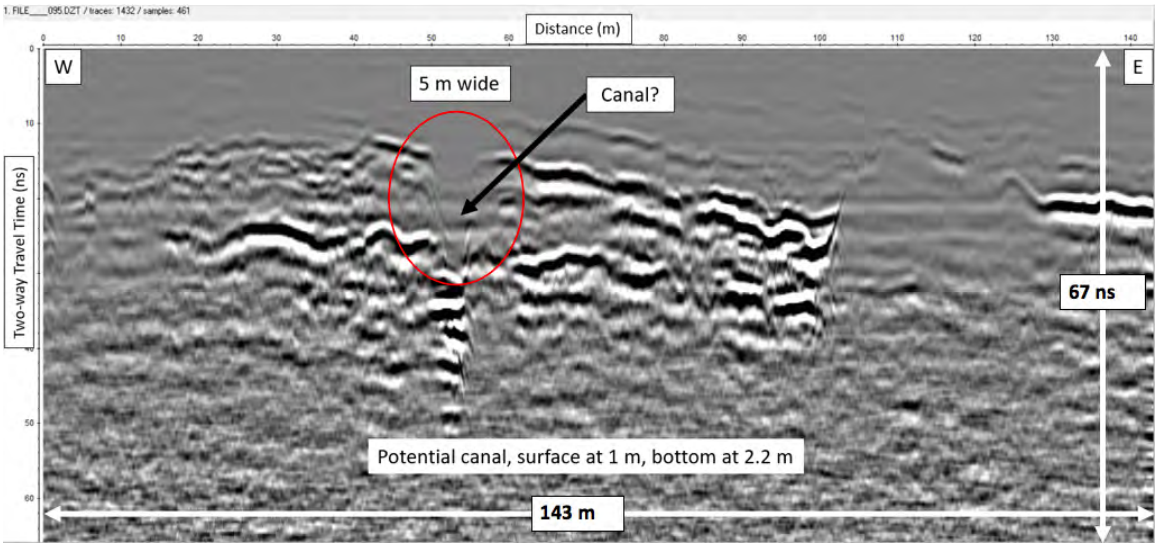

(a) Northmost traverse over anomaly.

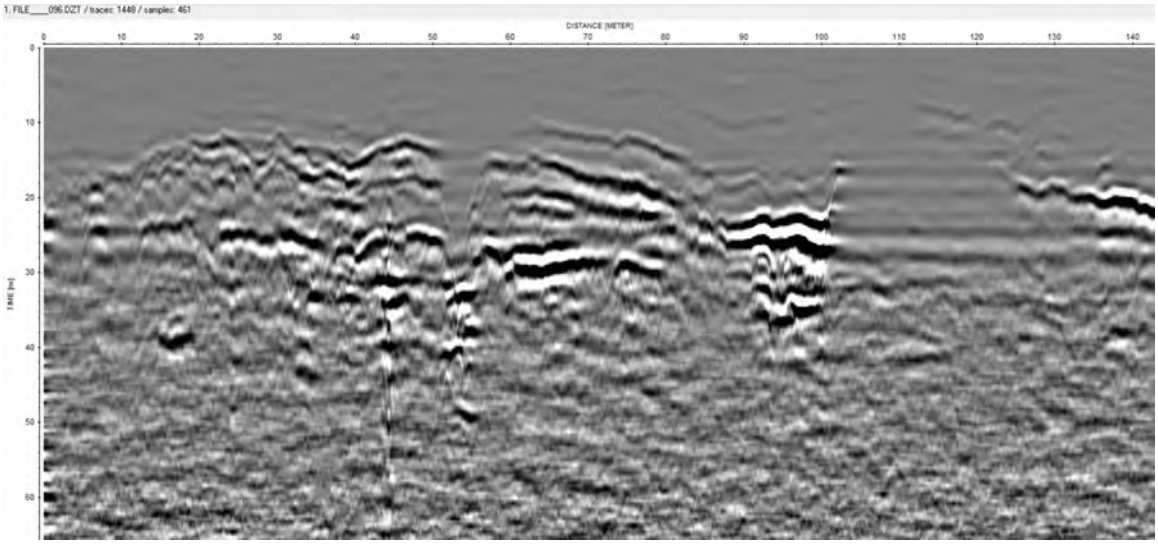

(b) Middle traverse over anomaly.

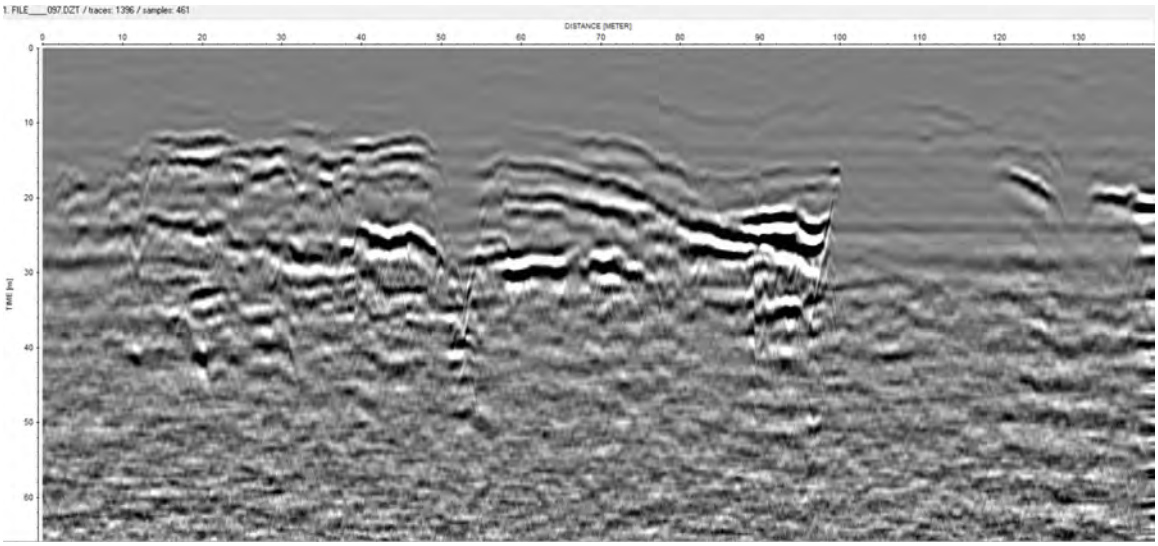

(c) Southmost traverse over anomaly.

Figure 39: GPR data acquired 7/18/2018 with SIR-3000 and 400 MHz antenna. Feature (circled in red) we hypothesize to be a continuation (or branch) of the canal in Figure 38. There is also a truncation of a high-amplitude anomaly on the eastern end of profiles that seems to break down more as profiles progress southwards. Depth of canal bottom is 2.1 m. Distance between each chosen traverse is 2 m.

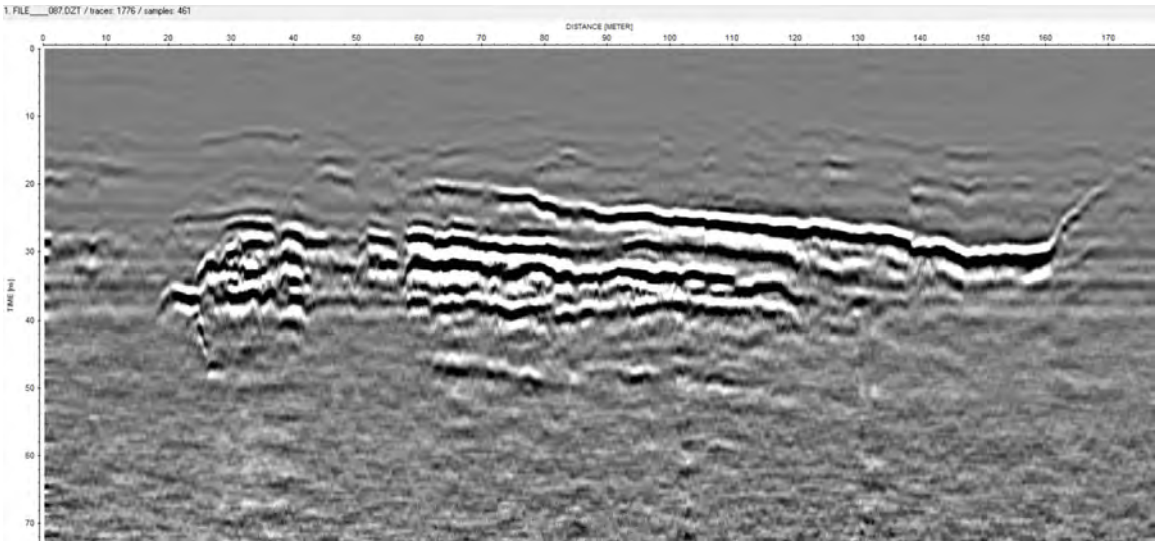

(a) Northmost traverse over anomalies.

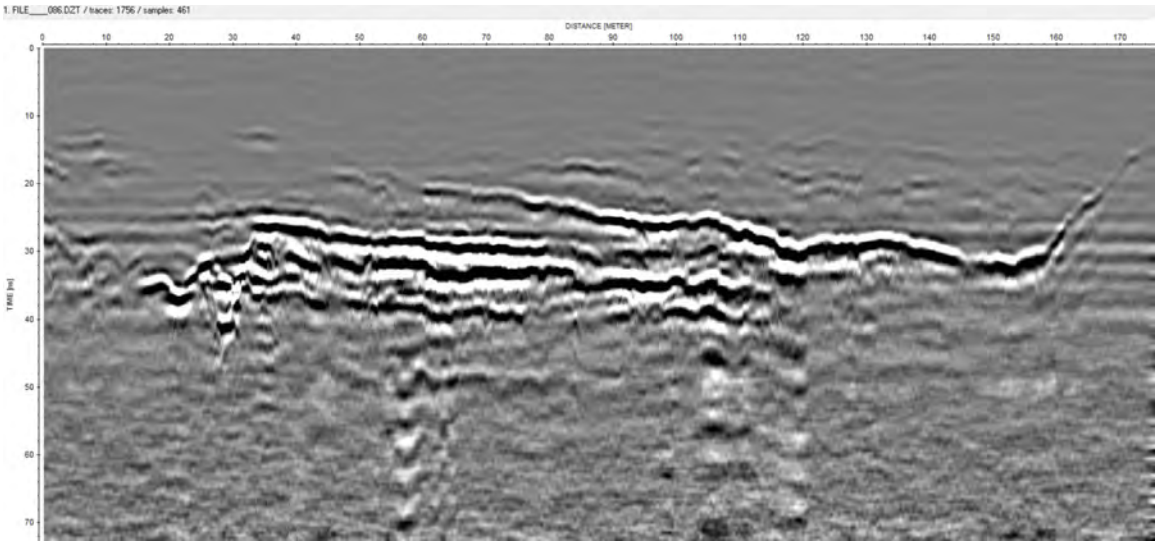

(b) Middle traverse over anomalies. Potential buried metal causing ”ring down.”

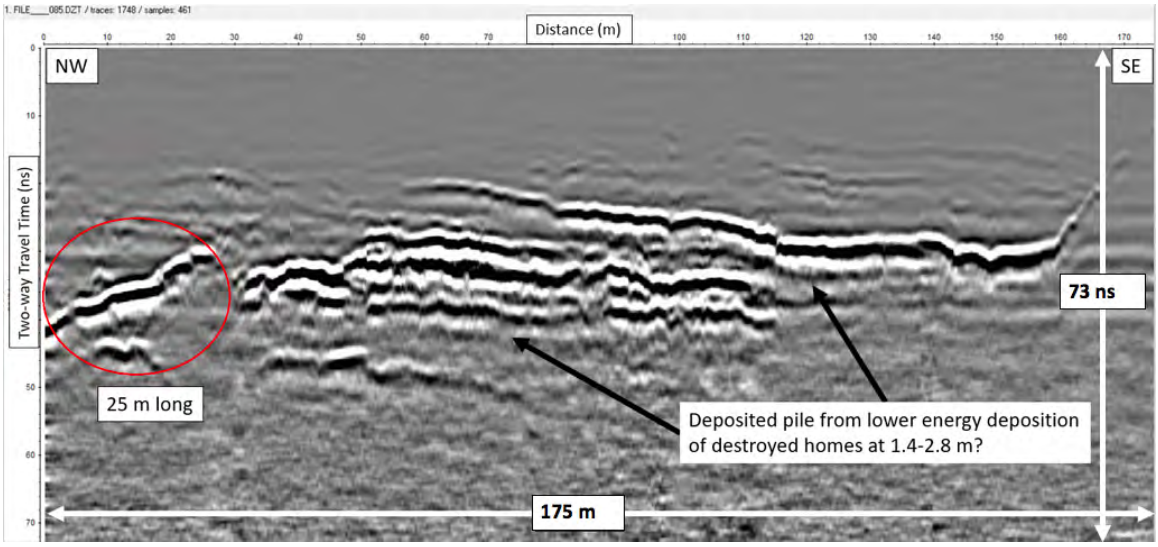

(c) Southmost traverse over anomalies.

Figure 40: GPR data acquired on 7/18/2018 with SIR-3000 and 400 MHz antenna. 130 m in length, high-amplitude cluster between depths of 1.4 - 2.8 m. There is a non-attached, high amplitude layer in (c) that either joins the cluster as seen in (b), or detached from it (circled in red). Distance between each chosen traverse is 1 meter. Location (see Figure 48) was tucked against the base of the hills, which would have been more protected from the full force of the flood. This makes it possible that the location was an area of lower-energy deposition.

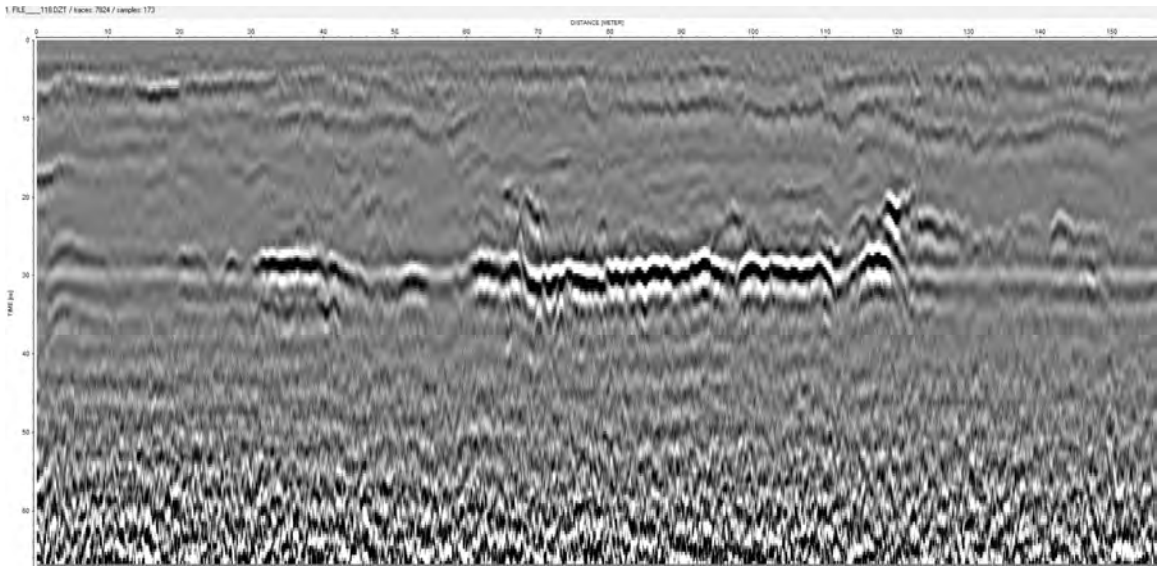

(a) Westmost traverse over anomaly.

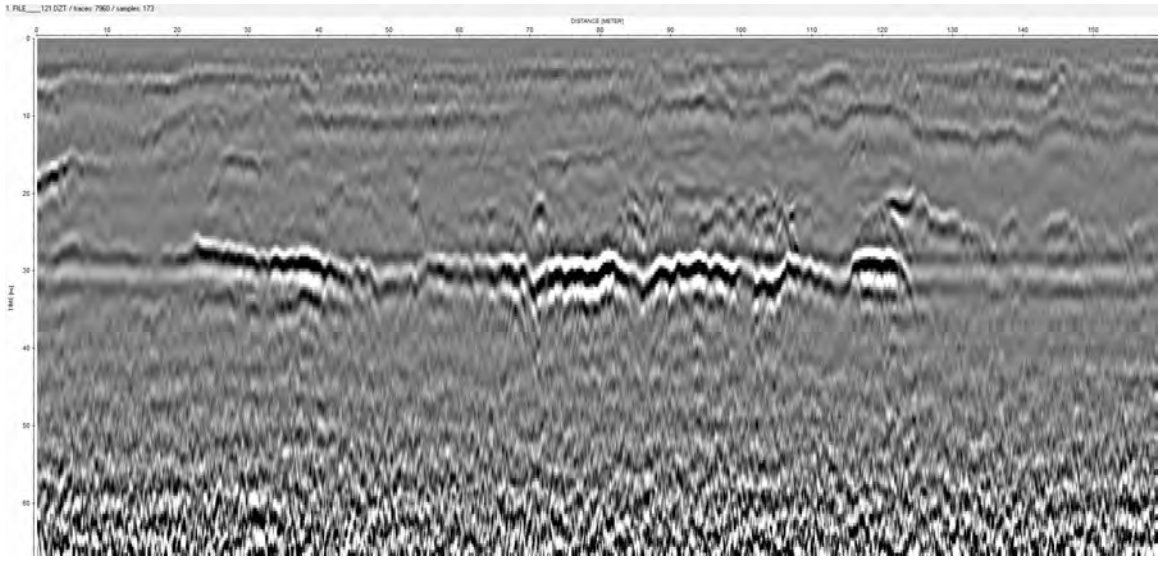

(b) Middle traverse over anomaly.

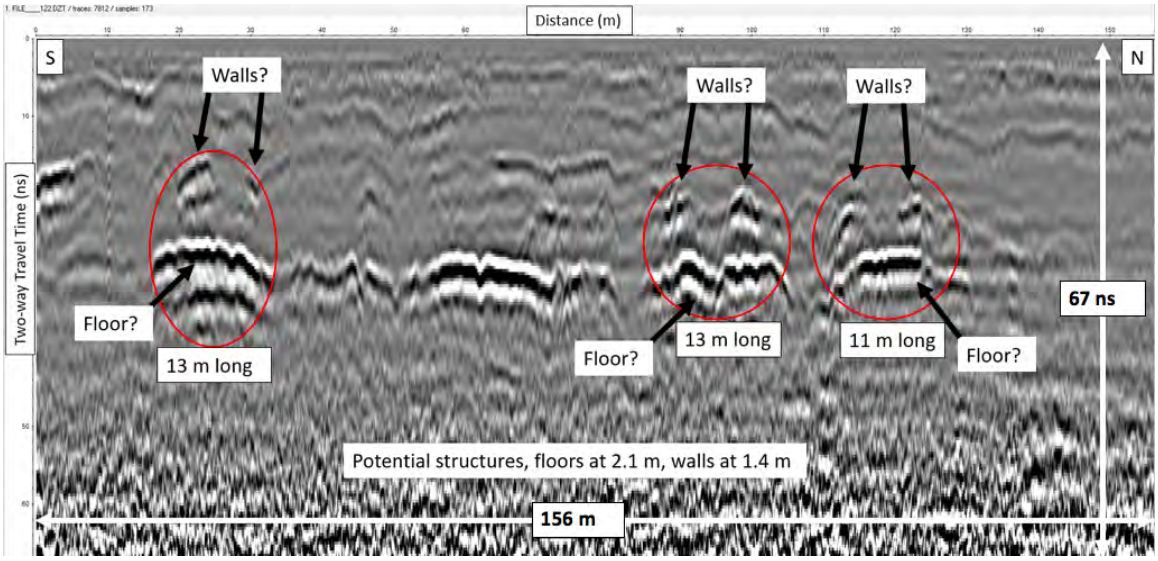

(c) Eastmost traverse over anomaly.

Figure 41: GPR data acquired 7/18/2018 with SIR-3000 and 400 MHz antenna. Features (circled in red) we hypothesize to be adobe structural remains, buried at 2.1 m. Planar, high amplitude layers are structure-sized, and each is framed by what could be walls. Profile furthest from SAR shows structures more intact (walls?). Distance between each chosen traverse is 2.5 m.

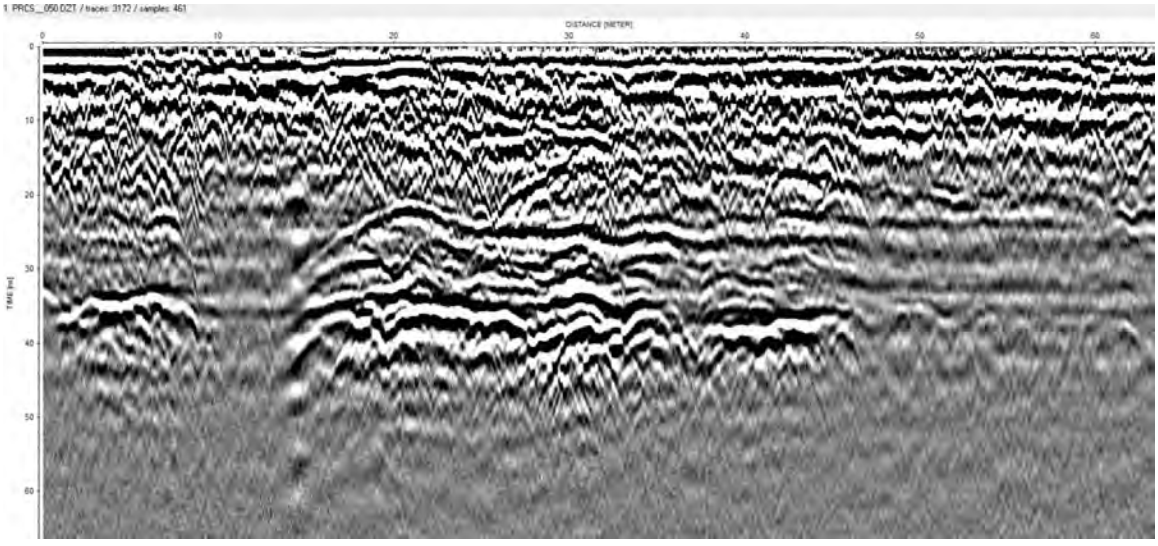

(a) Westmost traverse over anomaly.

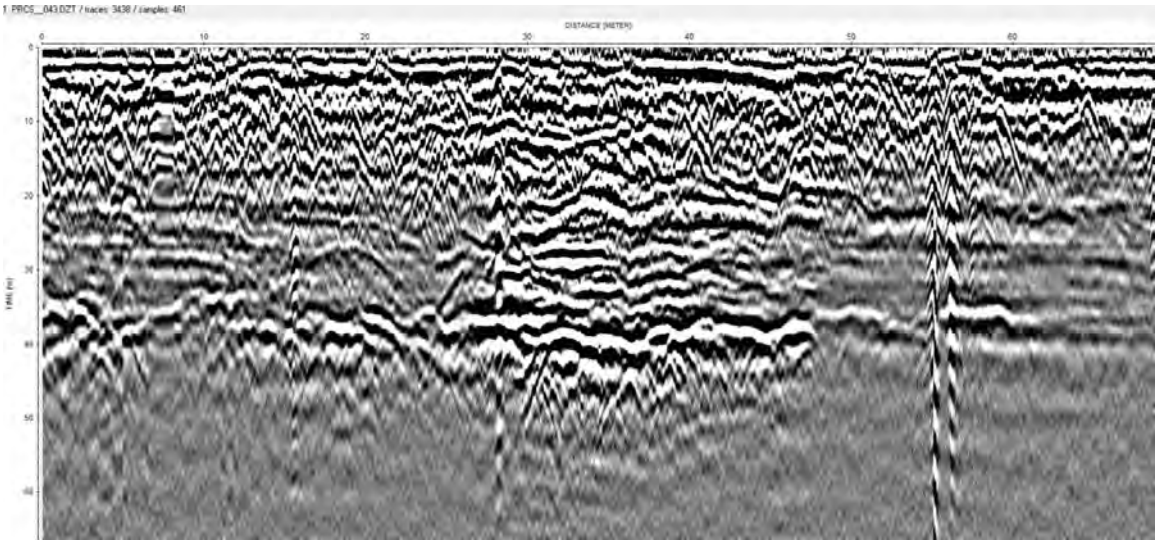

(b) Middle traverse over anomaly.

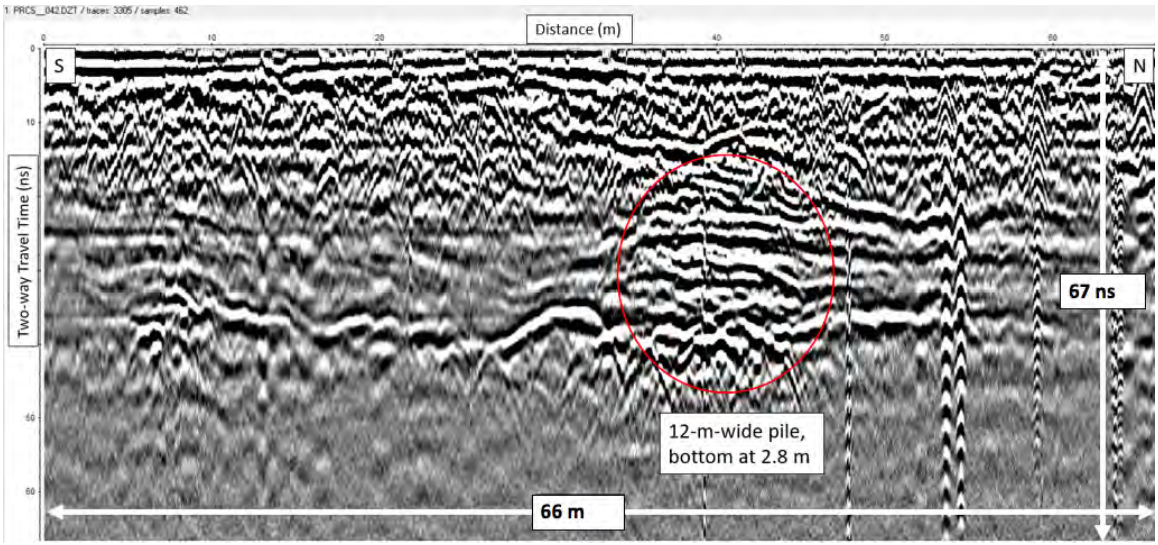

(c) Eastmost traverse over anomaly.

Figure 42: GPR data acquired on 11/26/2019 with SIR-4000 and 350 MHz HyperStacking antenna. High-amplitude layer at 2.8 meters depth seems to have a 10-20 m wide ”pile” on top of it. ”Pile” shifts northwards as profiles progress to the east. Distance between each chosen traverse is 2 m.

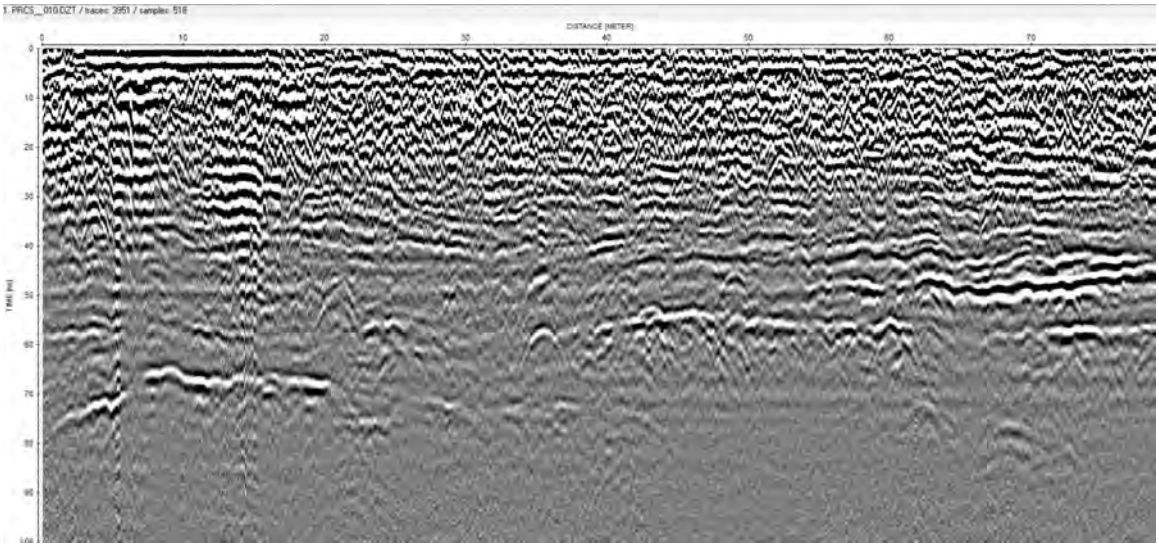

(a) Westmost traverse over anomaly.

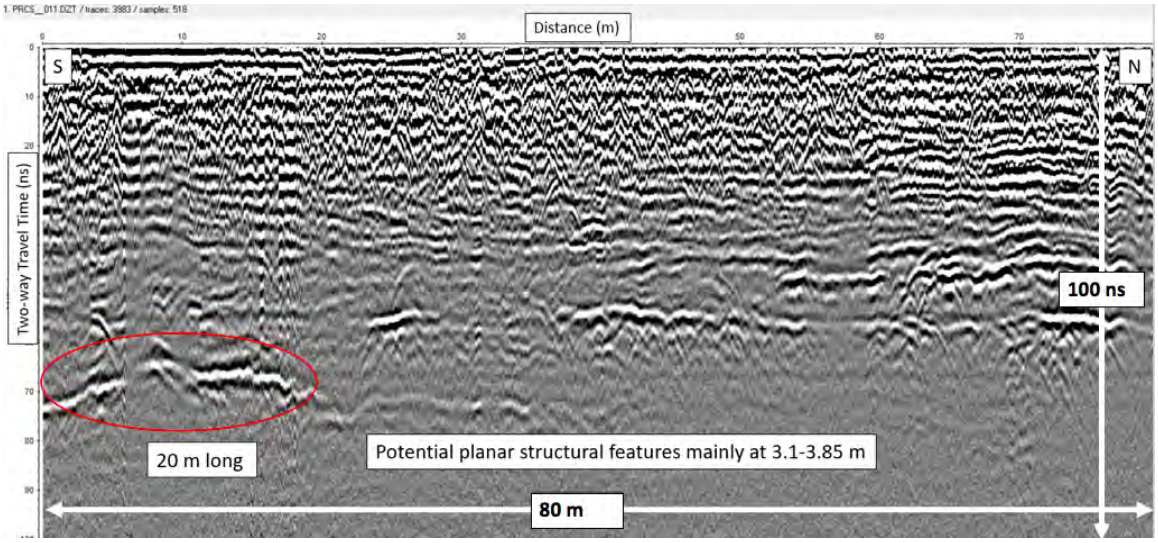

(b) Middle traverse over anomaly. At about 36 meters across the profile, at about 3.2 meters depth, we see a very strong hyperbolic reflection. This is likely to be a 3-meter, metallic artifact.

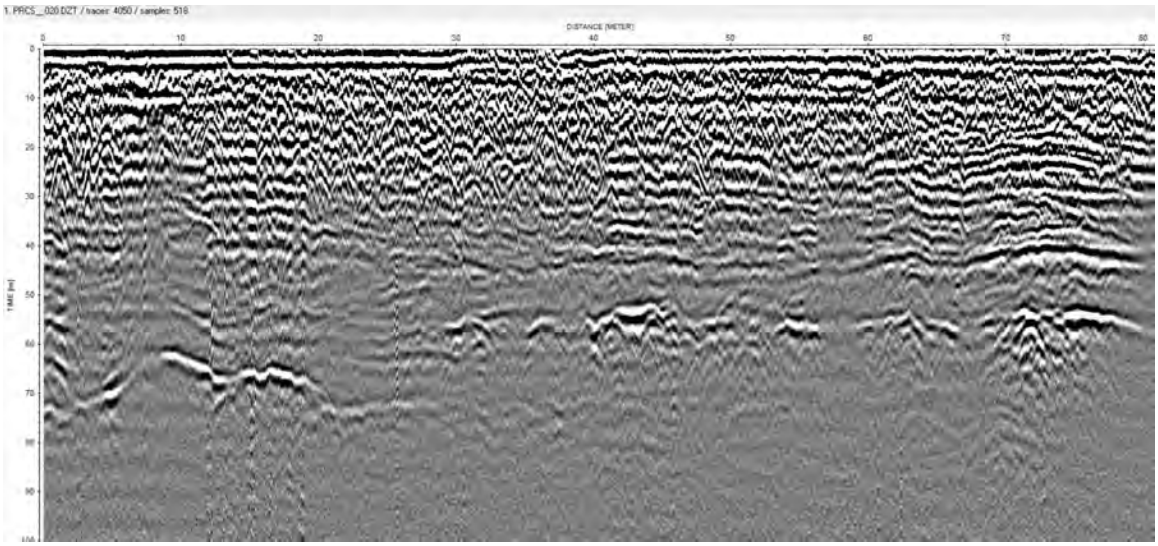

(c) Eastmost traverse over anomaly.

Figure 43: GPR data acquired 1/12/2020 with SIR-4000 and 350 MHz HyperStacking antenna. Many hyperbolas exist in these profiles, particularly (a) and (b), which indicate that large artifacts (2-3 m) could be buried here. Depth of circled anomaly at 3.8 m. Distance between each chosen traverse is 1 m.

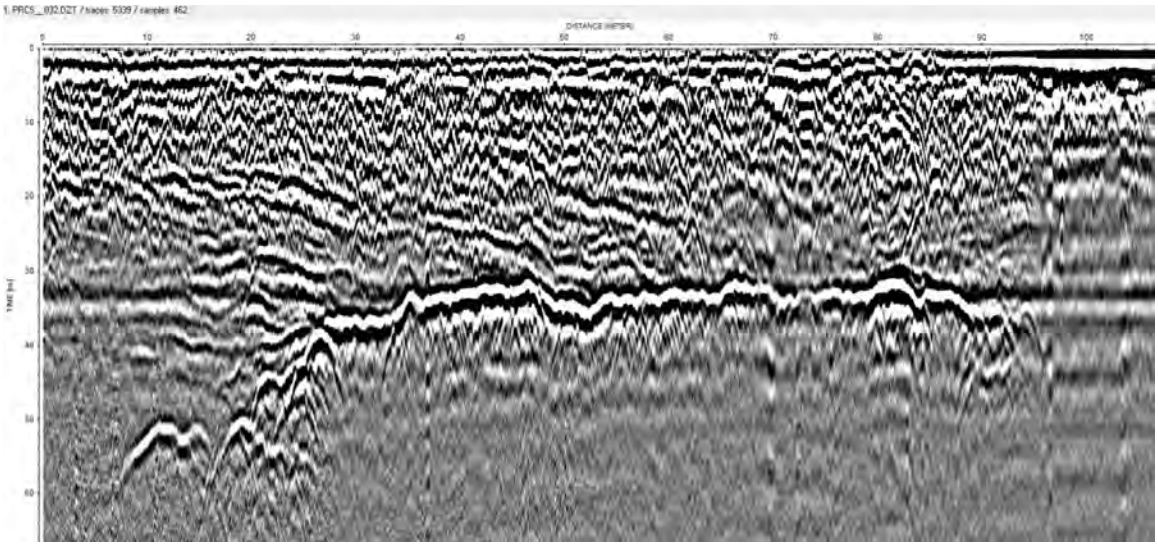

(a) Northmost traverse over anomaly (closest to SAR). There is an upper layer that is 70-meters long and a much smaller lower layer.

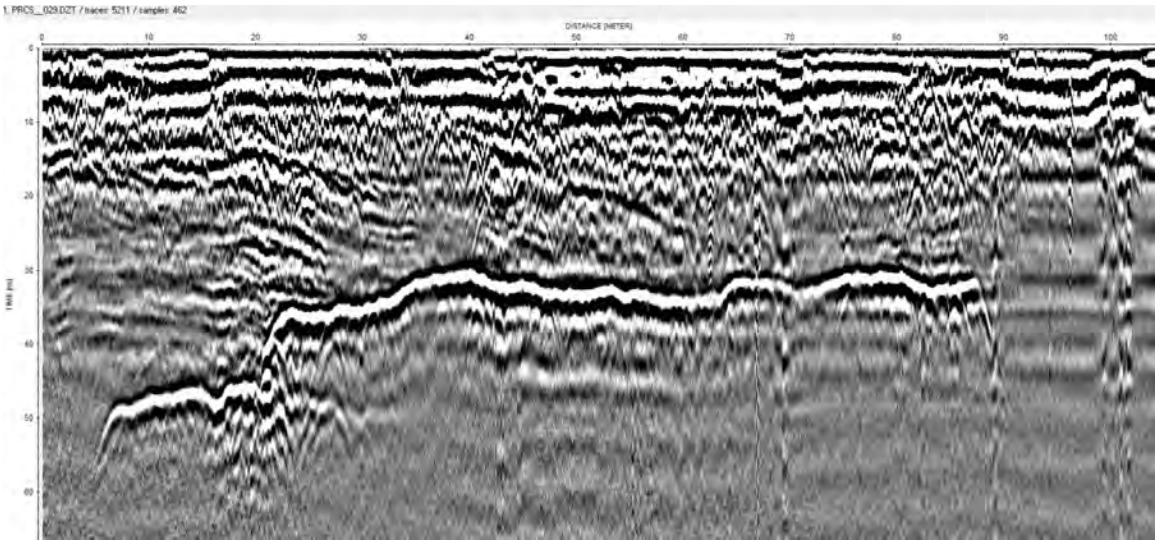

(b) Middle traverse over anomaly. Lower layer continues to grow, seemingly doing so at the expense of the upper layer, which is shrinking.

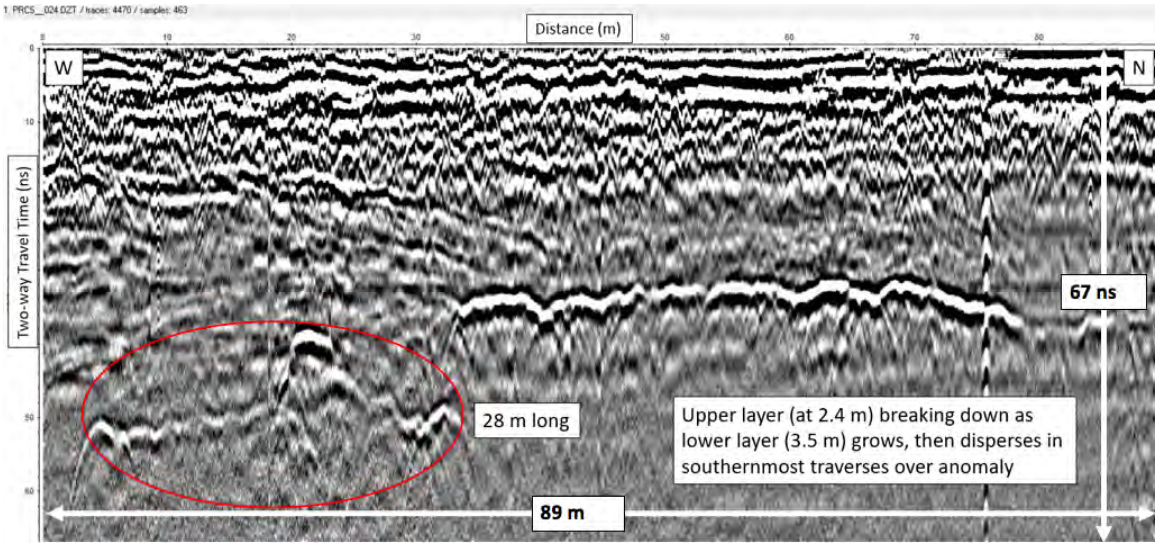

(c) Southmost traverse over anomaly (furthest from SAR). Lower layer has broken down to weak reflection and hyperbolas can be seen.

Figure 44: GPR data acquired 11/26/2019 with SIR-4000 and 350 MHz HyperStacking antenna. High-amplitude, varying-sized upper layer at 2.4 m depth, and varying-sized lower layer at 3.5 m depth that apparently grows from the top layer and then disperses (circled in red). Distance between each chosen traverse is 4 m.

3.3 Magnetic Gradiometer

In this study, over 25 km of gradiometer data was collected across Pellissier Ranch. Due to the abundance of modern debris at the surface and at shallow burial depth, processing and interpretation of data was difficult, but three major matches with GPR data have been selected and are presented in Section 3.4.

All gradiometer data collected across Pellissier Ranch was combined into one file, imported into Oasis Montaj, and the generated map of values was overlain onto Pellissier Ranch using Google Earth Pro (Figure 45). Combining gradiometer data from more than one day is possible, as while the magnetic field's strength varies from day to day, the magnetic difference between the local soil and the buried features will not vary (Ernenwein, 2007). As modern metal was unavoidable across the entire site, values above 20 nT/m and below -20 nT/m were removed from the data before processing to minimize their presence in generated maps. Previous geophysical surveys conducted in Egypt and Italy showed that ancient settlements made of earthen material are detectable only in magnetic gradient maps, and only after constraining the range of values to low values (Mekkawi et al., 2013), (Colombero et al., 2019).

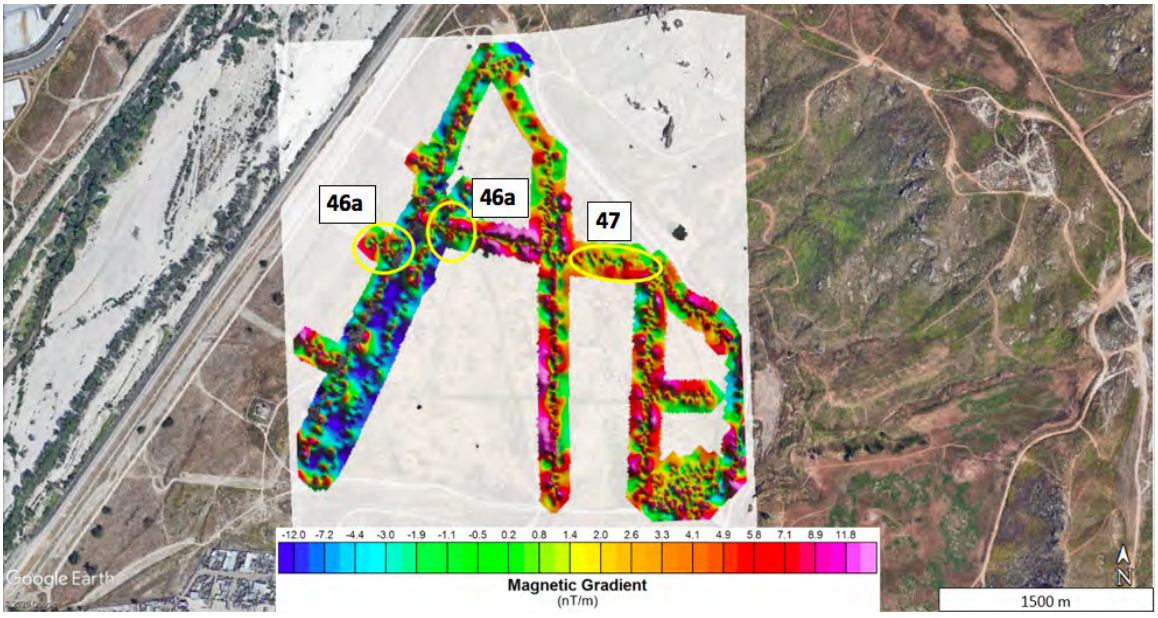

Figure 45: All gradiometer data collected at Pellissier Ranch between April 2018 and January 2020. Spacing varies from 1 meter to 1.5 meters between each traverse. Data was filtered to show only values of 20 nT/m and -20 nT/m in order to minimize noise from modern metal. Map is overlain on Google Earth Pro. Analysis of results was very difficult. Most anomalies can not be matched with GPR anomalies shown at depth. However, three locations (circled in yellow and labeled by Figure number) show anomalies in gradient values that correspond closely with anomalies imaged at depth in the GPR profiles.

3.4 Matching Significant Anomalies with GPR Anomalies

As mentioned in Section 2, the gradiometer was used as a complementary technique to the GPR. We used it to potentially verify anomalies that the GPR imaged. Across the site, the gradiometer did not have much success, which is attributed to the deeper burial of artifacts / features than the technique is capable of detecting. However, three locations of gradiometer anomalies could be matched with anomalies imaged at depth with the GPR. Not only did the anomalies match up in location, but their size was highly comparable as well (Figure 46).

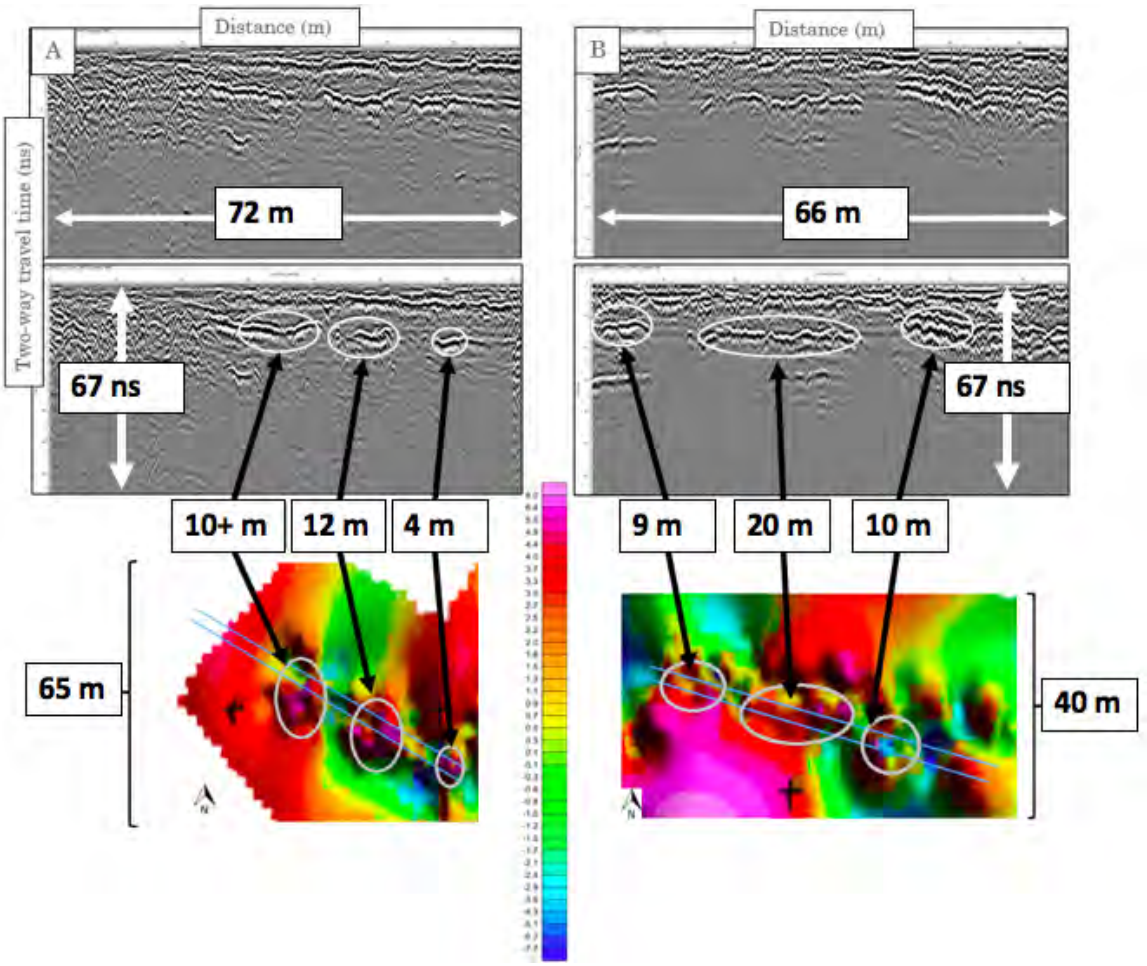

Figure 46: Two locations where GPR and magnetic gradiometer data positively correlated in location and size of anomalies. Four GPR profiles (represented by light blue lines on gradiometer data map) at 2 separate site locations. Gradiometer data processed using Oasis Montaj after excluding values above 20 nT/m and below -20 nT/m from the raw data file; GPR data processed using Reflex2DQuick. Length of GPR profile marked above as "A" extends beyond gradiometer data at this location, as caution was exercised with the gradiometer in avoiding power lines that border the northwestern edge of the site. 0.5-meter spacing was used between each gradiometer path through both locations, and a 1.5-meter GPR spacing. The GPR images the anomalies at a depth of approximately 1 meter. This explains why the gradiometer is able to detect the anomalies (per previous research that determined gradiometers are successful at imaging low strength magnetic material buried at depths of 2 meters or shallower (Clark, 1996).

During our analysis of the Oasis Montaj maps, we noticed the interpolation between measurements had created artifacts due to the relatively poor coverage of the area. We decided to import the gradiometer measurements into Google Earth Pro and test its usefulness

in analysis of results by applying a color ramp to plotted values (in nT/m) and checking if any anomalies were more readily detectable (Figure 47). Overall, detection of anomalies across the site was not improved, but we were able to clearly make out the potential continuous canal feature imaged in Figure 39 in magnetic gradient plotted values. The feature appears as a drop in nT/m (depicted by white color).

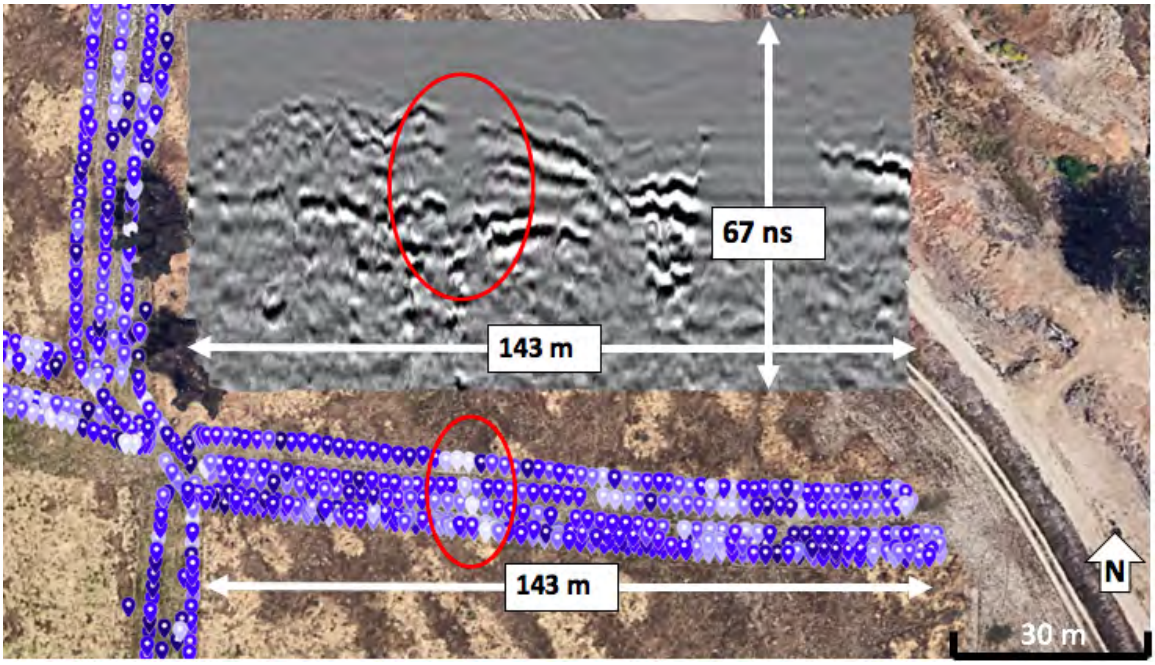

Figure 47: Gradiometer data collected at Pellissier Ranch on August 25, 2018 with overlain image from Figure 39b, a GPR profile taken at the same location. Values plotted using Google Earth Pro with a color ramp applied. Unfortunately, Google Earth Pro does not currently have the ability to create a legend showing the value range applied to each of the 12 color groups. From white to dark blue the values increase from -20 nT/m to 20 nT/m respectively. The potential canal feature appears markedly as a NW-SE trending, white (lowest values) feature. Spacing of 1 meter between each traverse. Data was filtered to show only values of 20 nT/m and -20 nT/m in order to minimize noise from modern metal in results.

3.5 Discussion of GPR and Magnetic Gradiometer Results

GPR profiles taken closest to the river show signatures of chaotic hyperbolas from lag deposits dropped when the flow velocity began to slow, and sloping layers characteristic of washover flood deposits in a floodplain. Across the site, we saw many profiles that

either contained no anomalies (as shown in Figure 33), or anomalies that were sub-2-meters deep (as shown in Figure 46 and 47). Anomalies in Figure 46 were excluded from our significant results, as we do not believe them to be related to the La Placita settlement for two reasons: archival research claimed they would be buried about 3 - 5 meters, and our 2-meter-deep test hole (Figure 6) did not get through the sandy flood deposits which blanketed the settlement during the Great Flood of 1862. We are confident that the bottom of the sandy deposits would be marked by a more loamy soil based on archival research stating that pre-flood, La Placita had fertile soil and post-flood, settlers were forced to abandon the farmland because they were not successfull in growing any crops on the newly deposited soil (Vickery, 1984). For Figure 47 however, we make an exception and include the feature in our significant results as the depth of the canal extends into potential La Placita depth and there is no disturbance of the material that filled in the void feature. This indicates that it could not have been a modern, man-made feature, but a feature filled in naturally, many decades ago.

When analyzing significant anomalies in GPR profiles, the deepest located reflectors do not exceed 3.8 meters depth (Figure 43, 44). This would put La Placita at the shallower end of the range given in archival research (personal communication STHF, 2018). Some profiles contain anomalies that extend from a La Placita range burial to shallower depths of 1.4 - 2 meters (Figure 37, 40, 42, 46). We still consider these as probably related to La Placita due to their deeper extension. For example, in Figures 37 and 41, it is in the easternmost (furthest from SAR) profiles of all traverses over the anomalies that reach shallower depths. It is probable that when the river hit the structures / features, it collapsed the side closest to the SAR as it took the brunt of the river's force and then effectively acted as a shield to the portion further from the SAR. This would explain the shallower depths of the structures / features in those profiles. Figures 40 and 42 on the other hand, had location-related advantages. Anomaly 40 was tucked up against the base of La Loma Hills, where it would have received far less of the river's energy than a location further

from the base of the hills. This would have led to less destruction and deposition of sandy flood deposits atop what may be structures / features that were melted / broken down and dropped off in this lower energy location. A similar situation exists for anomaly 42, which sits on the eastern border of the site at a location that would have received less of the river's energy than the middle and western portions of the site.

4 Conclusions

In this thesis, GPR and magnetic gradiometry techniques were applied to attempt to locate the buried settlement of La Placita de Los Trujillos in the subsurface of what is currently Pellissier Ranch. Eleven site visits were undertaken, totalling approximately 45 hours of data collection in the Colton, California vacant lot. Raw data acquired with GPR was processed using Reflex2DQuick. The velocity of the subsurface was determined through a hyperbola-fitting method, leading to extraction of approximate depths of anomalies. Depth information was an important factor in this study, as our interest was in anomalies buried at depth; particularly at burial depths greater than 2 meters, which is the minimum depth we could confidently accept of La Placita based on archival research and the 2-meter deep hole we dug.

Continuous-length reflectors that stretch over many meters seen in our data are highly comparable with reflectors seen in previous southwestern GPR studies that successfully located and unearthered 'adobe melt' and floors of buildings buried in fluvial environments (Conyers, 2013). Less commonly, hyperbolas were seen in GPR data at depths of 2 - 4 meters across the site. Per the general rule of thumb with GPR, objects can only be imaged if they are buried as deep as they are large (Ernenwein et al., 2007). This indicates that many of those artifacts are objects between 2 and 4 meters large. Larger household objects (ex. chairs, tables, beds) or large farming objects (ex. wooden posts used to tie up horses, large baskets / buckets for collecting crops, large equipment used to till the soil) are possible artifacts these anomalies could represent.

A hole was dug in the middle of Pellissier Ranch in attempt to either: locate artifacts / features or reach the bottom of the sandy flood deposits. Neither goal was accomplished due to the depth of the deposits exceeding the depth that a hole could be manually dug safely. As no confirmation of artifacts / features could be achieved, the results of this study are classified as the most probable locations of La Placita artifacts / features. This claim is

based on the similarity of our results with previous southwestern site studies, and the fact that anomalies are buried within a depth range acceptable for La Placita. Besides the land briefly being used as a dairy farm and vineyard by Antoine Pellissier in the early 1900s, the land that La Placita once occupied has remained largely untouched. As such, any anomalies buried at depth greater than 2 meters can be classified as related to La Placita with a high degree confidence.

Profiles taken a week after rain were able to image an anomaly's size and characteristics almost exactly as it did in dry conditions. The most significant GPR anomalies we saw in our surveys include what we hypothesize to be buried canals, structural walls, floors, and remains of adobe homes, seen as 'adobe melt' signatures, which contrast heavily with the sand that buried them (Figure 48).

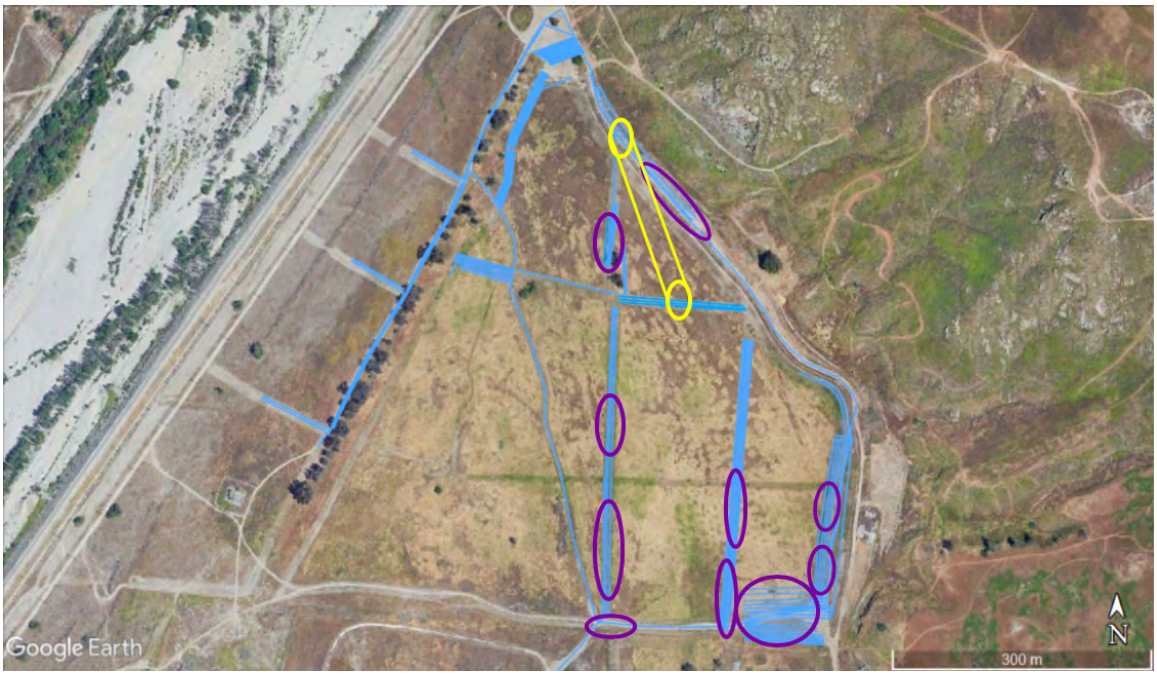

Figure 48: Map of all major GPR anomalies. The labels point out those shown in this section. Features are circled in purple and labeled by their Figure number. Yellow circles with connecting lines drawn as probable path of irrigation canal, based on GPR data at the two circled locations, which show a similar sized and structured canal, decreasing in width from 13 to 5 meters as its distance from the SAR increases. We hypothesize that in the 13-meter measurement of the canal, we had run more diagonal, instead of perpendicular, to the canal.

While interpretation of the magnetic gradiometer results to locate La Placita artifacts / structures was challenging, we were able to match three shallowly buried GPR anomalies with clearly higher (strong GPR reflectors) or lower (void; potential canal) gradiometer values (Figure 3.4). This observation illustrates the method's effectiveness in detecting features buried at sub-2-meter depths, as was reported by previous studies (Clark, 1996). However, with this shallow burial depth, we can not confidently consider two of these anomalies related to the pre-flood settlement, but do make an exception for the potential buried canal feature due to the depth it extends into the subsurface, with no evidence of modern day disturbance of the soil.

4.1 Suggestions for Future Work

If future surveys of the 200-acre Pellissier Ranch site are to be conducted, it is our recommendation to focus efforts in locations circled on the map (Figure 49) to attempt to further constrain promising anomalies (Figure 50, 51, 52).

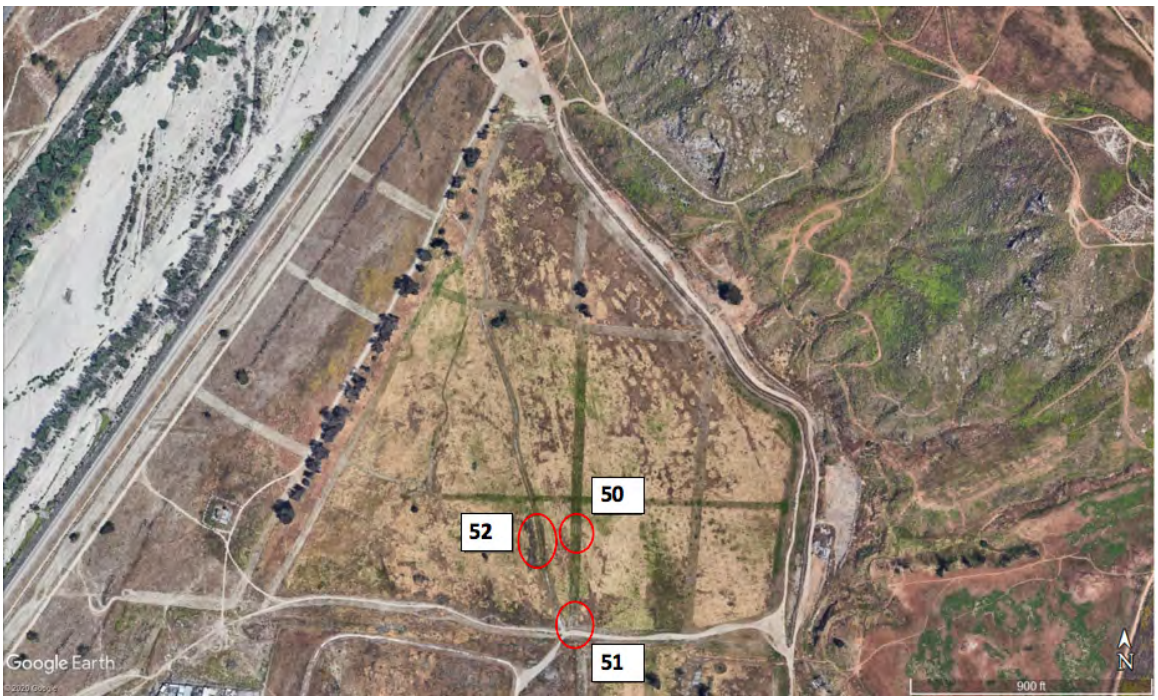

Figure 49: Map of Pellissier Ranch. Circled in red (and labeled with their corresponding Figure) are locations of promising anomalies that could be related to the original Trujillo Adobe or another family home. We strongly recommend that if future work is to be conducted at Pellissier Ranch in search of La Placita, these locations should be prioritized (Google Earth Pro, 2018).

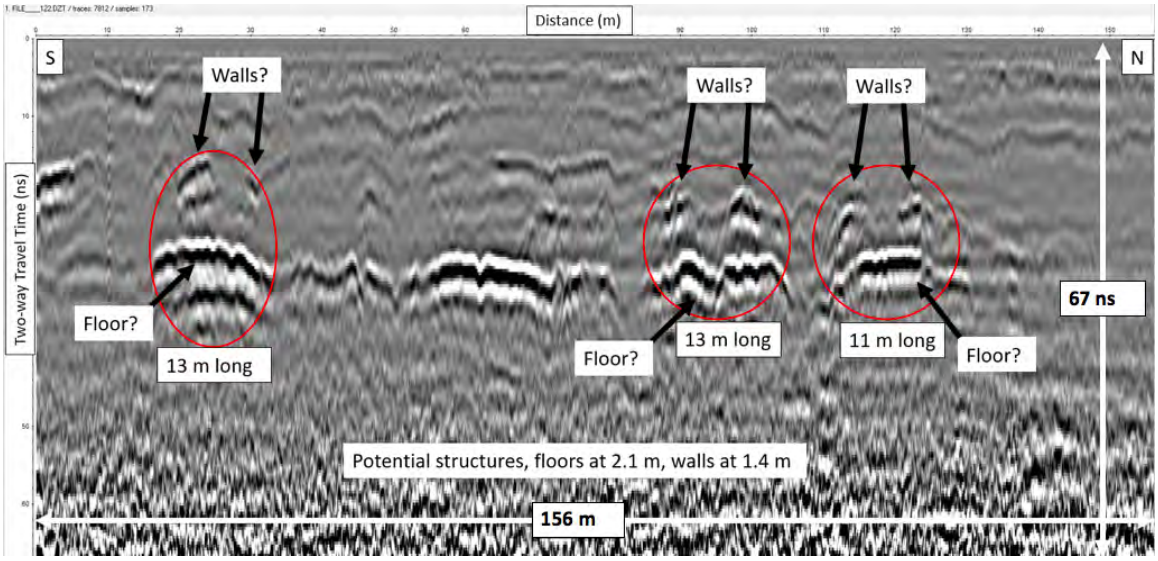

Figure 50: We believe this profile to be our most probable evidence of La Placita structures. Collected on 8/5/2018, several anomalies that resemble the shape and size of adobe structures are imaged at a depth of 2.3 meters. They all lie along the proposed path of where the original Trujillo Adobe was hypothesized to exist before it was destroyed by the flood (Figure 9).

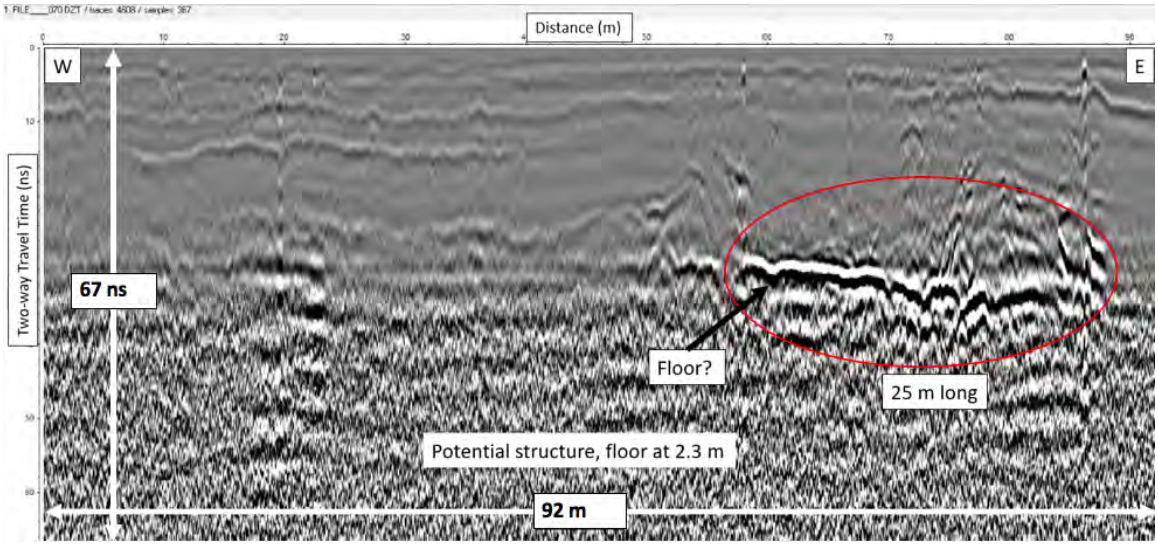

Figure 51: Promising anomaly seen in 4/28/2018 profile at a depth of 2.3 meters, which lies along the proposed path of where the original Trujillo Adobe was hypothesized to exist before it was destroyed by the flood (Figure 9), and is of the approximate size of an adobe structure that was turned into 'adobe melt' during the flood.

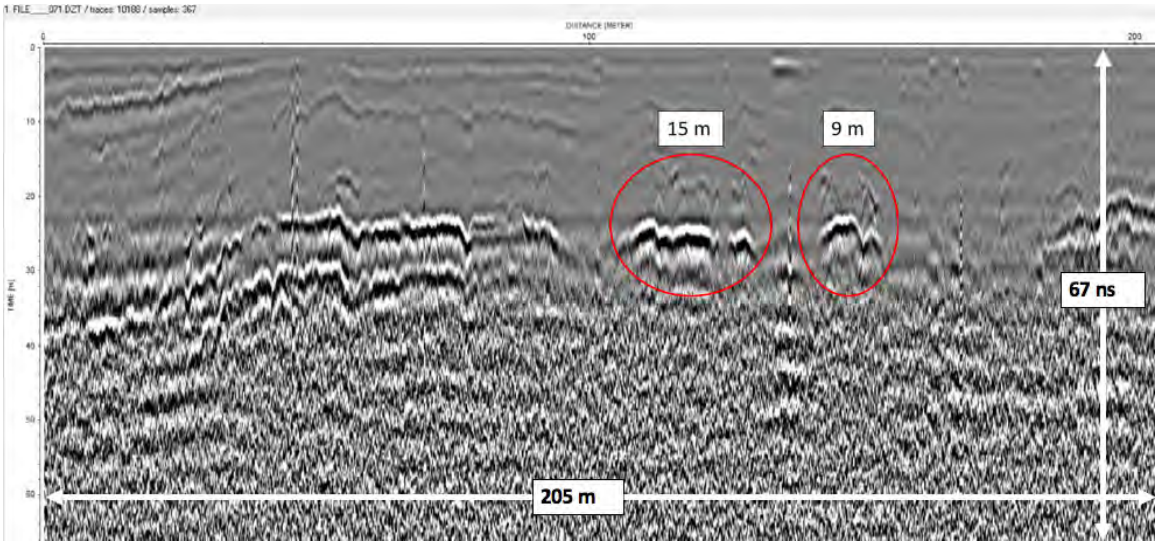

Figure 52: Promising anomaly seen in 4/28/2018 profile at a depth of 2.3 meters. Lies along the proposed path of where the original Trujillo Adobe was hypothesized to exist before it was destroyed by the flood(Figure 9).

Other methods that could produce successful surveys at the site include drone-based magnetics, electromagnetic profiling, and electrical resistivity. Drone-based surveys would greatly increase coverage of the 200-acre site, especially over areas that are not mowed and more difficult to traverse. A base station could be used to help correct for diurnal variations in the drone-captured total magnetic field intensity data. Electomagnetic profilers could be successful at Pellissier Ranch, if utilized in an area void of modern metal at or near the surface, and if the profiler used is capable of imaging to a depth of 4 meters. Electrical resistivity surveys should be performed over areas that are most likely to have features of interest in the subsurface as the set up is not time-efficient, but the technique could offer the opportunity to image features that were not previously measurable, or better define features that we saw in our own results.

References

Aitken, M. (1958). Magnetic prospecting i. *Archaeometry: vol. 1*, 16-20.

Atkinson, R. (1958). Field archaeology. *Methuer, London*.

Bevan, B. (1977). Ground-penetrating radar at valley forge. *Geophysical Survey Systems, North Salem, New Hampshire*.

Bristow, C. (2009). Ground penetrating radar in aeolian dune sands. ground-penetrating radar: theory and applications. *Elsevier Science, edited by Harry M. Jol*, 273-298.

Cassidy, N. (2009). Ground penetrating radar data processing, modelling and analysis. ground penetrating radar: Theory and applications. *Elsevier Science, edited by Harry M. Jol*, 141-176.

Colombero, C., Elia, D., Meirano, V., & Sambuelli, L. (2019). Magnetic and radar surveys at locri epizephyrii: A comparison between expectations from geophysical prospecting and actual archaeological findings. *Journal of Cultural Heritage*.

Conyers, L. (2012). Advances in ground-penetrating radar exploration in southern arizona. *Journal of Arizona Archaeology: vol. 2, no. 1*, 80-91.

Conyers, L. (2013). *Ground penetrating radar for archaeology*. AltaMira Press, Lanham.

Conyers, L. (2014). *Interpreting ground-penetrating radar for archaeology*. Routledge.

DataUSA. (2017). *Colton, ca.* Retrieved from `https://datausa.io/profile/geo/colton-ca. Accessed [08/26/2018]`

David, A. L., Linford, N., & Linford, P. (2008). Geophysical survey in archaeological field evaluation. *English Heritage*.

Ernenwein, E., & Hargrave, M. (2007). Archaeological geophysics for dod use: a guide for new and novice users. *Environmental Securty Technology Certification Program*.

Eula, M. (1993). Thinking historically: Using theory in the introductory history class. *The History Teacher*, 203-209.

Harley, R. (2003). An early riverside suburb at la placita. *Journal of the Riverside Historical Society No. 7*, 13-24.

Jasper, H., Candel, M., Kleinhans, B., Wim, Z., Cindy, Q., & Jakob, W. (2018). Late holocene channel pattern change from laterally stable to meandering – a palaeohydrological reconstruction. *Earth Surface Dynamics: vol. 6*.

Jones, L. (2018). *The big ones: How natural disasters have shaped us (and what we can do about them)*. Doubleday.

Landis, M. (2017). Mount slover's fame is set in stone. *San Bernardino Sun*.

Leckebusch, J. (2003). Ground-penetrating radar: A modern three-dimensional prospection method. *Archaeological Prospection: vol. 10*, 213-240.

Mekkawi, M., Arafa-Hamed, T., & Abdellatif, T. (2013). Detailed magnetic survey at dahshour archeological sites southwest cairo, egypt. *NRIAG Journal of Astronomy and Geophysics: vol. 2*, 175-183.

Peninou, E. (2004). A history of the seven viticultural disctricts of california - los angeles viticultural district. *Nomis Press. Santa Rosa, CA*, 67.

Rolfes, T. (2017). *Natural resources conservation service, united states department of agriculture.* Retrieved from `https://websoilsurvey.nrcs.usda.gov/`

Sidler, W. (1968). *Agua mansa and the flood of january 22, 1862 santa ana river*. California: San Bernardino County Flood Control District.

Smekalova, T., Voss, O., & Smekalov, S. (2008). *Magnetic surveying in archaeology*. Publishing House of the Polytechnical University, St. Petersburg.

Vickery, J. (1984). Defending eden: New mexican pioneers in the san bernardino valley. *Riverside, CA: Riverside Museum Press*.

Weymouth, J. (1976). A magnetic survey of the walth bay site. *Occasional Studies in Anthropology No. 3*.

5 Appendix A: Elevation Analysis of Pellissier Ranch with ArcMap

The USGS's (United States Geological Survey) "The National Map" GIS (Geographic Information System) resource for topographic information provided the DEM (Digital Elevation Model) raster datasets used in this study. The format they were given in was ".xml", which is not directly usable with ArcMap. 7-Zip 18.05 and uGet 2.2.1 had to both be used to convert the files into usable image format from their original ".xml" format. Once they were usable disc images, all 23 DEM files, which had cell sizes of 3'x3' and followed the North America Datum 83 coordinate system, were added to the map. Each contained 1000 rows and 1000 columns, with a band number of 1, a source type Generic, and a pixel type and depth of floating point and 32 Bit respectively. Angular units were given in degrees and linear units in feet. A total area of approximately 5.6 km in a north-south direction and 8.8 km in an east-west direction, was analyzed with the DEM data.

Initially, all the DEM datasets had scales that were independent of each other. One dataset's scale would color an area white (low elevation) where another dataset would show the same elevation as gray (intermediate elevation). To solve this issue, a uniform dataset had to be created by combining all 23 datasets into a single dataset. ArcMap's Mosaic to New Raster tool was employed to accomplish this. This was possible as the number of bands (1) and pixel depth (32 Bit) matched for all DEM datasets. All 23 DEM files were input into the tool and the single output dataset was named "Combined_Elevation_Raster." This successfully was able to combine all 23 datasets into one with a single scale. It was then possible to use ArcMap's Spatial Analyst tools to investigate the site for various features.

First analyzed was the change in slope across the DEM with the Slope tool. The single dataset was set as the input and the output was named "combined_slope", with a value of degree and a Z factor of 1. As the change in slope across the river and the area of Pellissier Ranch was minimal, a large class value of 20 was chosen to show the minimal changes

and the color ramp was set to purple and blue hues (with green to yellow to red reflecting greater slopes respectively, seen mostly in La Loma Hills to the north of the ranch).

Next, ArcMap's Spatial Analyst tool, Contour, was employed to further delineate boundaries of the potential river flow during the Santa Ana River's Great Flood of 1862. The single output dataset was set as the input and "converted to vector representations using conventional image processing techniques" (Greenlee, 1987). This output was named "Contour (asl) in 10' increments". As the change in elevation across the river and area of Pellissier Ranch is minimal, a contour interval of 10' was chosen. The contour line color was set to fire red and labels set to peach to easily see them overlain on the dark-colored DEM map.

ArcMap's Spatial Analyst tool was then used to derive a Flow Direction raster dataset. This raster's use was in deriving a Flow Accumulation raster dataset, called "Flow_Accumulation" in which each "grid cell is treated as a point on a continuous surface on which a unit of flow package is generated and flows to the next downhill point(s)" (Zhou et al., 2011). This method has been found to be successful in the past, as "digital comparisons of the Big Tujunga Reservoir watershed and a digitized version of the manually delineated watershed indicated 98 percent agreement" (Jenson and Domingue, 1988).

The Flow Accumulation raster's symbology was adjusted to pronounce changes in the map as much as possible. Even after adjustments were made, it was difficult to see the accumulations. To fix this, the Spatial Analyst tool, Focal Statistics, was used to derive another Flow Accumulation dataset, "Flow_Accumulation_2," which was able to enhance the flows visualized on the map.

A workflow of all inputs and outputs for this project is shown in Figure 53 below.

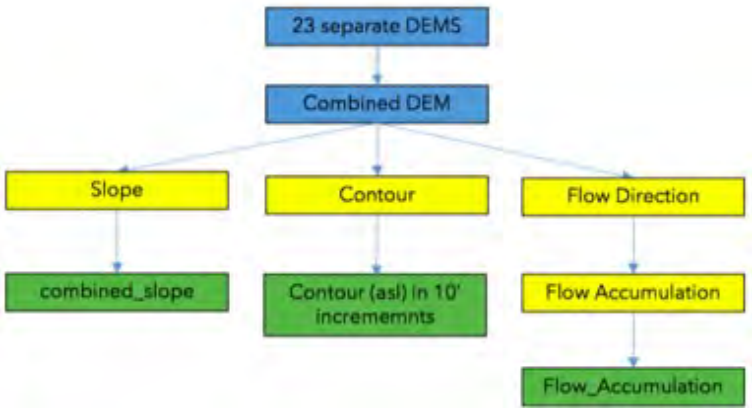

Figure 53: Workflow for the ArcMap elevation study of Pellissier Ranch. Blue = input raster datasets; Yellow = Spatial Analyst tools; Green = output raster datasets (ArcMap, 2018).

The combined DEM dataset created from 23 DEM datasets able to give us a visual overview of elevation changes along the Santa Ana River as it flows southwest towards Pellissier Ranch (Figure 54). In the northeast corner of the map, it is clearly observed that the river is the darkest feature (lowest elevation) when compared to its surroundings. When the river reaches La Loma Hills in the middle of the map, it is forced to flow directly west. Here we see the largest contrast with the highest elevation (whitest color) at La Loma Hills very near the lowest elevation of the Santa Ana River. As the river passes this point, it is observed that the contrast of the river and its immediate surroundings lessens. The low elevation of the river (darkest color) matches the equally low elevation of Pellissier Ranch. A flooding situation in this elevation circumstance is easy to imagine. Resolution for this DEM is 1-meter.

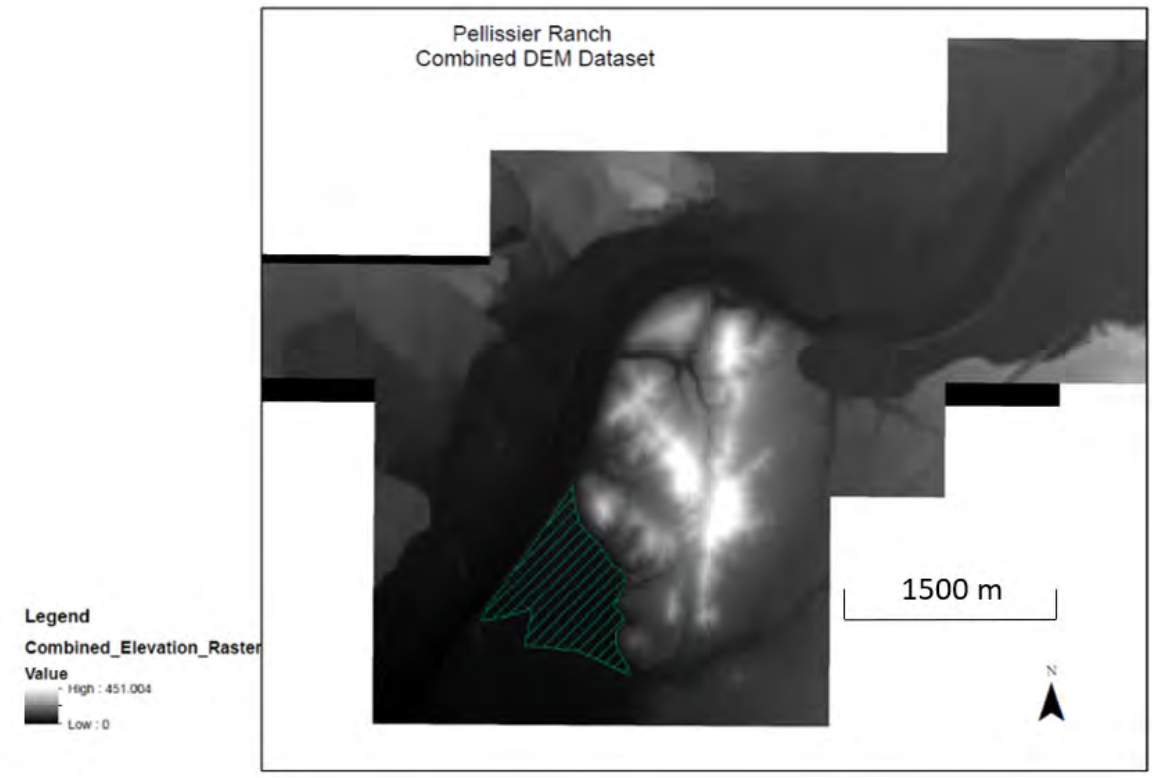

Figure 54: Single elevation raster from 23 combined DEM datasets obtained from the USGS's "National Map." Combined with Mosaic to New Rasster tool. White showing highest elevation changes and black showing lowest elevation changes. Hashed, aqua colored area denotes Pellissier Ranch (ArcMap, 2018).

The Slope tool (shown also in the Introduction section of this thesis), set with 20 classes of slope values, was able to show very small (1-3°) changes in slope across the entire area (Figure 55). Slopes across Pellissier Ranch are very low, mostly in the 0-1° range. The highest value seen in the area occurs sporadically and at approximately 6°. Looking at the southwest corner of the map, there is a definite sloping (5°) towards the southwest, causing a quicker drop in elevation in this area of the river than the northeast area.

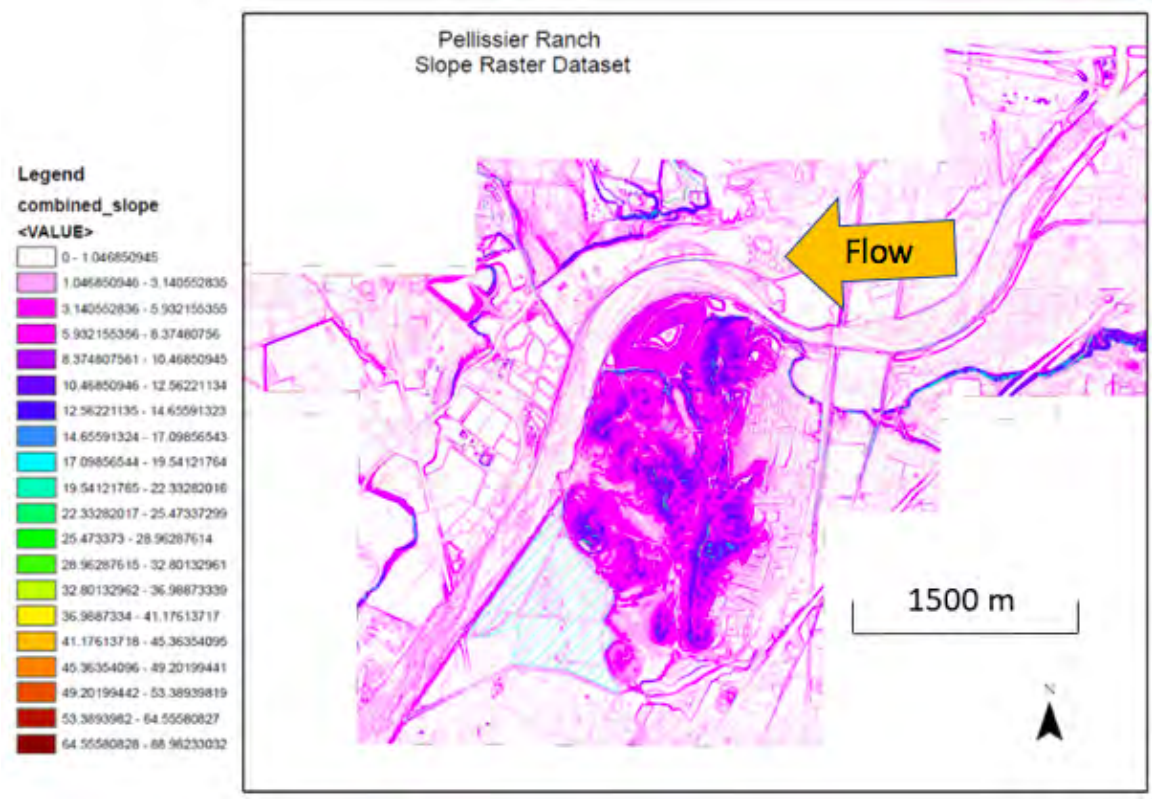

Figure 55: Slope raster derived from elevation raster showing 20 different classes of slope values to identify smallest changes in slope. Pellissier Ranch slopes are mostly in the 0-1° range. Hashed, aqua colored area denotes Pellissier Ranch (ArcMap, 2018).

The Contour tool (shown also in the Introduction section of this thesis), set at an interval of 10 meters, was able to delineate the lowest elevations in the area (Figure 56). A decreasing elevation is observed from the northeast corner of the map down to the southwest corner. The lowest elevation (in the river) is present in the southwest corner at 250 meters, while the highest is in the northeast at 290 meters. The decrease of 40 meters in elevation occurs in this shown stretch of the river (approximately 10 km length). In the middle of the map, it is seen that the river flows through a relatively narrow portion were its maximum width is limited to 500 meters. A river that flowed 9,000 m^3/s through this point is easy to imagine when you consider that the areas of the river directly above and below this point are almost three times the width at around 1300 meters.

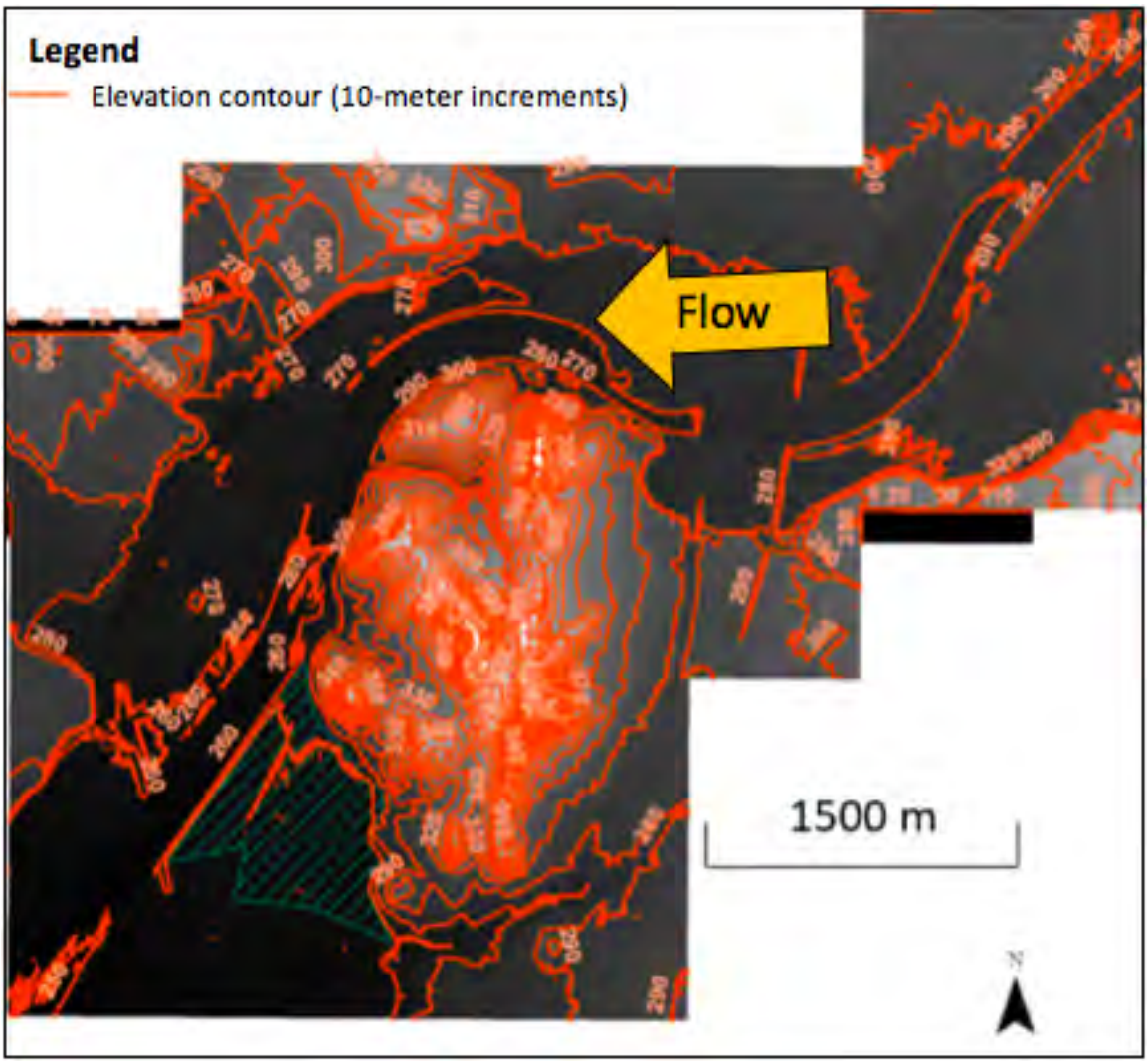

Figure 56: Contour raster derived from elevation raster showing an interval of 10 meters. The highest elevation is in the northeast corner of the map and the lowest elevation is in the southwest corner. Hashed, aqua colored area denotes Pellissier Ranch (ArcMap, 2018).

The Flow Accumulation tool with the Focal Statistics tool applied to show more pronounced maximum values of accumulation, was only useful for showing how water flowed on La Loma Hills to he north of the site (Figure 57). The minor changes across the site were too small for the 1-meter DEM to have been able to derive useful information from. As it has been found that "practically all channel networks have these lower elevation properties, it is sensible that they should be present in networks extracted from DEMs" (Tarboton et al., 1991).

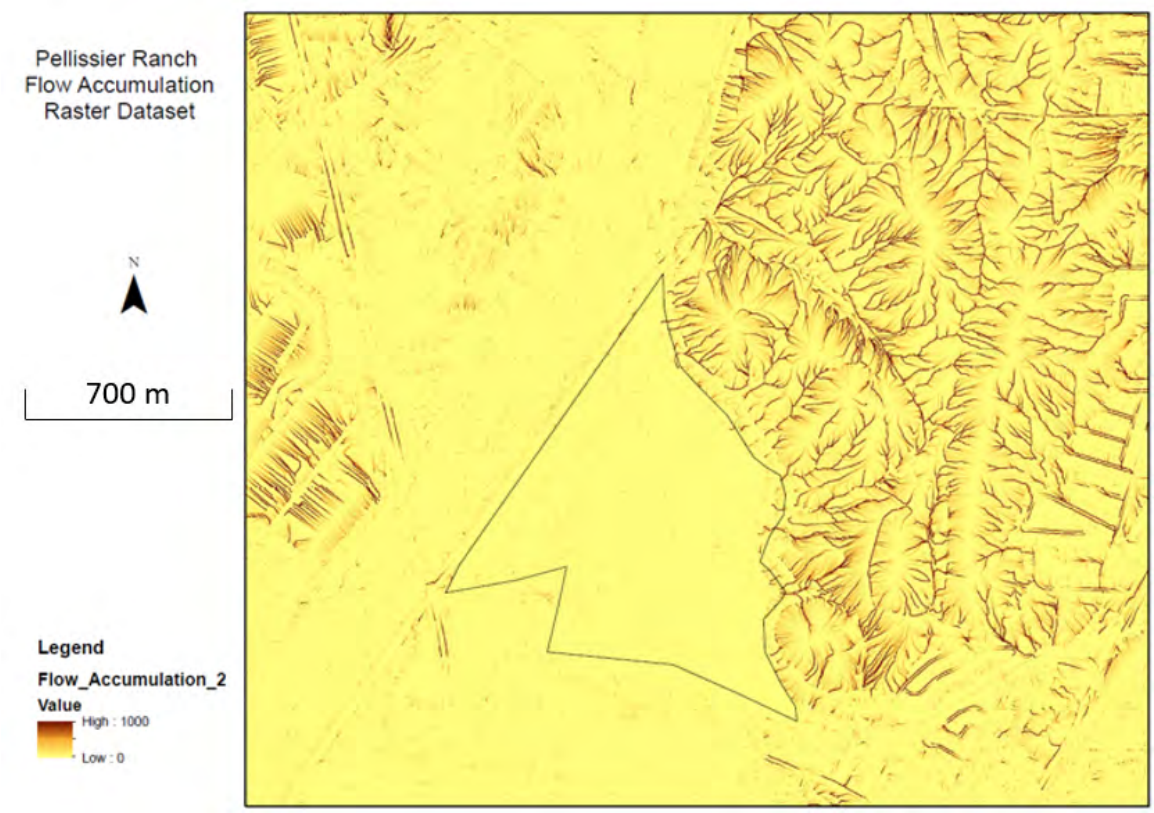

Figure 57: Flow Accumulation raster derived from the Focal Statistics tool after original Flow Accumulation raster was derived from the elevation raster. Black outlined area denotes Pellissier Ranch. Flow across Pellissier Ranch unable to be determined based on extremely flat properties (ArcMap, 2018).

When looking at both the slope raster and the contour raster, a path for an overwhelmed Santa Ana River can be hypothesized. The northeast portion of the map has a wide area which would have allowed the Santa Ana River to spill into as it travels along its path. As it reaches the middle portion of the map, topographic highs on either side of the river force it through a relatively narrow width.

During an overwhelming of the river, it would cause a heavy build up and strong flow through this portion as it forces itself through. Once making it through this narrow portion, it would have spilled over in great force and flowed towards the lowest elevation (the 250' elevation contour in the southwest corner). The greater width past the narrow portion would be filled, this includes Pellissier Ranch.

A limitation to this DEM study was not being able to access Riverside County DEM

datasets. San Bernardino County, which contains the northern half of Pellissier Ranch and all areas north of it, provided free and easily accessible datasets. Riverside County, which contains the southern half of Pellissier Ranch, did not have DEM datasets accessible to the public. While San Bernardino's datasets included enough of the northern border of Riverside County to show the entire Pellissier Ranch and a little south of it, a more conclusive study would have included areas further south.

This would have better shown how far south artifacts might have been taken before being deposited. Based on the two derived raster datasets in this study, it is possible to hypothesize that the Santa Ana River did indeed inundate the entire extent of Pellissier Ranch, which was once La Placita. The strongest force would have been experienced in areas in the southwest portion of the ranch due to the elevation and slope gradient seen in the river. An improved resolution for this survey could be accomplished with a drone, which would provide more minute changes in elevation to derive Flow Accumulation raster datasets of Pellissier Ranch from.